MASTER

Moment transmitting dvw reinforced timber connection with internal steel plate and expanded tube fasteners
influence of restrain effects on the behaviour

Brandon, D.

Award date:
2011

Moment transmitting dvw reinforced timber connection with internal steel plate and expanded tube fasteners -

Influence of restrain effects on the behaviour

APPENDICES

prof.dr.ir. A.J.M. Jorissen

D.Brandon

Graduation project
Eindhoven University of Technology

Supervisors:
prof.dr.ir.A.J.M.Jorissen
dr.ir.A.J.M.Leijten
ing.E.Luning

May 17, 2011

Apendices

Table of contents

Apendices

Apendices

Appendix 1: Results of numerical approach of inverse force displacement curves of tubular fasteners

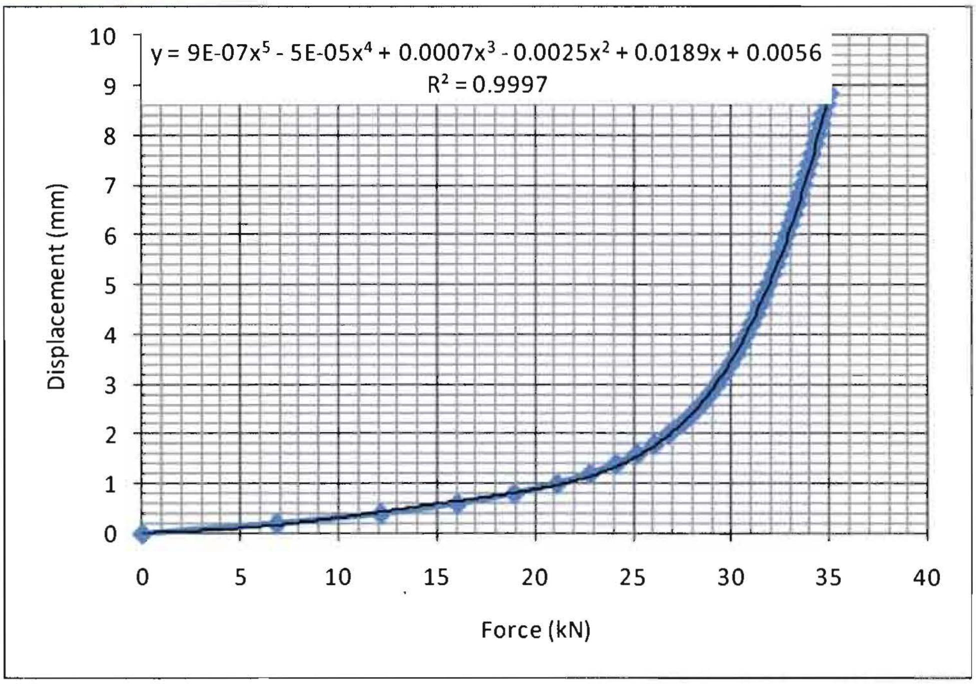

Figure 1: Numerical estimation of inverse of force-displacement curve for 18 mm tubes

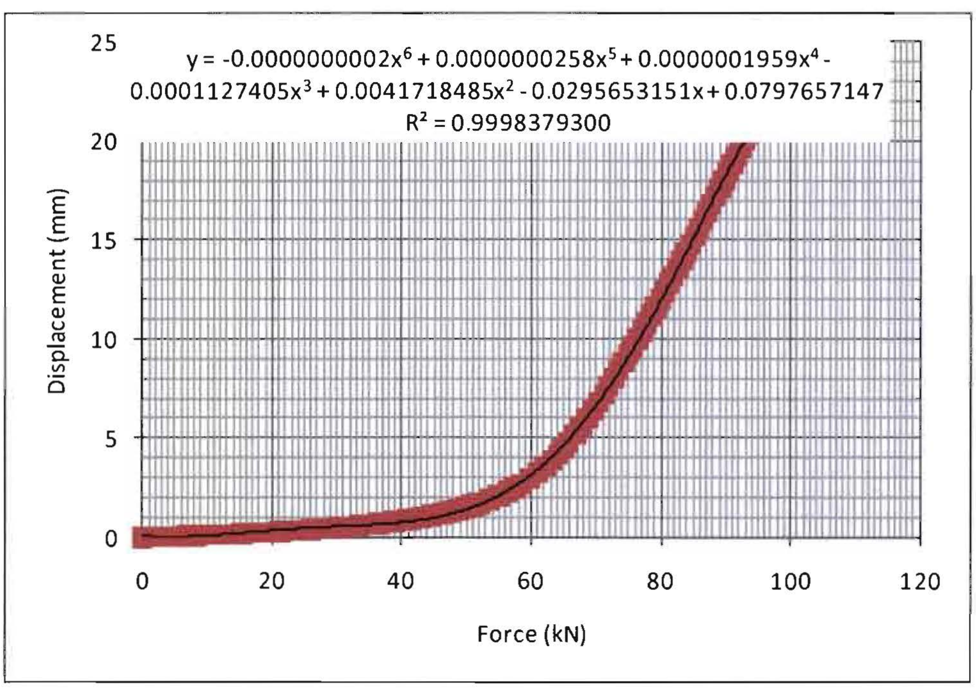

Figure 2: Numerical estimation of inverse of force-displacement curve for 35 mm tubes

Appendix 2: Results of analytical approach of connection with occurrence of gap closure due to bending moment

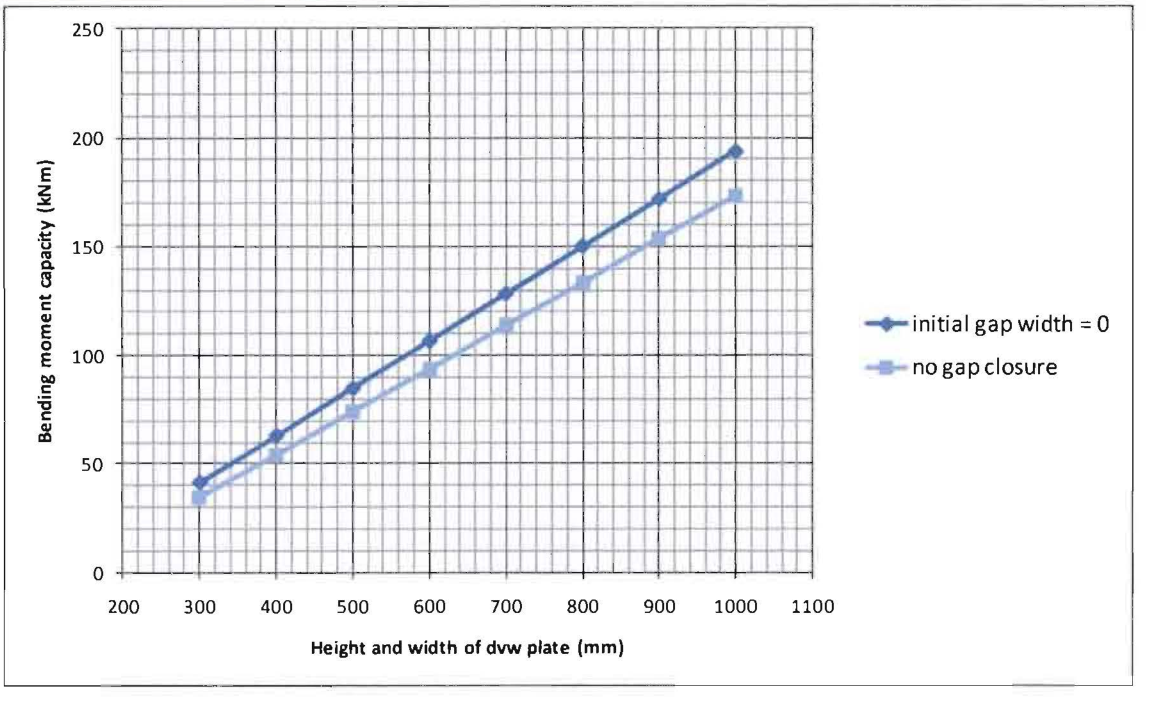

Figure 3: Moment capacity of connection with four tubes and an edge distance of 3.5 d; b=h; d=18mm; t=12mm; β=0,8.

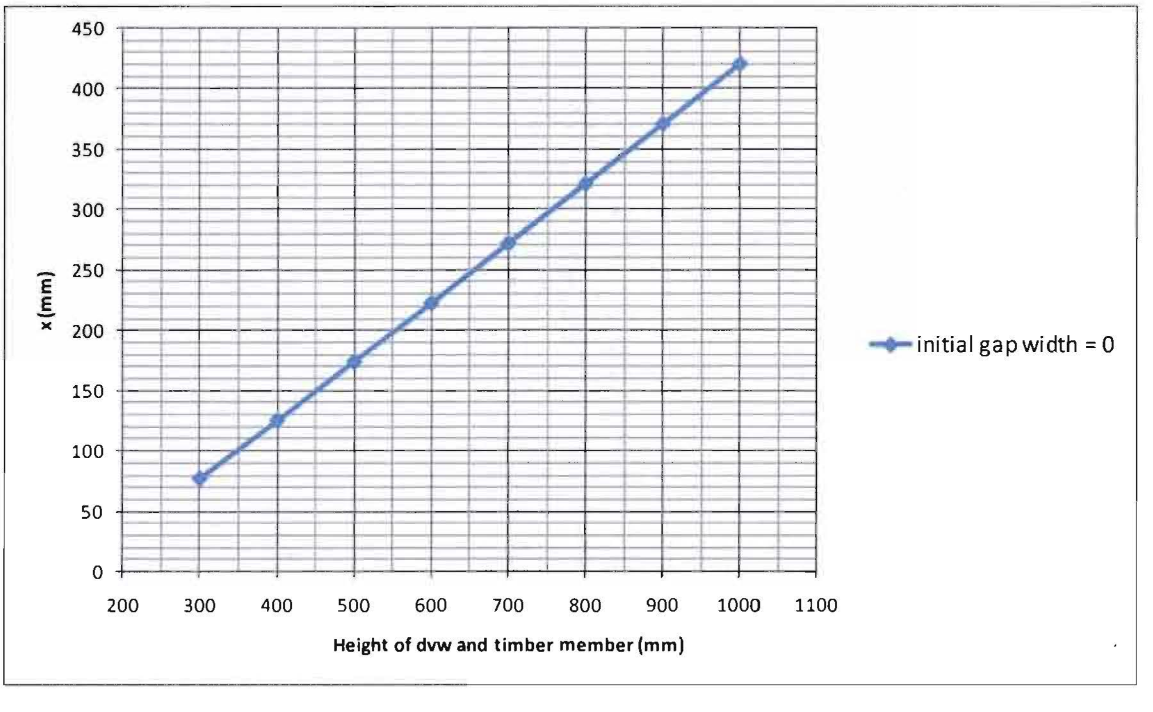

Figure 4: x_v at maximum capacity of connection with four tubes and an edge distance of 3.5 d; b=h; d=18mm; t=12mm; β=0,8.

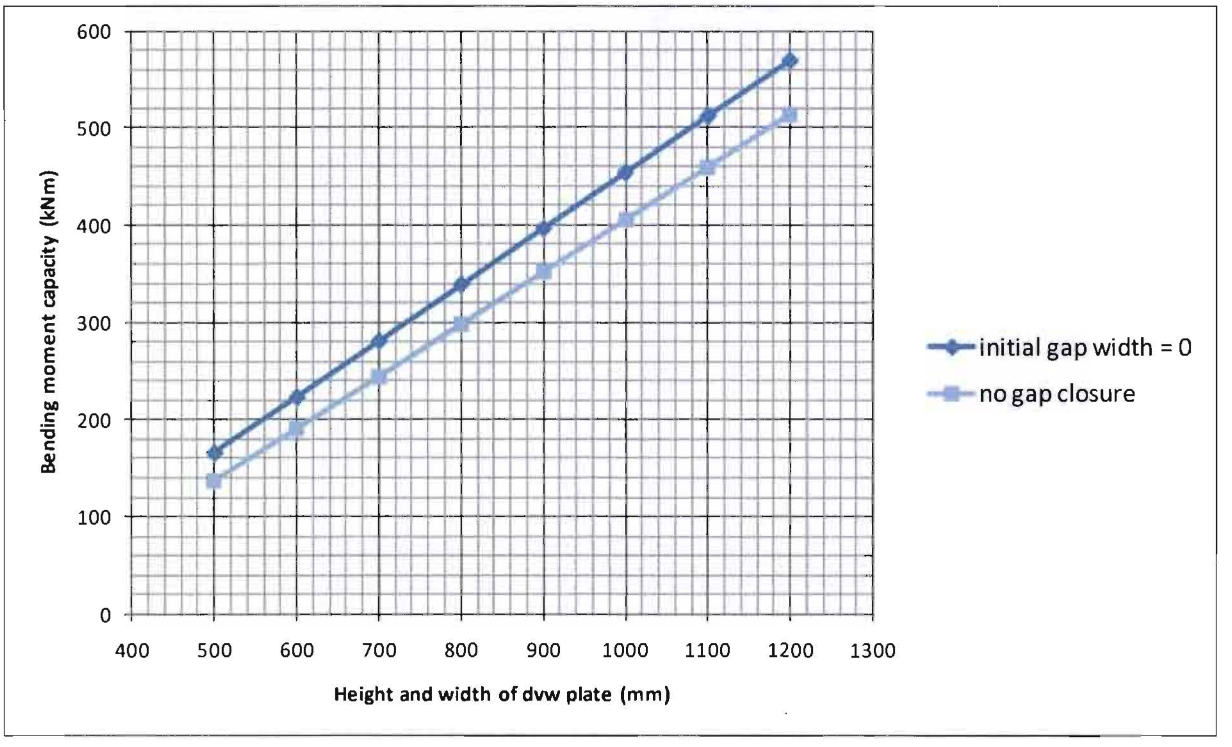

Figure 5: Moment capacity of connection with four tubes and an edge distance of 3.5 d; b=h; d=35mm; t=12mm; β=0,8.

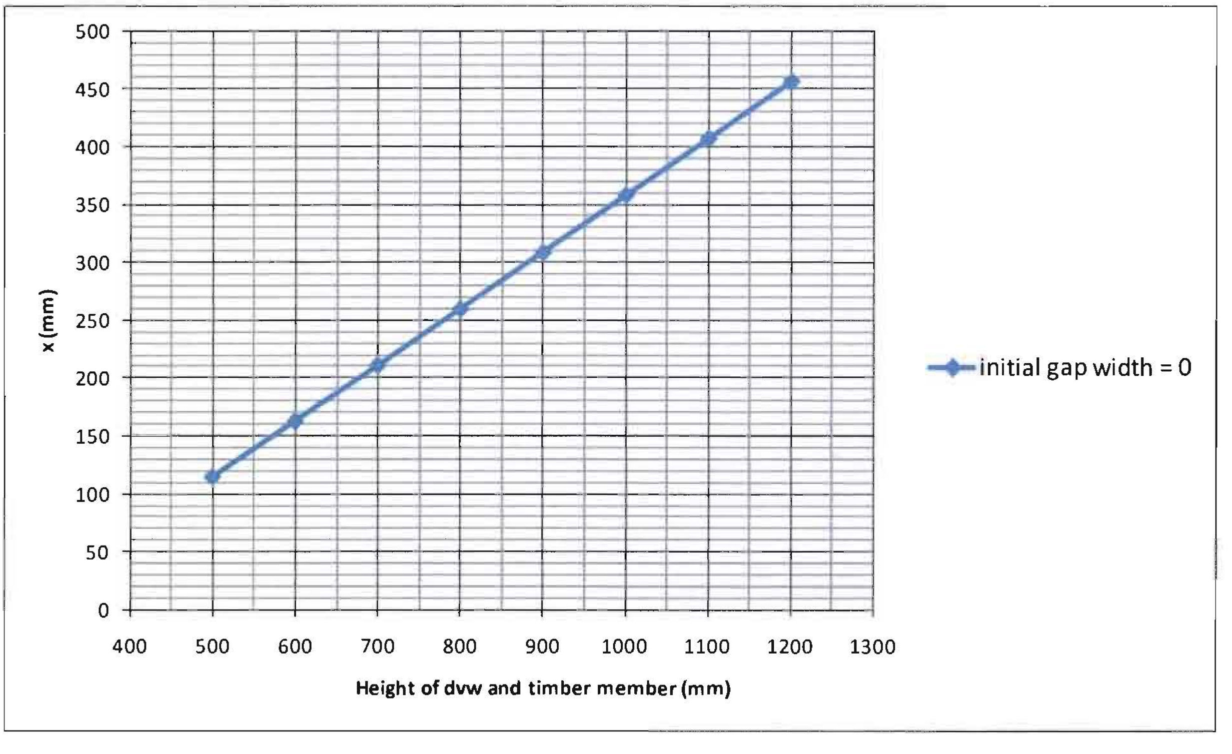

Figure 6: x_v at maximum capacity of connection with four tubes and an edge distance of 3.5 d; b=h; d=35mm; t=12mm; β=0,8.

Appendix 3: Benchmark C3D8R

The 8-node element C3D8R is able to describe normal and shear strain accurately. To gain insight of the ability to describe bending strain, a benchmark is made. Figure 7 illustrates the shape and boundary conditions of the model. Length, height and depth are respectively 150mm, 5mm and 2.5mm. The results are compared to the solution of equation 1.

$$\delta = \frac{Pl^3}{EI} \qquad (1)$$

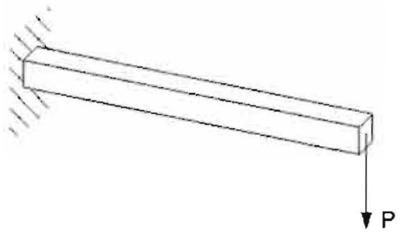

Figure 7: Benchmark model

First the results with fully integrated 8-node and 20-node elements are compared.

Element	Number of elements (Height × Length)			
	1 × 6	2 × 12	4 × 12	8 × 24
C3D8	0,077	0,248	0,243	0,563
C3D20	0,994	1,000	1,000	1,000

Table 1: Displacement by Abaqus divided by displacements according to equation 1

From Table 1 it can be concluded that the C3D8 element acts too stiff to accurately describe the deformation. The 20-node element describes the deformation accurately regardless to the number of elements. The 20-node element requires more calculation time than the 8-node element, which is problematic when used in models with a large amount of elements.

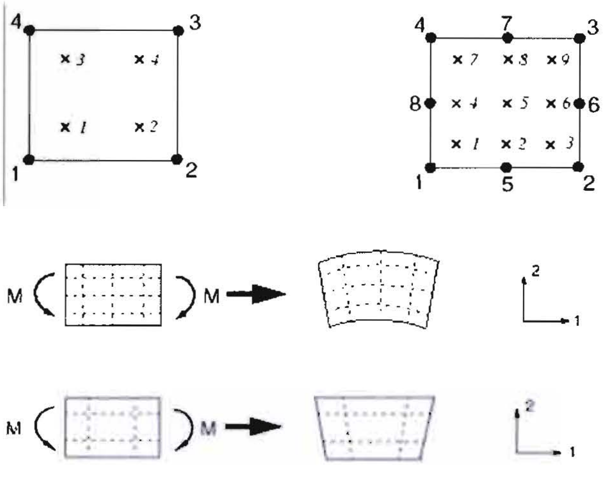

Figure 8: 4-node (2D) and 8-node (2D) elements and their integration points

Secondly elements with reduced integration are tested. With reduced integration the number of integration points per element is reduced, resulting in less required calculations. The ideal location of these Gauss-integration points often leads to more accurate results.

Element	Number of elements (Height × Length)			
	1 × 6	2 × 12	4 × 12	8 × 24
C3D8R	70,1	1,323	1,063	1,015
C3D20R	0,999	1,000	1,000	1,000

Figure 9 : Displacement by Abaqus divided by displacements according to equation 1

From Figure 9 it appears the 8-node elements tend to behave too flexible when reduced integration is implemented. An 8 node element has only one integration point and therefore only one strain (or stress) output value. The 2-dimensional 4-node element of Figure 10 represents similar problems. The length of the dotted lines in Figure 10 will not change due to pure bending moment in the elements. This results in zero strain values, zero stress values and zero energy. This specific behavior due to *zero energy modes* which can occur in 4-node 2D elements and 8-node 3D elements is called *hourglassing*.

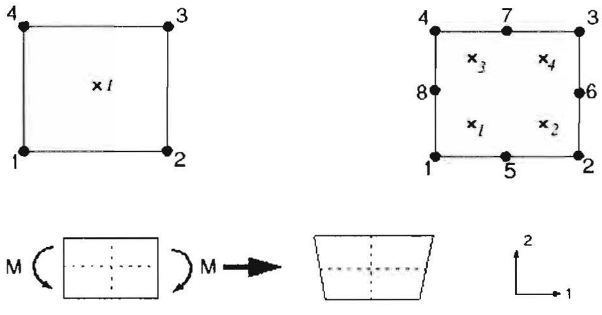

Figure 10: 4-node (2D) and 8-node (2D) elements and their Gauss-integration points

Enhanced hourglass control in Abaqus/CAE can be used to solve this particular problem. An additional stiffness based on the pure stiffness method is implemented to gain reliable results.

Element	Number of elements (Height × Length)			
	1 × 6	2 × 12	4 × 12	8 × 24
C3D8R	0.992	1.000	1.000	1.000

Figure 11 : Displacement by Abaqus divided by displacements according to equation 1

The accuracy of the 8-node element, C3D8R, with enhanced hourglass control is comparable to the accuracy the 20-node element. A significant advantage of the 8-node element is the low costs (or calculation time).

Appendix 4: Determination of l_{eff} for simplified strain calculation

A simple finite element model is made to determine the value of l_{eff} that can be in the simplified strain calculation discussed in paragraph 7.1.2 of the report. Hook's law is used, but instead of using the full length of the beam (l), l_{eff} is used to compensate the fact that the beam is not compressed homogeneously by gap closure. Equation 2 is implemented for the strain calculations. l_{eff} is determined in this appendix by numerical analyses.

Figure 12 shows the geometry of the finite element model. A rigid surface with height h_c is introducing the compressive force in the timber and dvw member. As shown in Figure 12 one side of the rigid surface is moved for a distance equal to Δl. The beam length in the model is taken 10 times the beam height. The input variable of the finite element analyses is Δl and the strain ε output is used to determine l_{eff}.

$$\varepsilon = \frac{\Delta l}{l_{eff}} \qquad 2$$

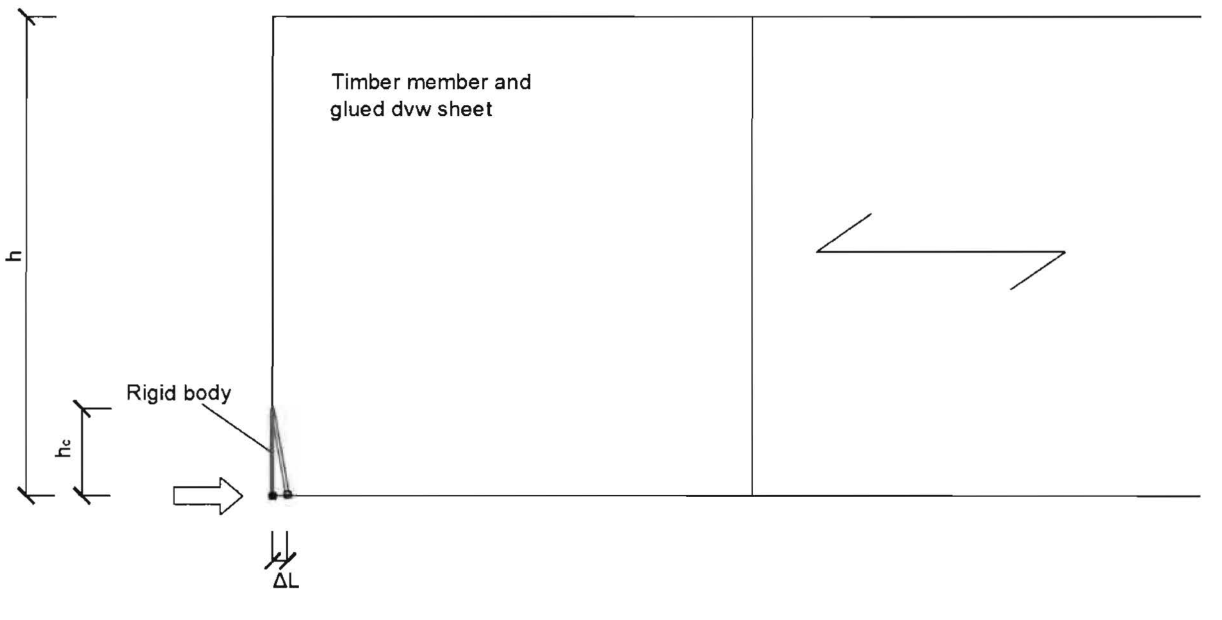

Figure 12: FEM model for determining l_{eff}

Figure 13: Strain in dvw and timber (back) with h_c/h= 0.2 and Δl=2.3911E-04 mm

Figure 14: Strain in timber with h_c/h= 0.2 and Δl=2.3911E-04 mm

The effective length corresponding to the strain values given in Figure 13 and Figure 14 can be determined with;

$$\varepsilon_{dvw} = \frac{\Delta l}{l_{eff;dvw}}$$

$$l_{eff;dvw} = \frac{2.3911^{-4}}{1.304 \cdot 10^{-6}} = 183.4mm = 0.61h$$

$$\varepsilon_{timber} = \frac{\Delta l}{l_{eff;timber}}$$

$$l_{eff;timber} = \frac{2.3911^{-4}}{9.326 \cdot 10^{-7}} = 256.4mm = 0.85h$$

Figure 15: Strain dvw and timber (back) with h_c/h= 0.3 and Δl=1.4980E-04 mm

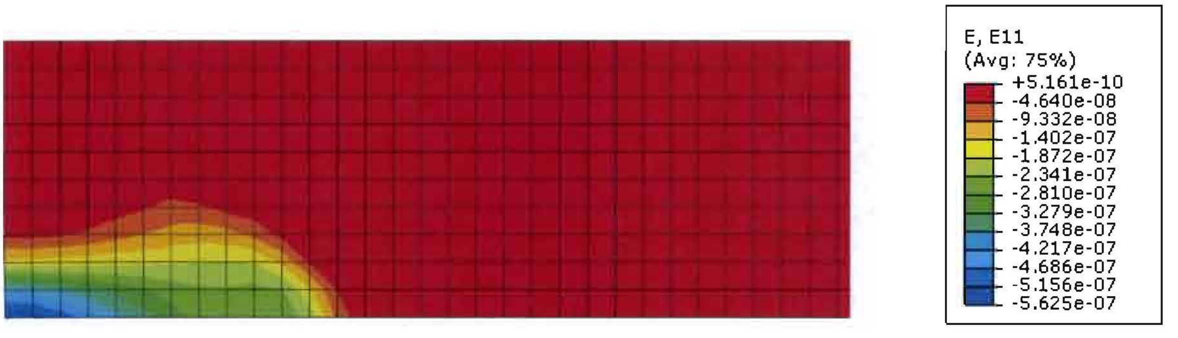

Figure 16: Strain timber with h_c/h= 0.3 and Δl=1.4980E-04 mm

The effective length corresponding to the strain values given in Figure 15 and Figure 16 can be determined with;

$$\varepsilon_{dvw} = \frac{\Delta l}{l_{eff;dvw}}$$

$$l_{eff;dvw} = \frac{1.4980 \cdot 10^{-4}}{7.478 \cdot 10^{-7}} = 200.3mm = 0.67h$$

$$\varepsilon_{timber} = \frac{\Delta l}{l_{eff;timber}}$$

$$l_{eff;timber} = \frac{1.4980 \cdot 10^{-4}}{5.625 \cdot 10^{-7}} = 266.3mm = 0.89h$$

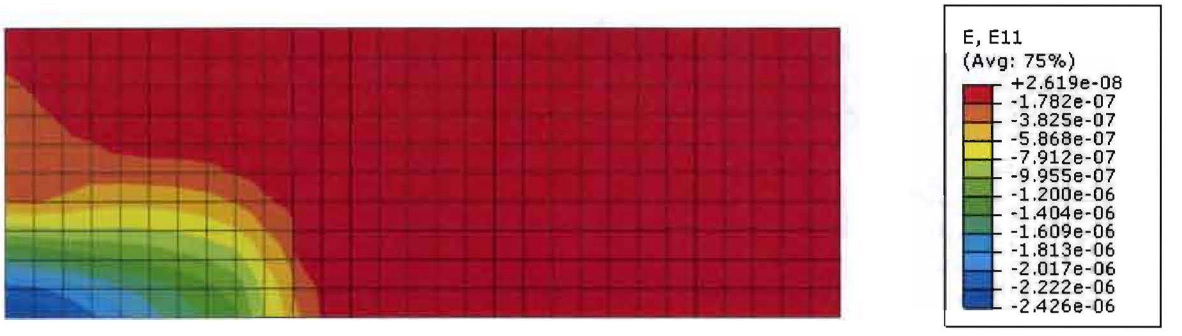

Figure 17: Strain dvw and timber (back) with h_c/h= 0.5 and Δl=5.7500E-04 mm

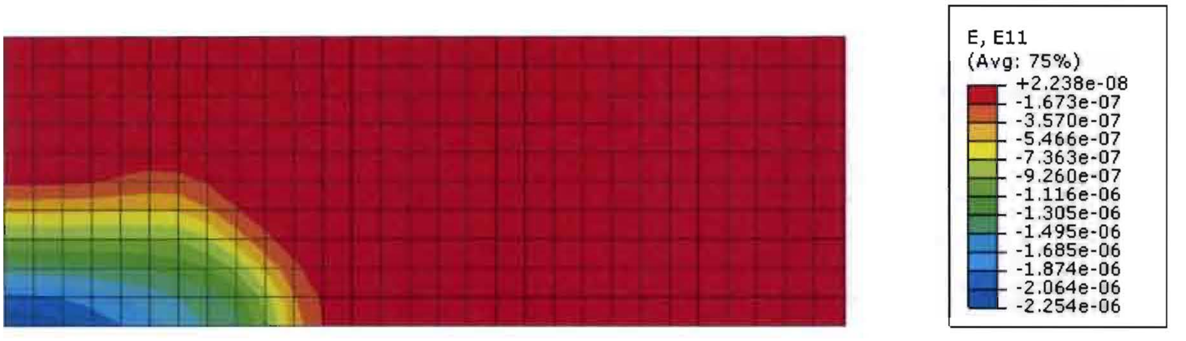

Figure 18: Strain timber with h_c/h= 0.5 and Δl=5.7500E-04 mm

The effective length corresponding to the strain values given in Figure 17 and Figure 18 can be determined with;

$$\varepsilon_{dvw} = \frac{\Delta l}{l_{eff;dvw}}$$

$$l_{eff;dvw} = \frac{5.7500^{-4}}{2.426 \cdot 10^{-6}} = 237.0mm = 0.79h$$

$$\varepsilon_{dvw} = \frac{\Delta l}{l_{eff;dvw}}$$

$$l_{eff;dvw} = \frac{5.7500^{-4}}{2.254 \cdot 10^{-6}} = 255.1mm = 0.85h$$

Figure 19 shows that the effective length is approximately constant for the different values of h_c that are implemented in this analysis.

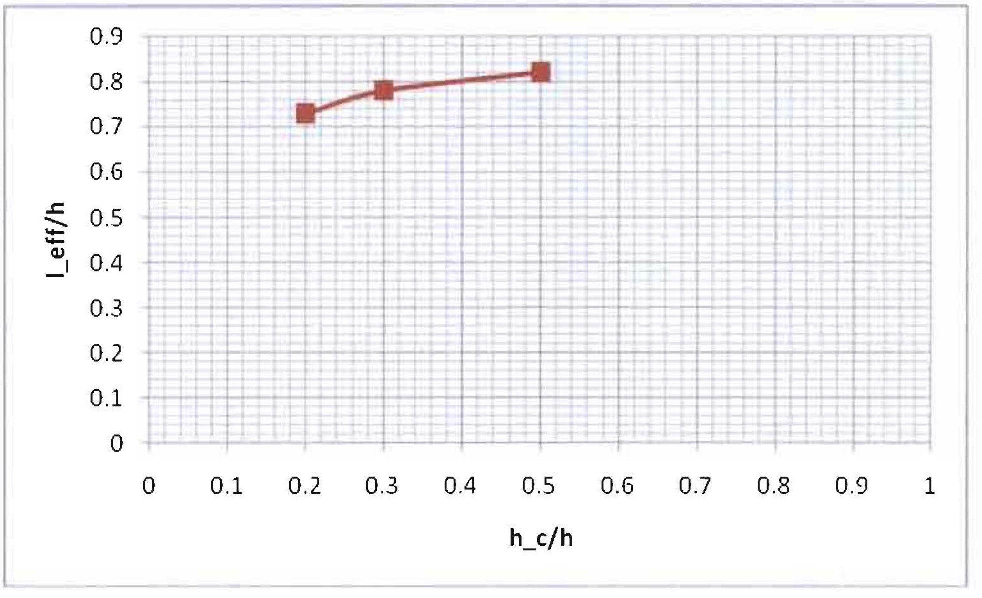

Figure 19: l_{eff} for different values of h_c/h

Appendix 5: Benchmark for cohesive elements

Cohesive elements are used to simulate delamination in finite element analyses. To monitor the reliability of the simulation, benchmarks are compared to the results of studies made by Per Johan Gustafsson and Erik Serrano [5]. To control the accuracy of cohesive elements the creep dissipation due to viscous damping should be a fraction of the total internal energy. An analysis with creep dissipation less than three percent of the internal energy is defined accurate for this study.

The set-up of Figure 21 is modeled in Abaqus. The glue length L is taken 400 mm and the height of the glued surface is taken 150 mm (similar to the analyses of Gustafsson and Serrano and the experiments of Glos and Horstman). Table 2 shows the results of the benchmark (FEA Brandon). The results are comparable with the results of Gustafsson and Serrano.

Figure 23 shows the determined bond line capacity for different load to grain angles. The grain angle of the middle beam of Figure 21 is herewith adapted. From the results it can be concluded that the results of the analyses discussed in this appendix (FEM Brandon) mainly coincide with the FEA results of Gustafsson and Serrano and the experimental results of Glos and Horstman.

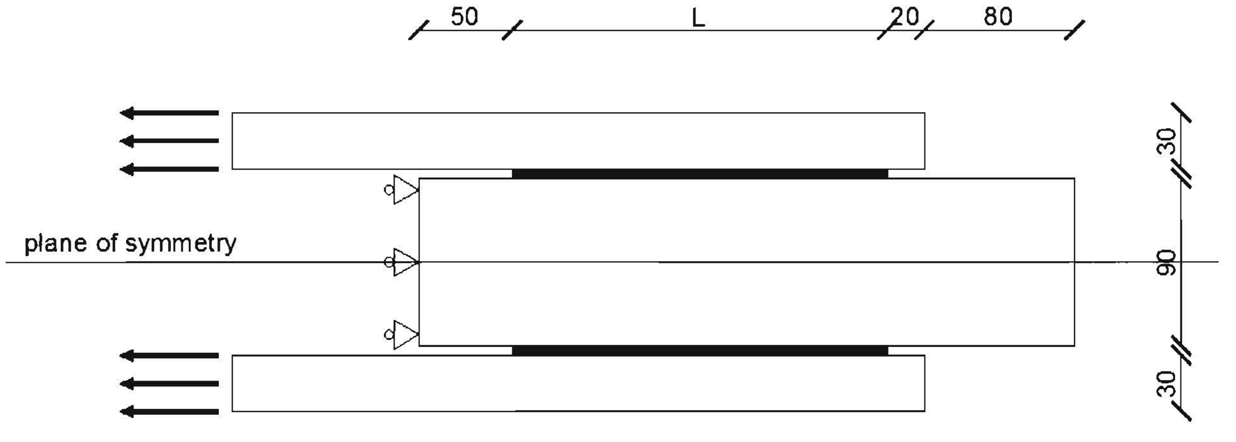

Figure 20: Geometry of finite element model; L = 400 mm [5]

Adhesive type	R/P	Epoxi	PVAc
Fracture energy (J/m2)	800	1400	1600
Gustafsson and Serrano (kN)	167	214	230
FEA Brandon (kN)	175	232	250
Deviation (%)	4.8	7.8	7.9

Table 2: Comparison of results of two finite element analyses; L = 400 mm

Apendices

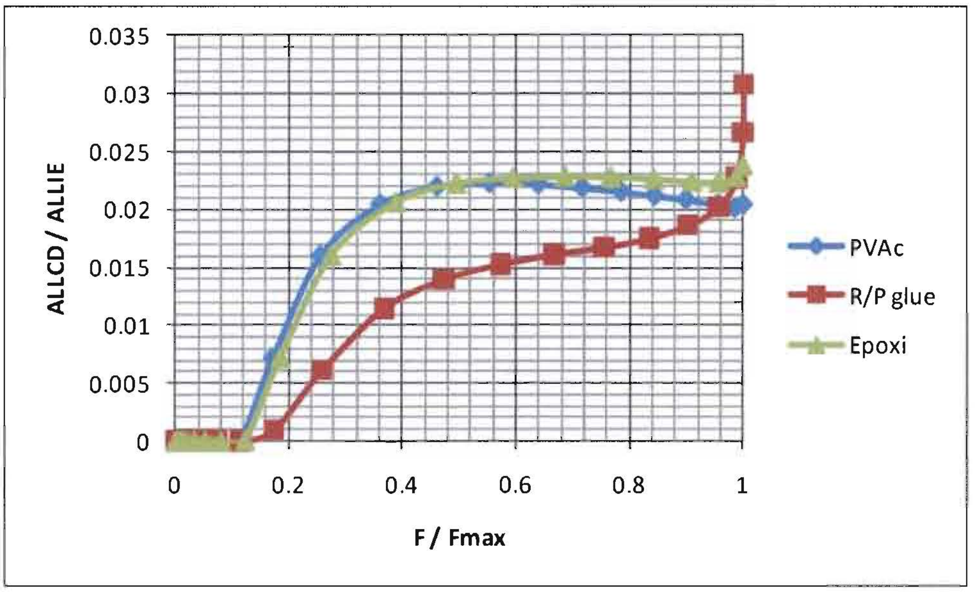

Figure 21: Total creep dissipation due to viscous damping divided by total internal energy

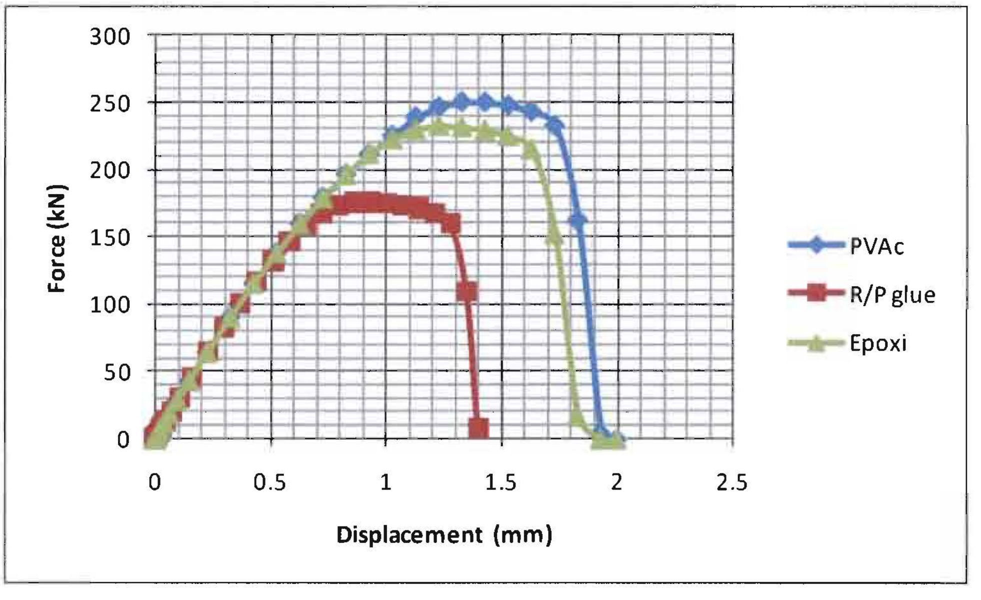

Figure 22: Force-displacement curve of benchmark

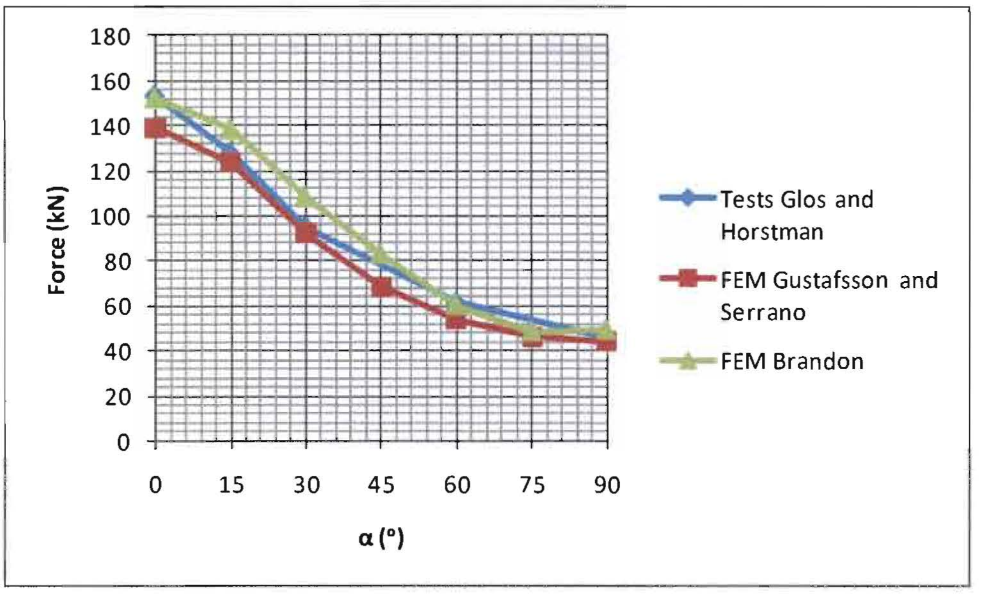

Figure 23: Force versus angle to grain direction referred to previously published results [5]

Appendix 6: Analyses of tube deformation without internal steel plate 35 mm tube

tube diameter (d)	35 mm
displacement at step time = 1.0 ($\delta_{1.0}$)	18 mm
edge/end distance	3.5d
timber thickness (t_{timber})	55 mm
dvw thickness (t_{dvw})	18 mm

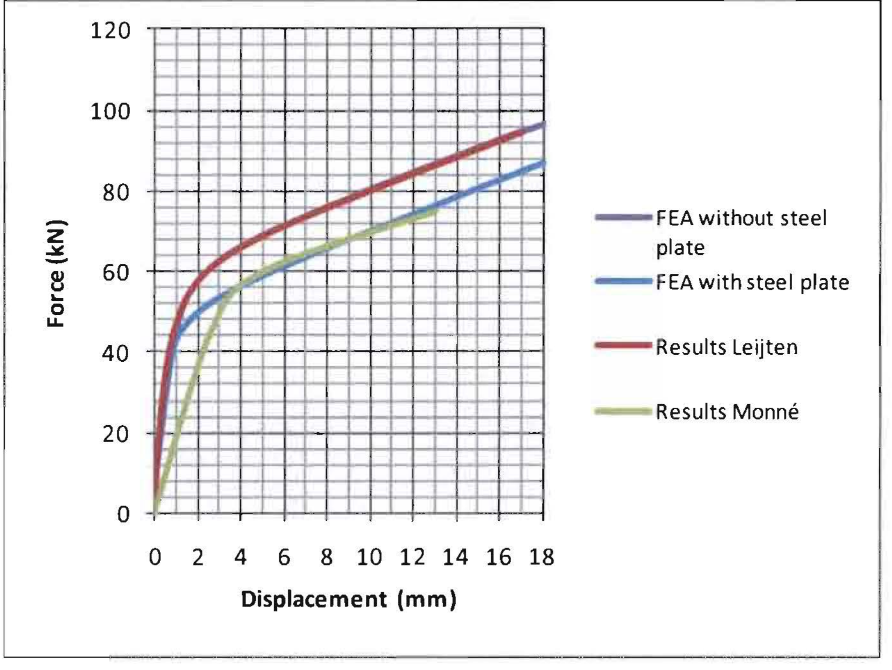

Figure 24: Tube force per shear plane versus displacement of different analyses and published test results [1] [3]

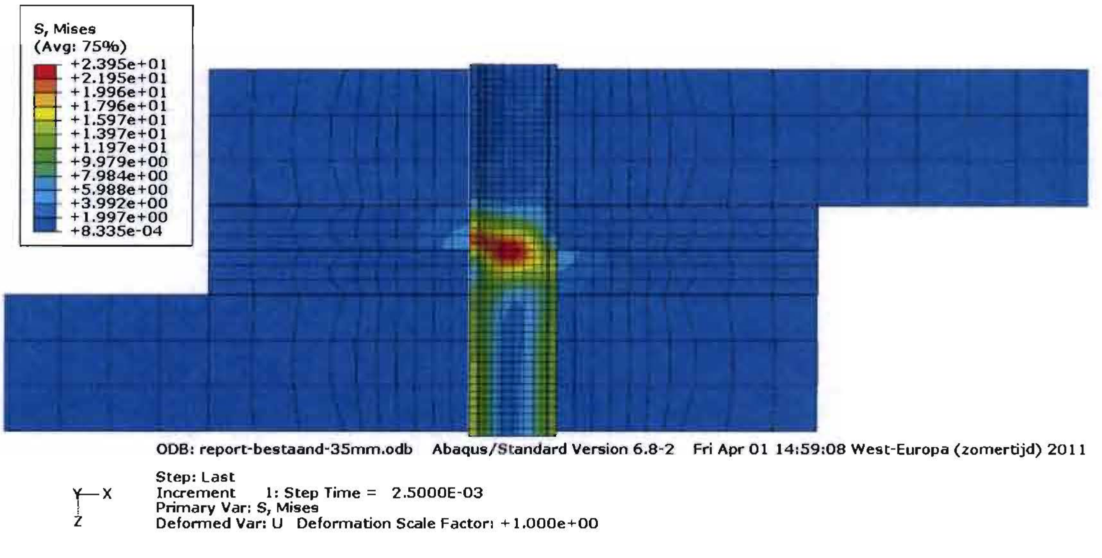

Figure 25: von Mises stress; step time = 0.0025

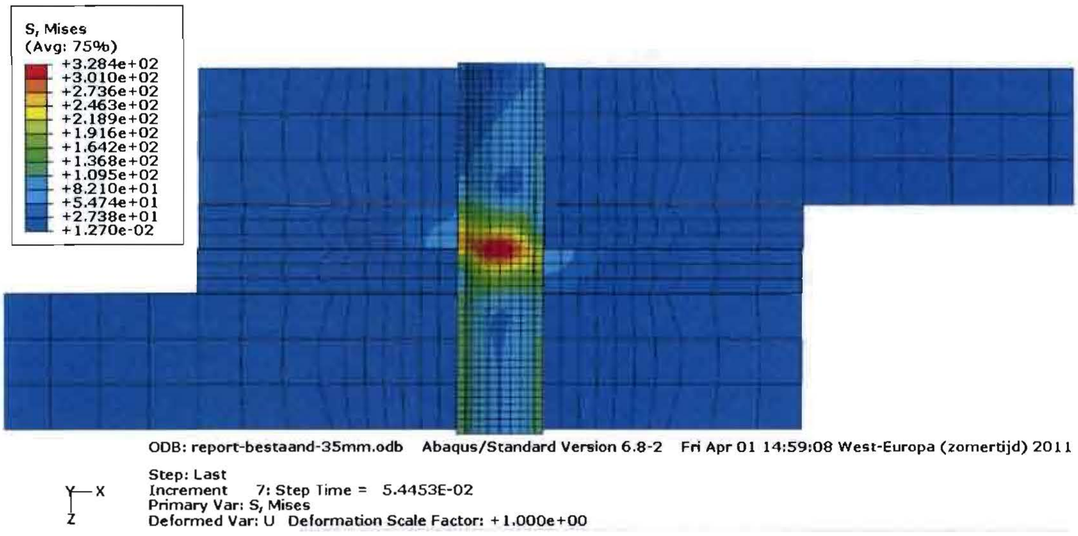

Figure 26: von Mises stress; step time = 0.0544

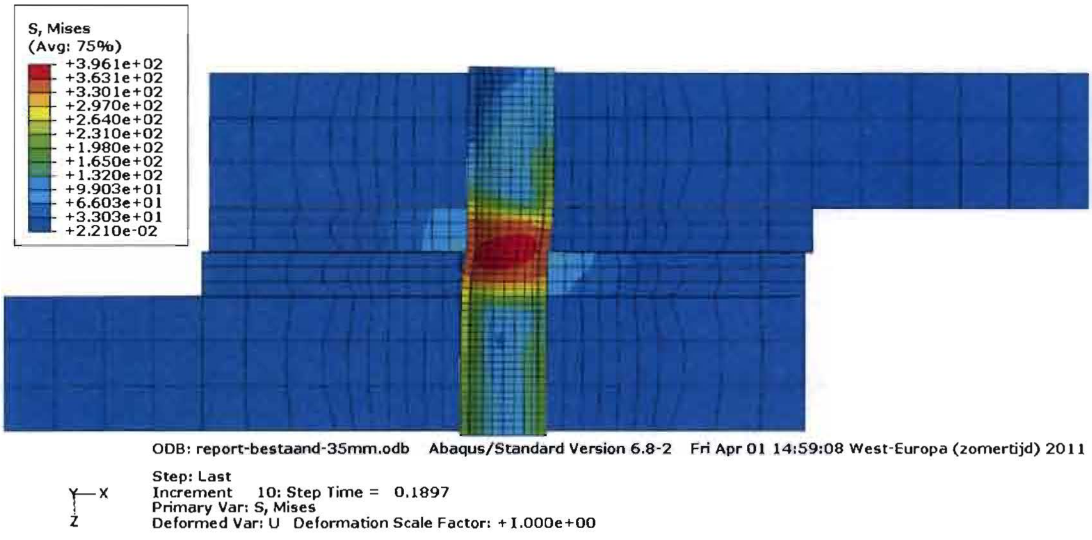

Figure 27: von Mises stress; step time = 0.1897

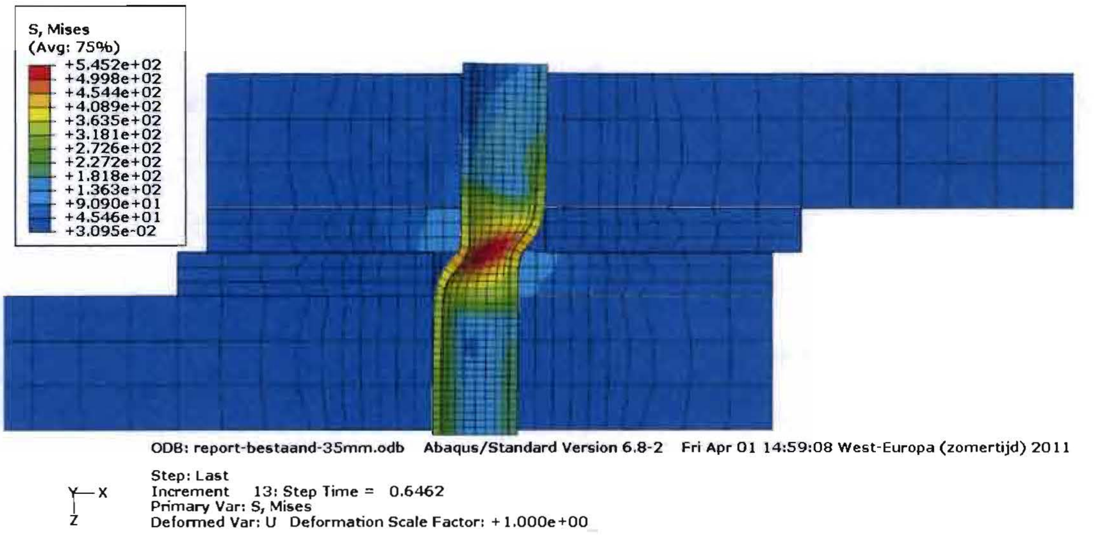

Figure 28: von Mises stress; step time = 0.6462

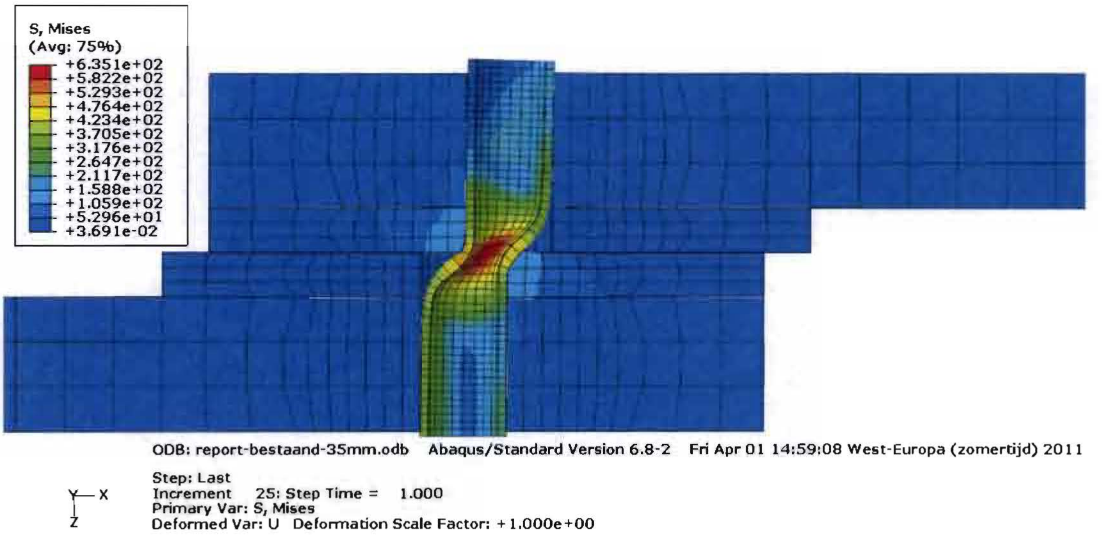

Figure 29: von Mises stress; step time = 1.0000

Appendix 7: Analyses of tube deformation with internal steel plate and 35 mm tube

tube diameter (d)	35 mm
displacement at step time = 1.0 ($\delta_{1.0}$)	18 mm
edge/end distance	3.5d
timber thickness (t_{timber})	55 mm
dvw thickness (t_{dvw})	18 mm
adhesive	PU
bond line thickness	0.2 mm

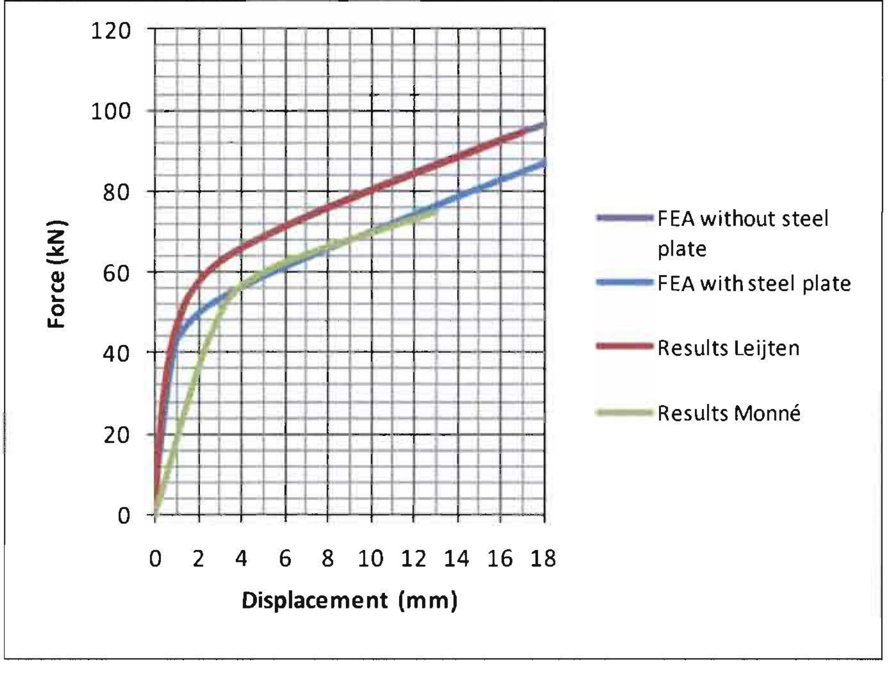

Figure 30: Tube force per shear plane versus displacement of different analyses and published test results [1] [3]

Appendix 7 A: Von Mises tube stresses

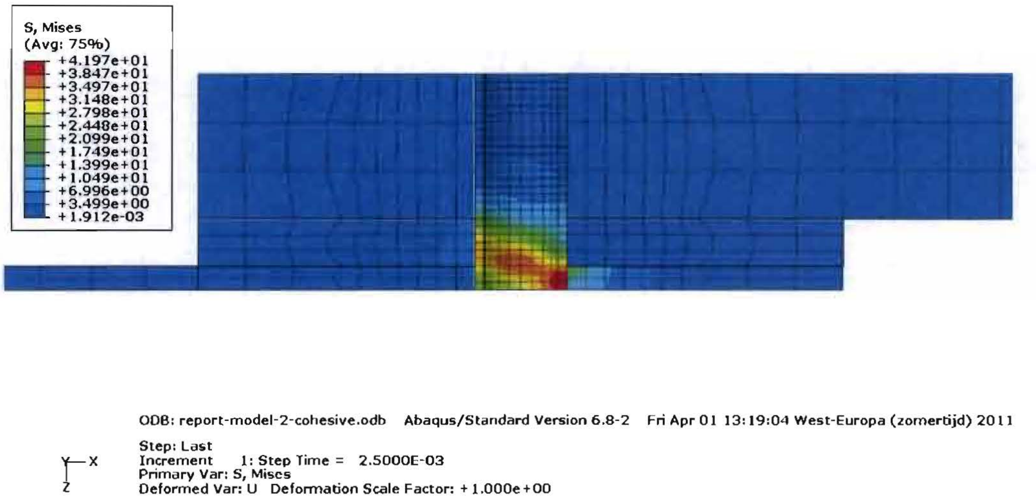

Figure 31: von Mises stress; step time = 0.0025

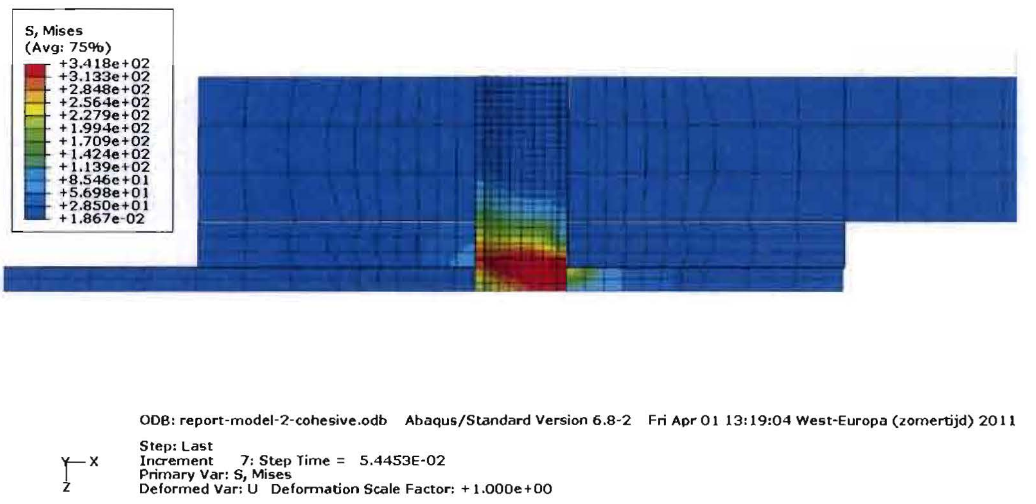

Figure 32: von Mises stress; step time = 0.0544

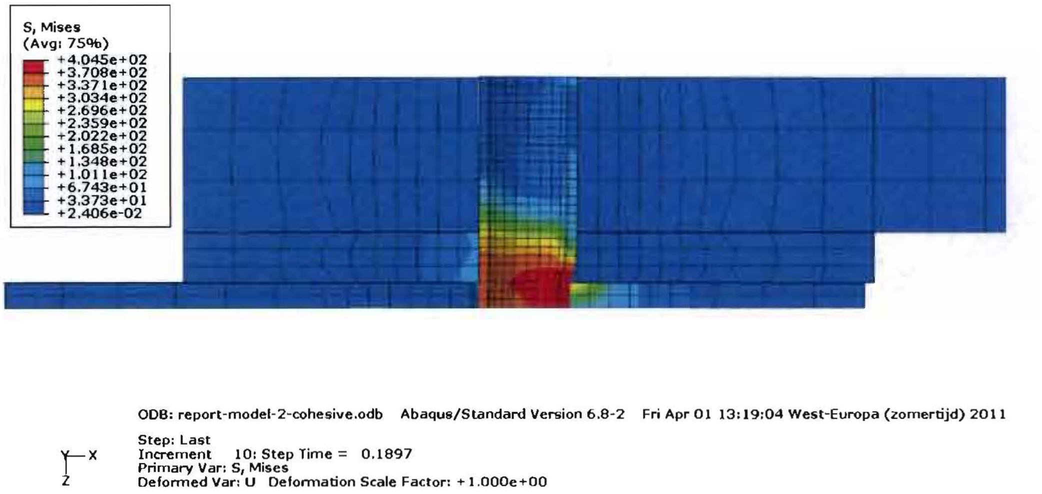

Figure 33: von Mises stress; step time = 0.1897

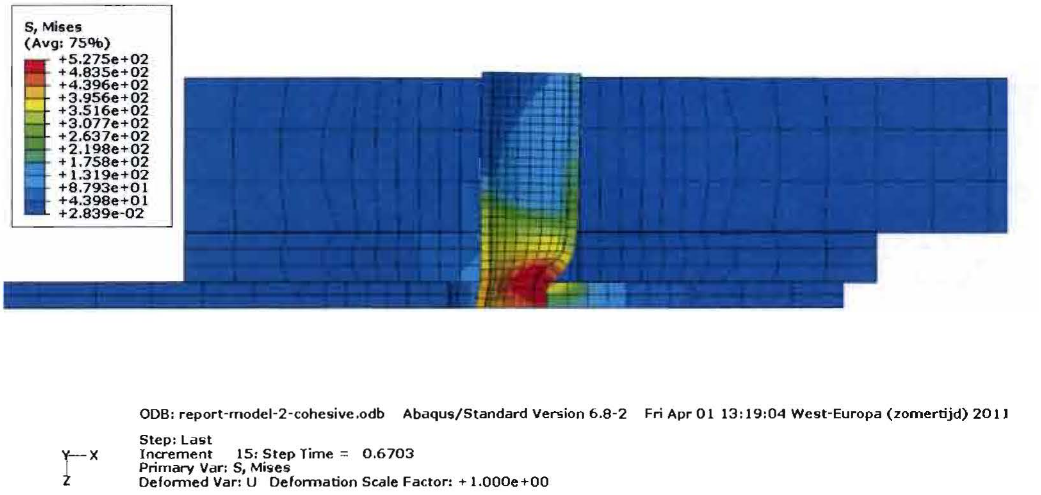

Figure 34: von Mises stress; step time = 0.6462

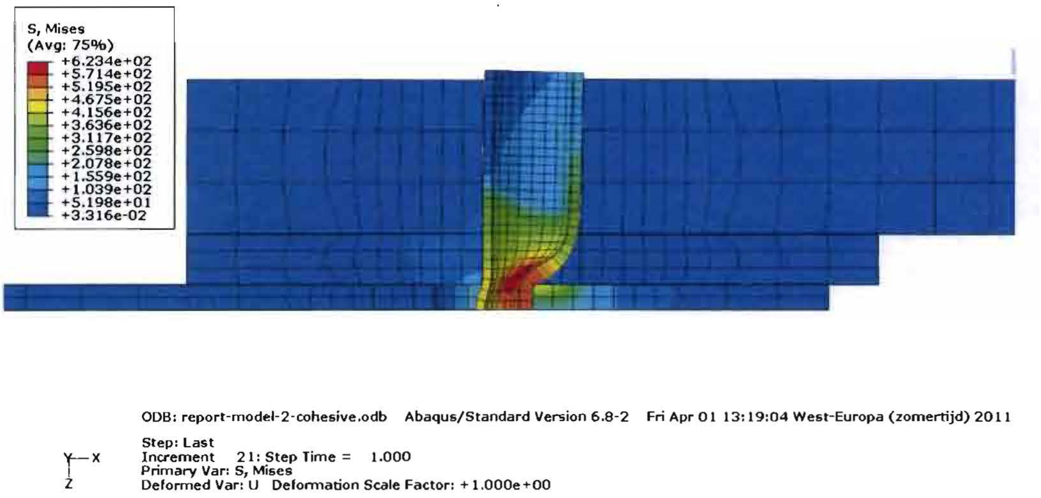

Figure 35: von Mises stress; step time = 1.0000

Appendix 7 B: Shear stress parallel to grain in bond line

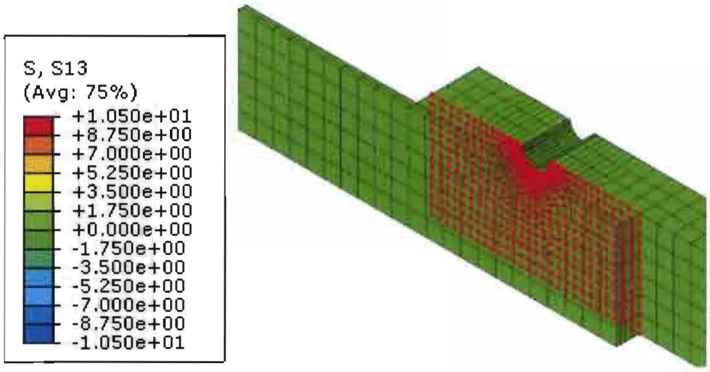

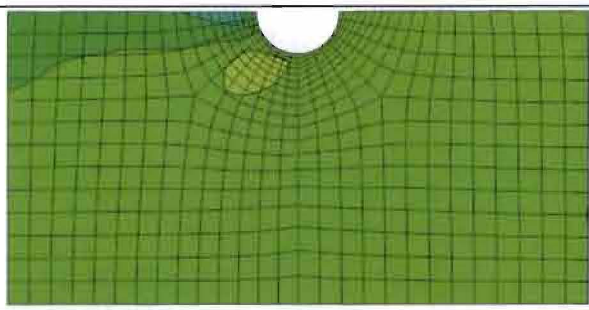

Step time: 0.1256
Diplacement: 2.2608mm

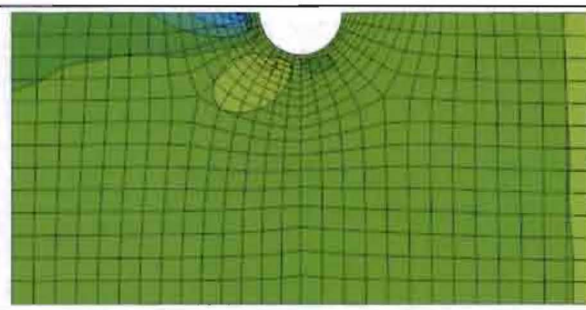

Step time: 0.0.3819
Diplacement: 6.8742mm

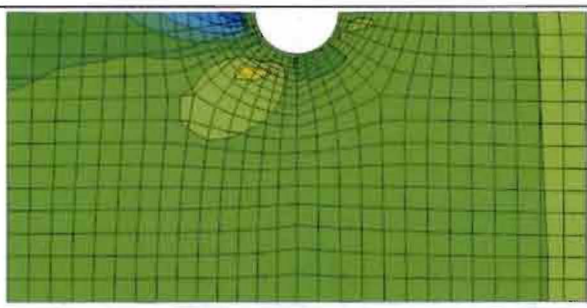

Step time: 0.8625
Diplacement: 7.7625mm

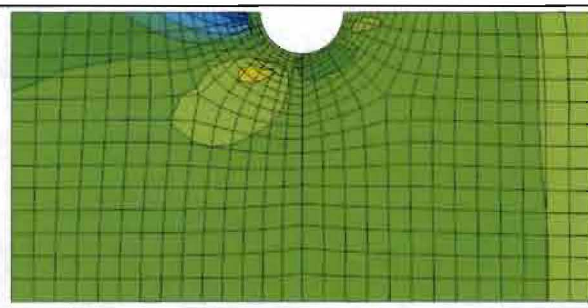

Step time: 1.0000
Diplacement: 9mm

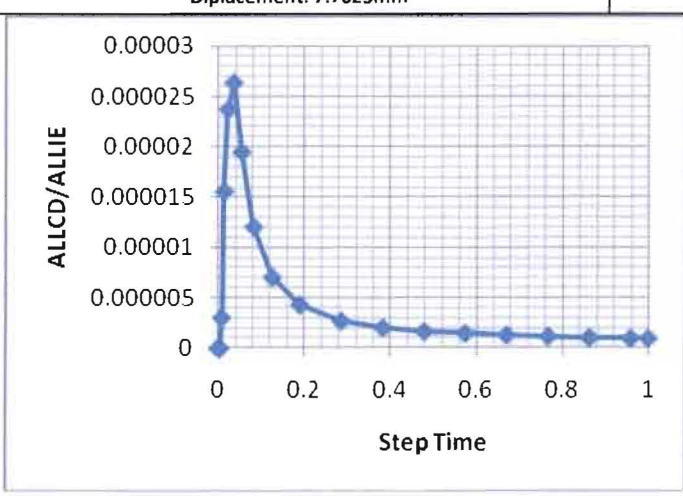

Figure 36: Energy due to creep dissipation divided by total internal energy through time

Appendix 8:Analyses of tube deformation without internal steel plate 18 mm tube

tube diameter (d)	18 mm
displacement at step time = 1.0 ($\delta_{1.0}$)	9 mm
edge/end distance	3.5d
timber thickness (t_{timber})	55 mm
dvw thickness (t_{dvw})	12 mm

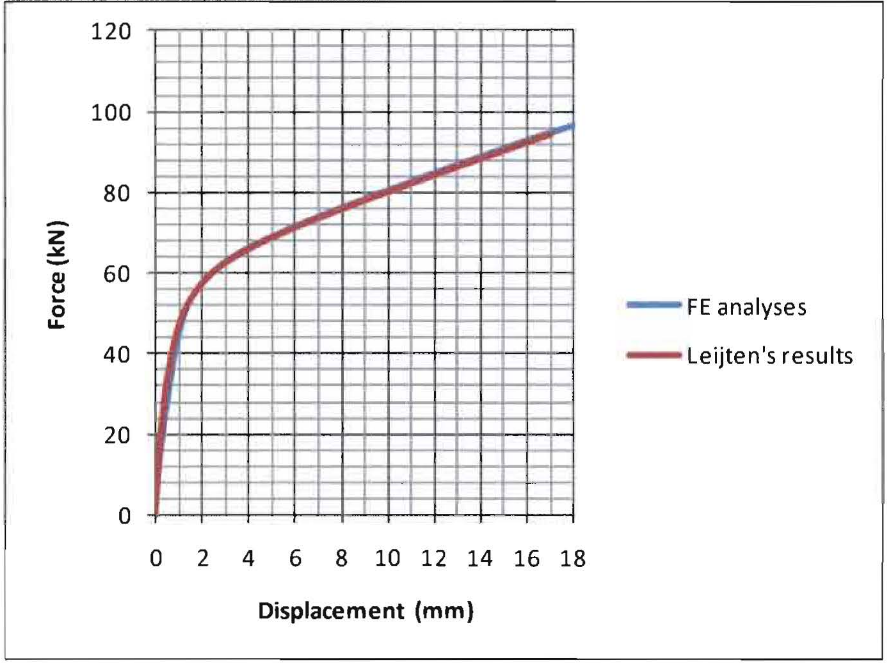

Figure 37: Tube force per shear plane versus displacement of FEA and published test results [1]

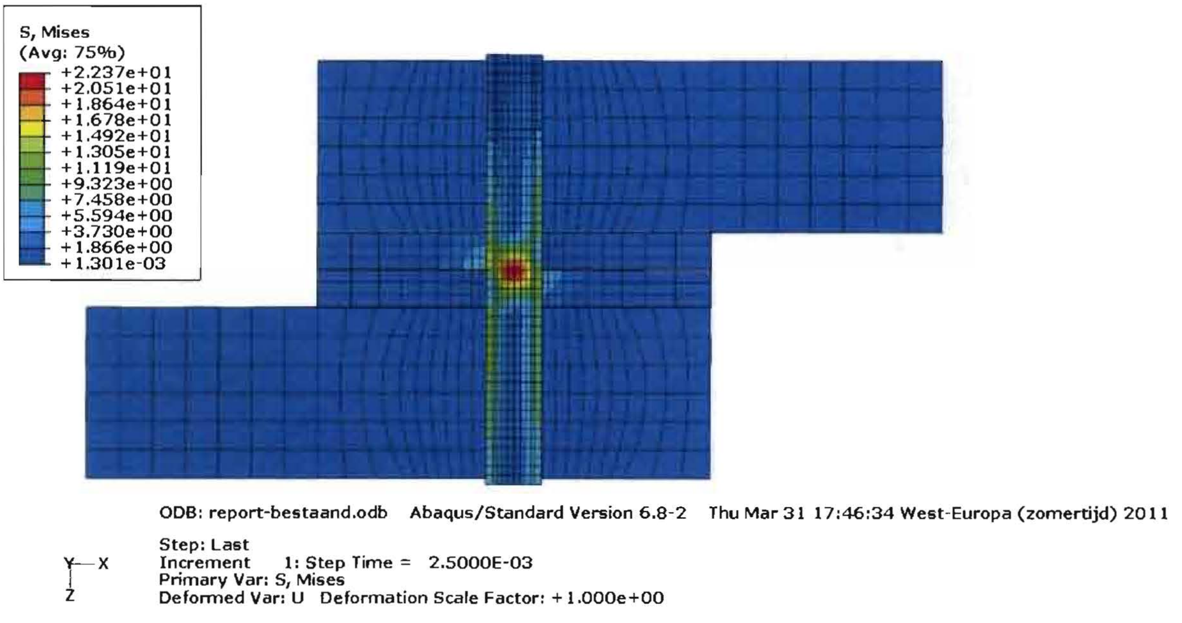

Figure 38: von Mises stress; step time = 0.0025

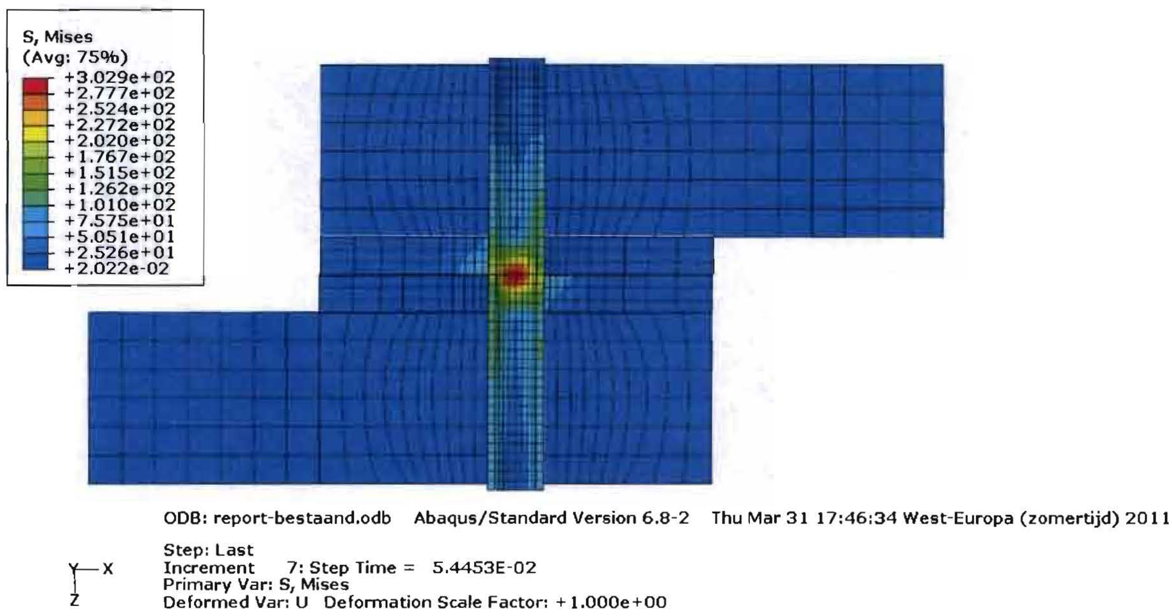

Figure 39: von Mises stress; step time = 0.0544

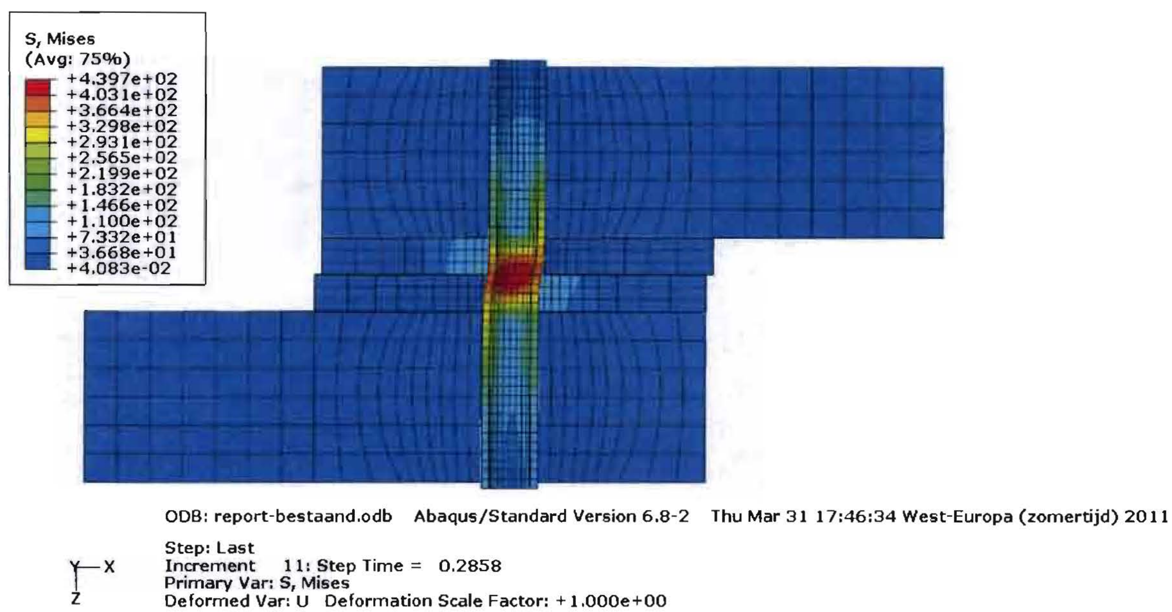

Figure 40: von Mises stress; step time = 0.2858

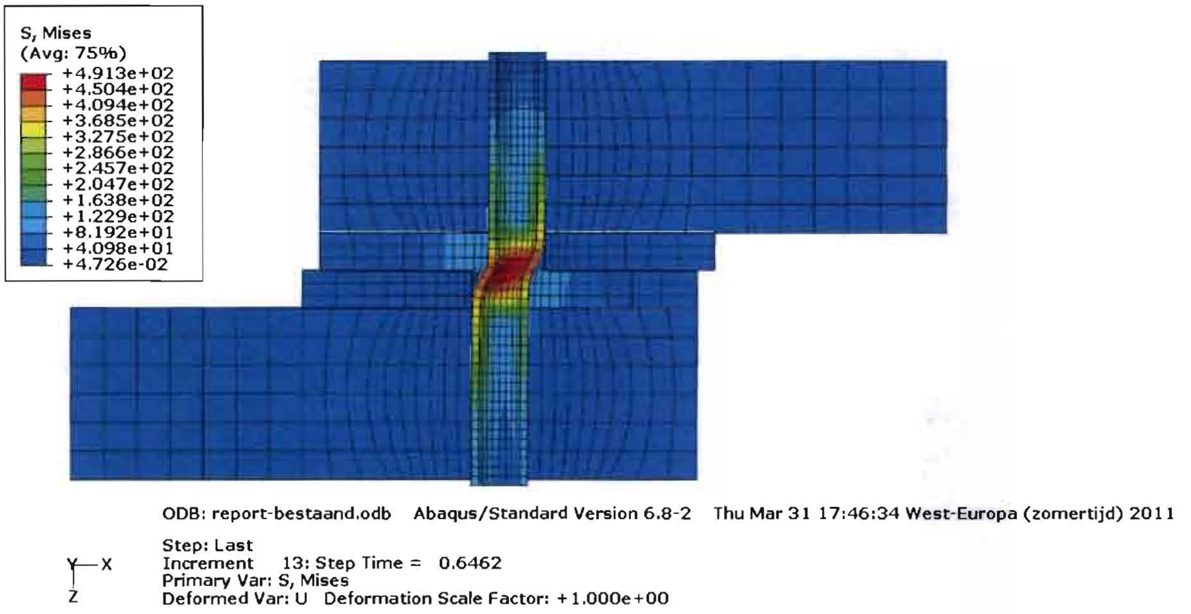

Figure 41: von Mises stress; step time = 0.6462

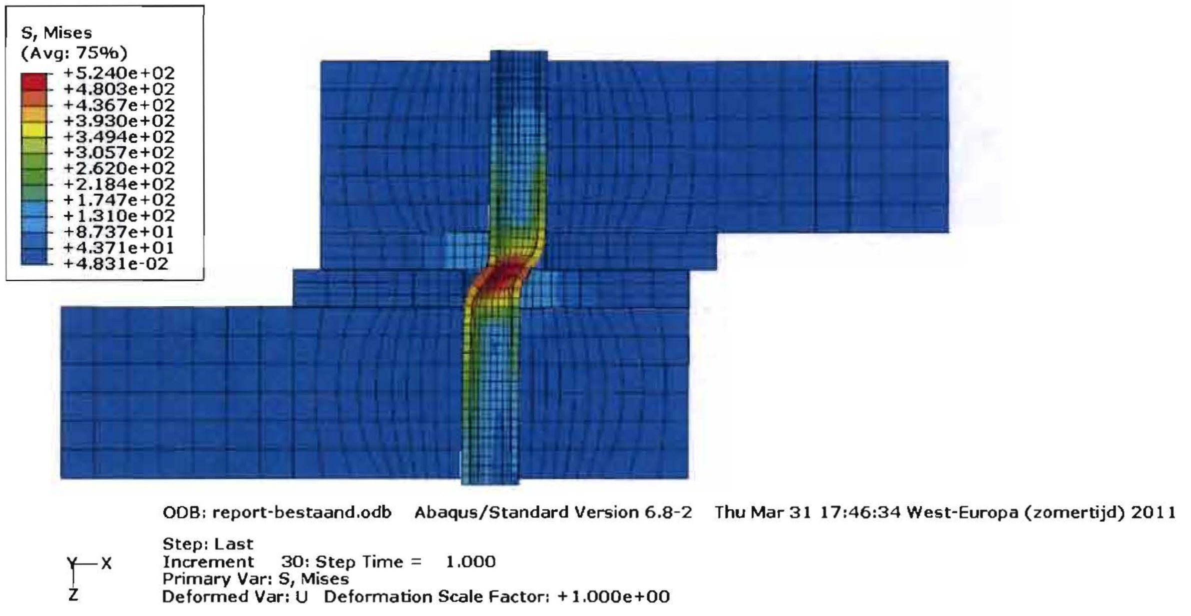

Figure 42: von Mises stress; step time = 1.0000

Appendix 9: Analyses of tube deformation with internal steel plate and 18mm tube

tube diameter (d)	18 mm
displacement at step time = 1.0 ($\delta_{1.0}$)	9 mm
edge/end distance	3.5d
timber thickness (t_{timber})	55 mm
dvw thickness (t_{dvw})	12 mm
adhesive	PU
bond line thickness	0.2 mm

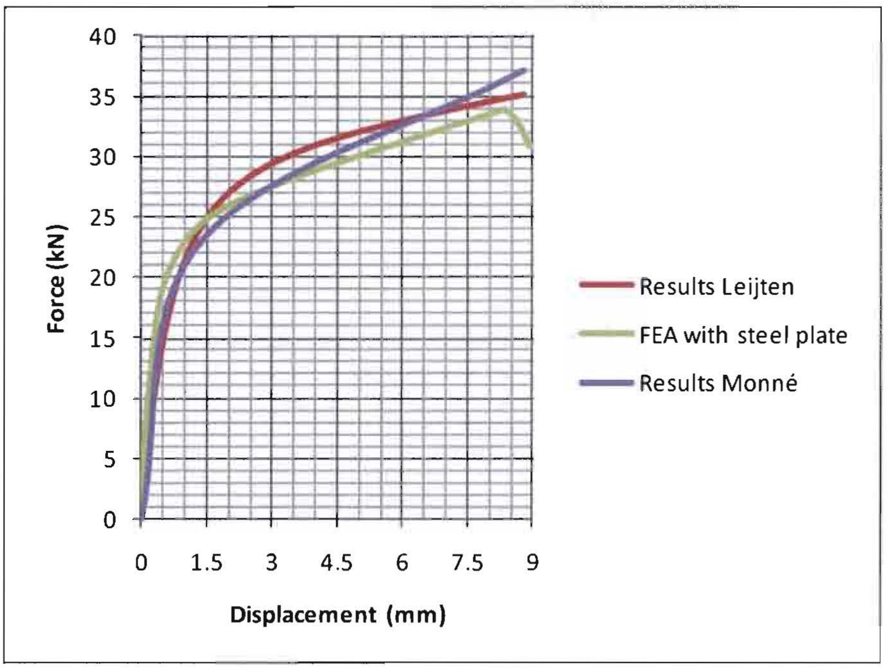

Figure 43: Tube force per shear plane versus displacement of FEA and published test results [1] [3]

Appendix 9 A: Von Mises tube stresses

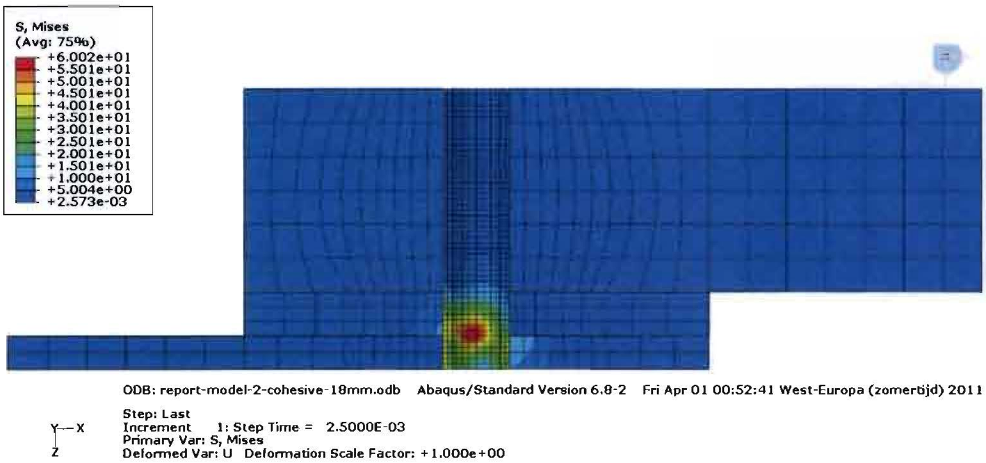

Figure 44: von Mises stress; step time = 0.0025

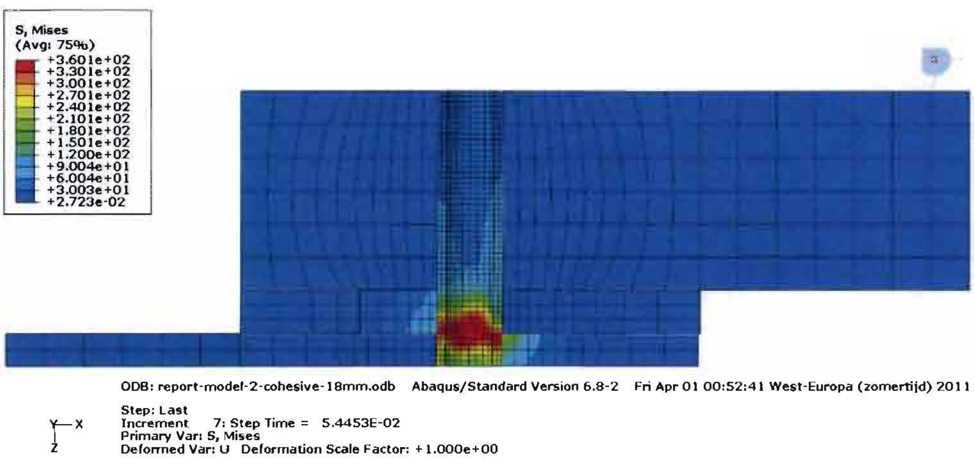

Figure 45: von Mises stress; step time = 0.0544

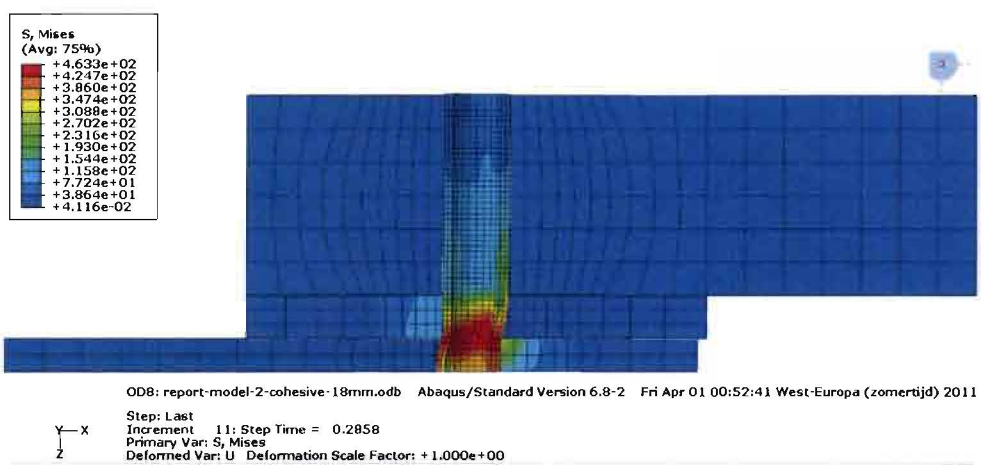

Figure 46: von Mises stress; step time = 0.2858

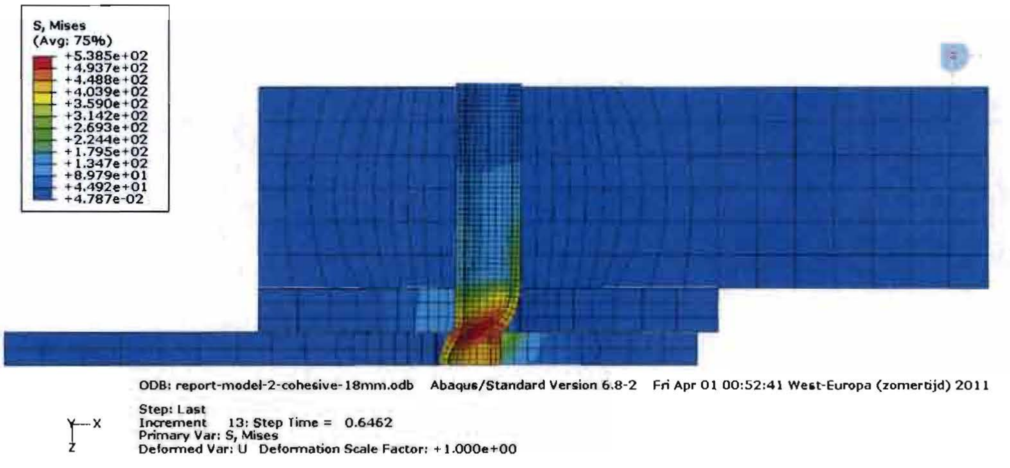

Figure 47: von Mises stress; step time = 0.6462

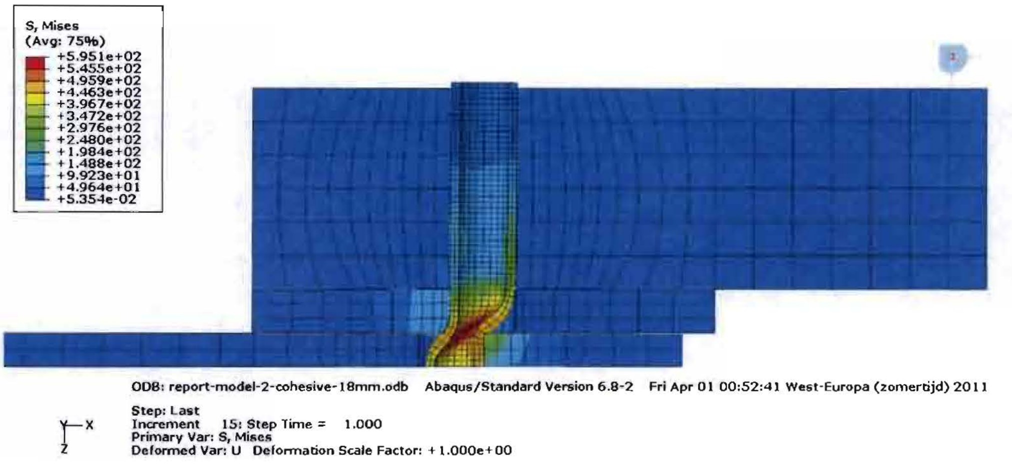

Figure 48: von Mises stress; step time = 1.0000

Appendix 9 B: *Shear stress in bond line near tube*

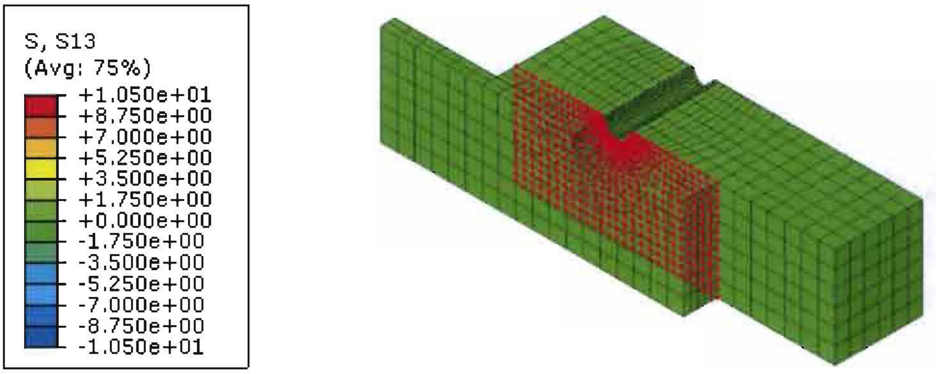

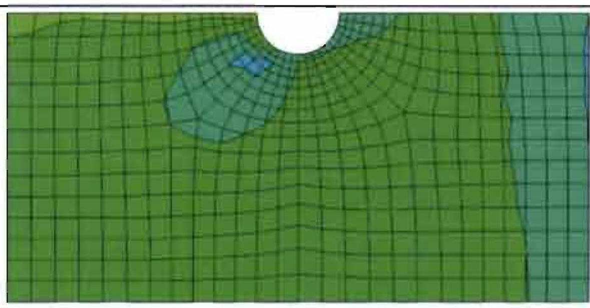

Step time: 0.1256
Diplacement: 1.1304mm

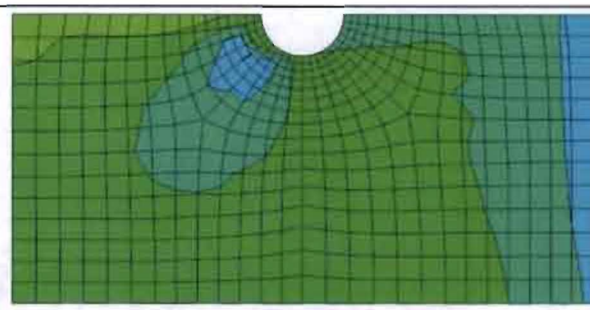

Step time: 0.4300
Diplacement: 3.87mm

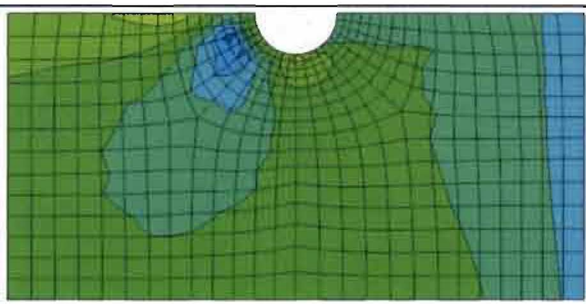

Step time: 0.8625
Diplacement: 7.7625mm

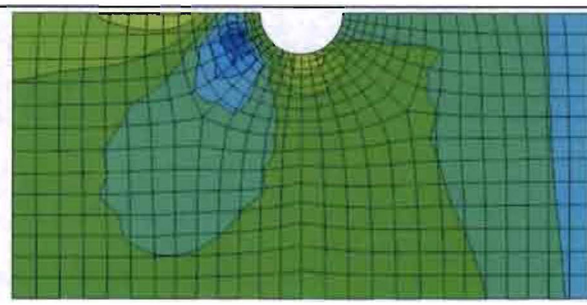

Step time: 1.0000
Diplacement: 9mm

Appendix 10: Applied tube parameters for global models and corresponding results

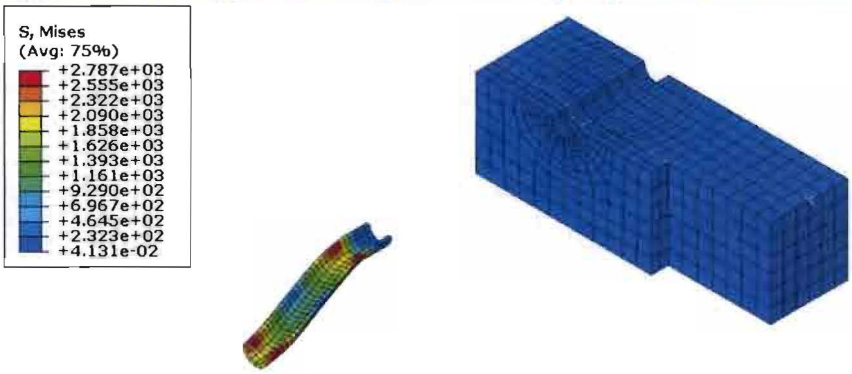

Figure 49: von Mises stresses in the deformed tube for global models

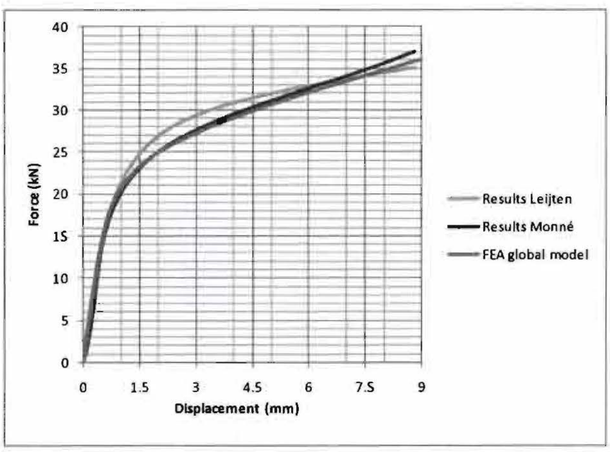

tube diameter (mm)	18
length (mm)	120
modulus of elasticity (N/mm^2)	1100000

yield stress (N/mm^2)	plastic strain (-)
1300	0
1700	0.005
2900	0.05
6500	0.5

Figure 50: Force displacement curve fitted on experimental results and corresponding material properties

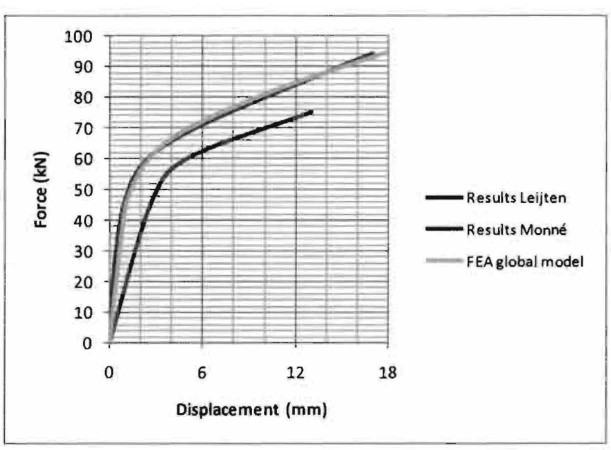

tube diameter (mm)	35
length (mm)	200
modulus of elasticity (N/mm^2)	1100000

yield stress (N/mm^2)	plastic strain (-)
1050	0
1400	0.005
2250	0.05
4500	0.6

Figure 51: Force displacement curve fitted on experimental results and corresponding material properties

Appendix 11: Benchmark for determining suitable size of cohesive elements

This benchmark is performed to determine the suitability of different cohesive element sizes. Figure 52 shows the finite element model used for this benchmark. The dvw plate (thin member) is translated 3.5 mm into the negative x-direction. The timber end (right side) is fixed in the x-direction. Results of different cohesive element sizes of 5 mm, 10 mm and 15 mm are studied. In all three analyses the element size of the adherents is exactly double the element size of the cohesive elements. Figure 53 shows that the results are practically similar for the different element sizes. Figure 54 shows that the energy due to creep dissipation ALLCD exceeds 4% of the total internal energy ALLIE, indicating that these analyses are not reliable from that point. However the shear capacity is already reached when the calculation becomes unreliable. The results of the bond line capacity are therefore reliable.

width of glued surface (mm)	245
height of glued surface (mm)	30
adhesive type	PU
glue thickness	0.2

Table 3: Properties of finite element model

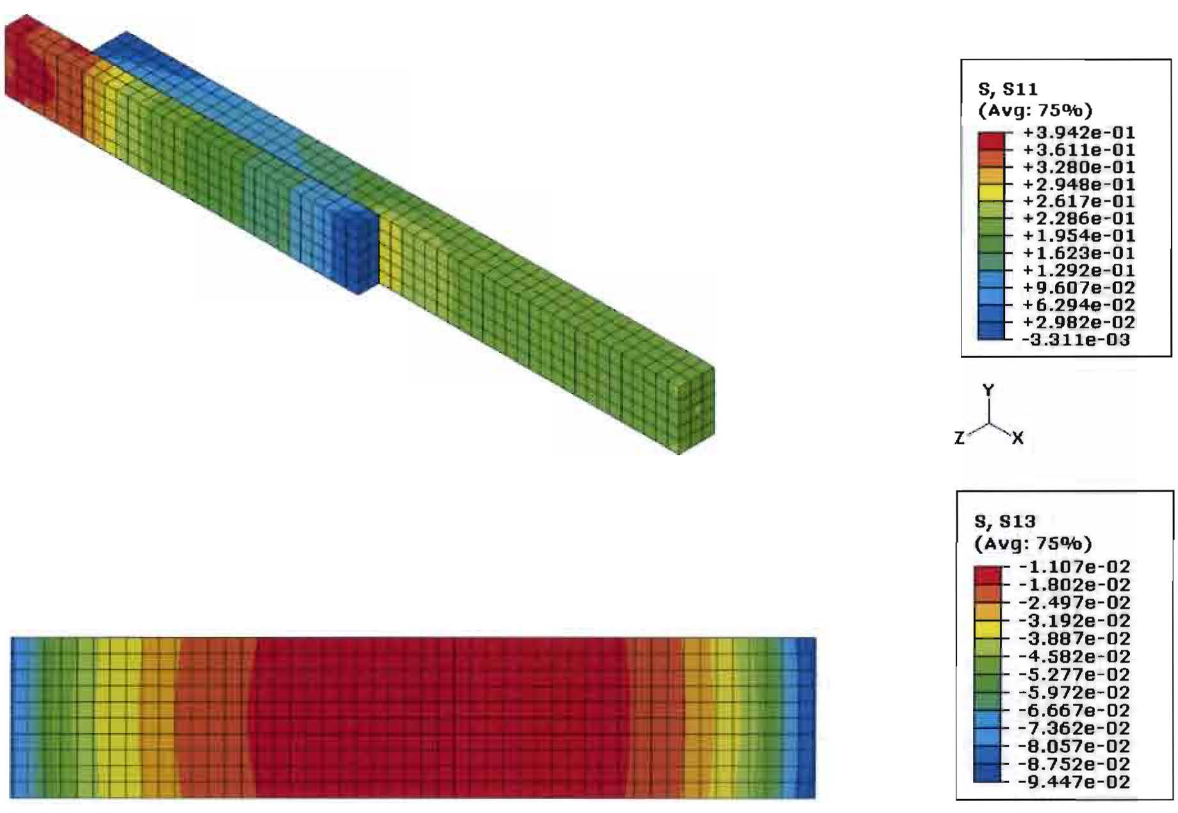

Figure 52: Parallel to grain stress and shear stress parallel to grain in bond line; coh. element size = 5mm; step time = 0.0025

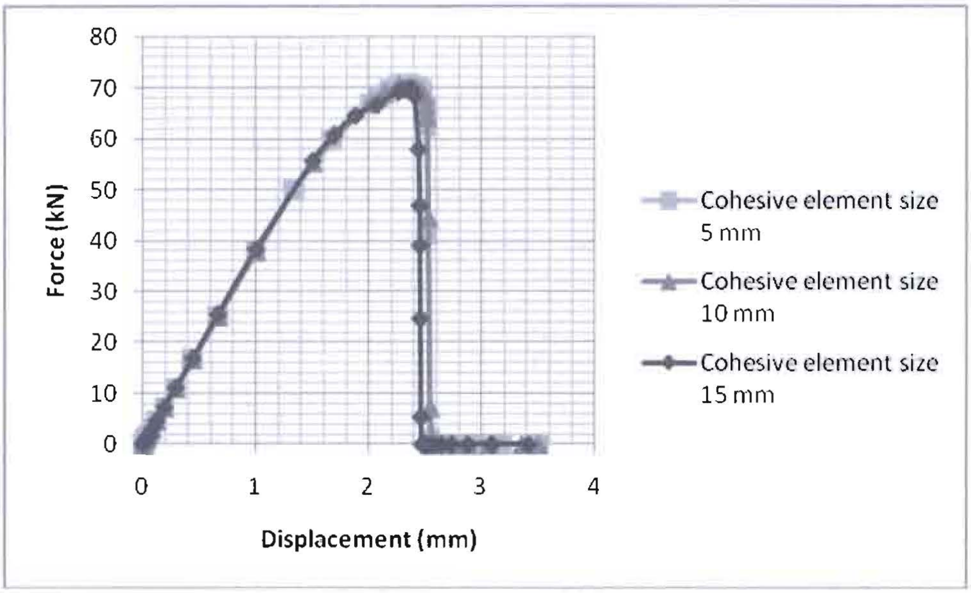

Figure 53: Force displacement curve of benchmark with different cohesive element sizes

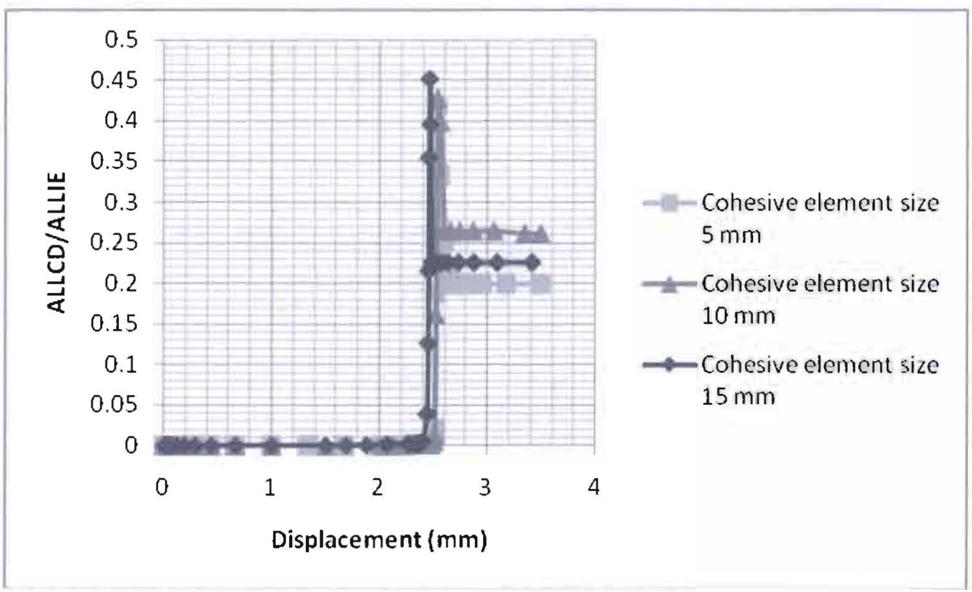

Figure 54: ALLCD/ALLIE of benchmark with different cohesive element sizes

Appendix 12: Photo report of glue process

Figure 55: Measurement of adherent thickness before gluing

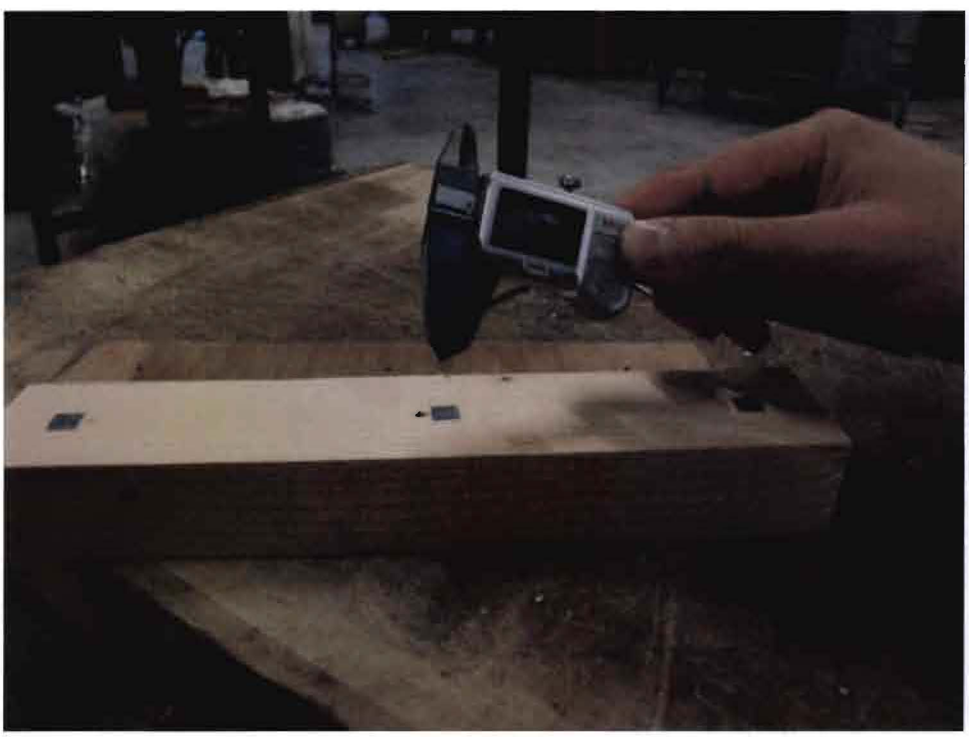

Figure 56: timber member with distance sheets near drill holes

Figure 57: preparation for gluing

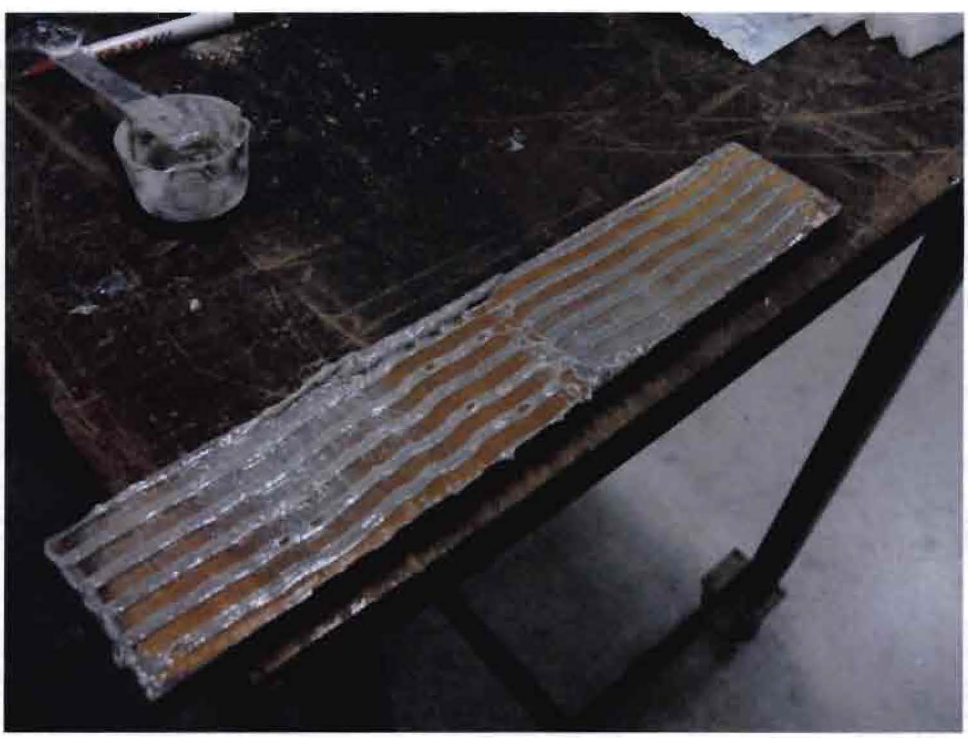

Figure 58: Surface glued by using a comb.

Figure 59: Screws as clamps

Figure 60: measurement of member thickness after gluing

Figure 61: Separation of adherents

Figure 62: Separated adherents after four hours of drying time; 100% of surface is glued

Appendix 13: Photo report of tube assembly

Figure 63 (left): Tube placed over rod that is placed in mold, tempex placed as support

Figure 64 (right): Tape the lower ring to prevent it from falling on the mold

Figure 65 (left): Placement of members to connect on top of the tempex

Figure 66 (right): Placement of upper steel ring

Figure 67 (left): Placement of upper mold

Figure 68 (right): Placement of upper mold base

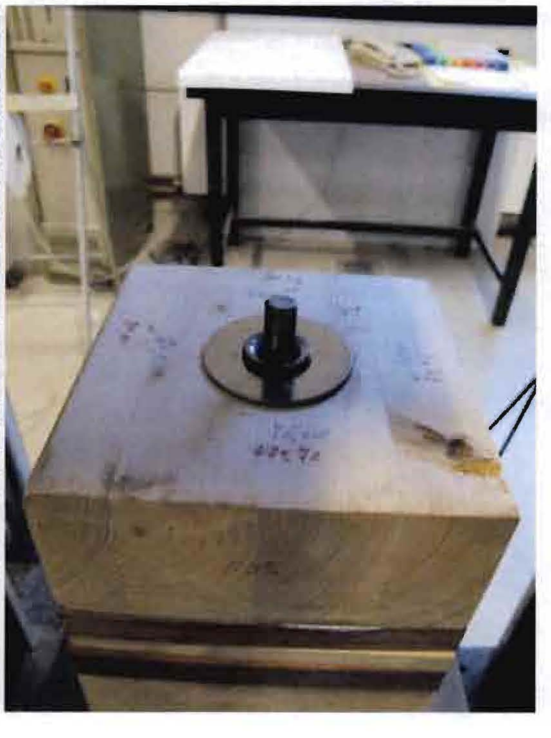

Figure 69 (left): Expanding of the tube

Figure 70 (right): Deformed tube end

Appendix 14: Photo report of tube assembly with portable hydraulic jack

Figure 71: Placement of the tube and upper ring

Figure 72: Placement of lower ring

Figure 73: Placement of upper mold and (high capacity) threated rod and nut

Figure 74: Placement of foam as distance holder

Figure 75: Placement of lower mold and nut

Figure 76: Placement portable hydraulic jack

Figure 77: Placement of nut for fastening the rod to the hydraulic jack

Figure 78: Placement of protection to prevent launching of the rod due to rod failure

Figure 79: T.J.van de Loo increasing the tensile force up to 85-90kN (for 18mm tubes)

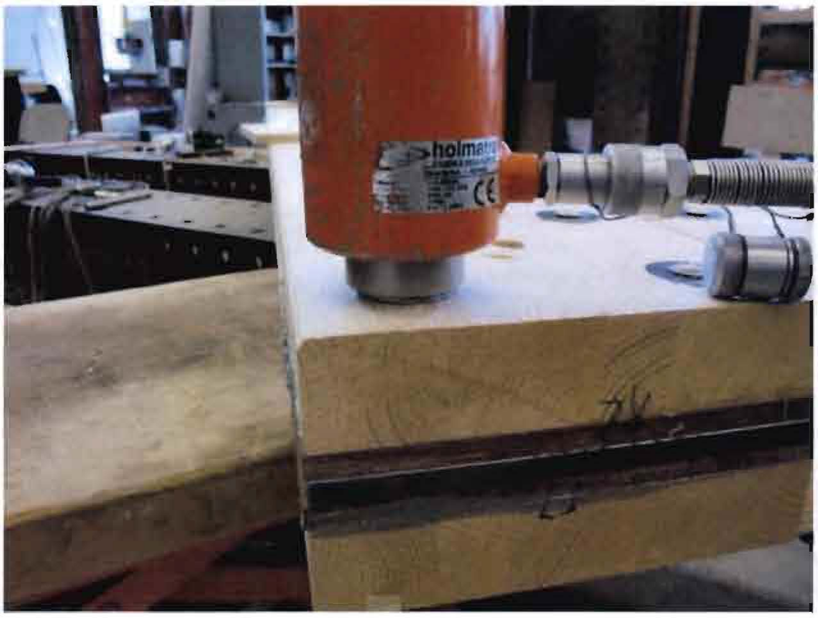

Figure 80: Removal of distance foam when hydraulic jack starts to move down

Figure 81: End of loading process followed by disassembly

Appendix 15: Results of tests of straight connection

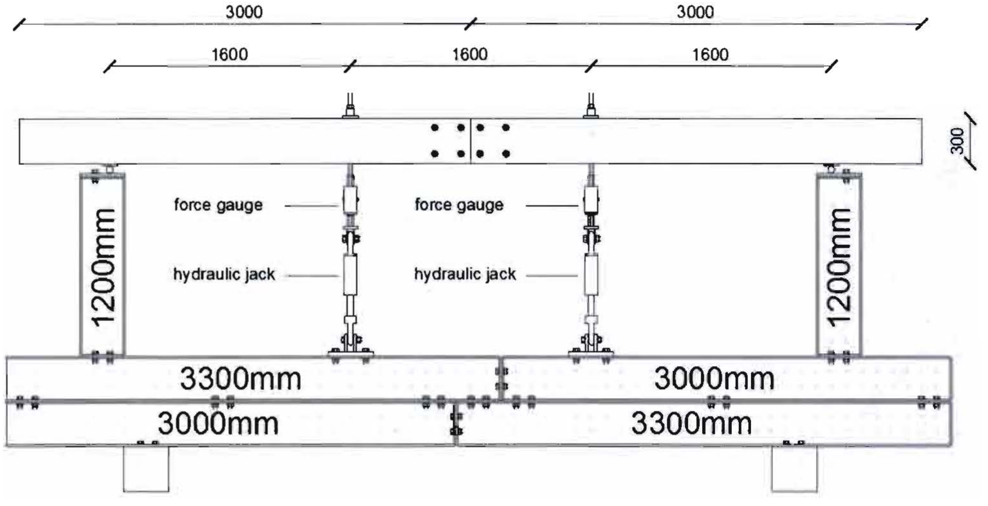

Figure 82: Set-up of four point bending test

timber beam height	300 mm
timber beam thickness	60 mm
dvw thickness	12 mm
steel thickness	15 mm
adhesive type	Poly-Urethane (DuoCol)
glue line thickness	0,4mm - 0,5mm

Appendix 15 A: sample 0-1

Ultimate bending moment	40.374 kNm
Rotation at ultimate load	0.92 rad
K_s	1601 kNm/rad (see comment)
K_i	1835 kNm/rad (see comment)
K_e	5443 kNm/rad (see comment)
Initial gap width (compressed side)	1mm<t_s<1.5mm
Type of failure	tube failure
Comments	• Connection was not supported in out-of-plane direction. The timber members were rotating out of plane. Test is paused and continued with support.

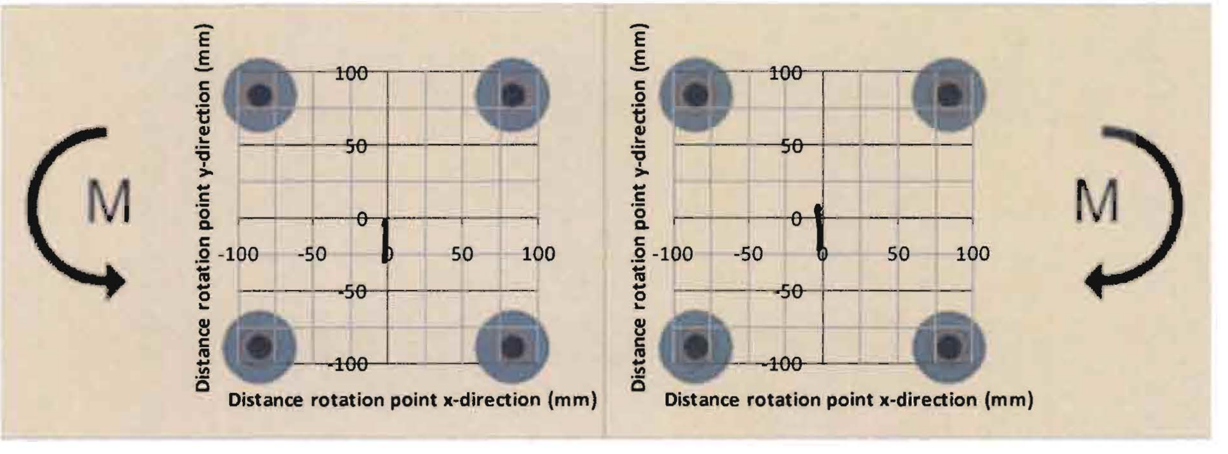

Figure 83: Measured path of rotation point (sample 0-1)

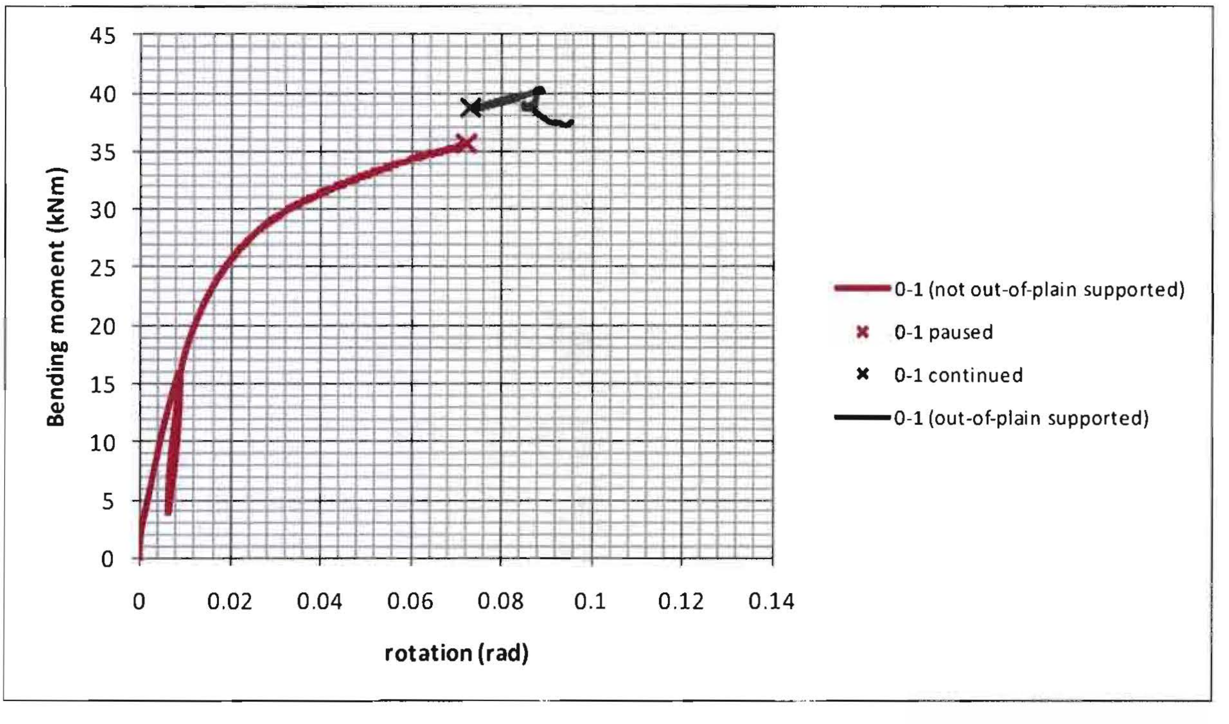

Figure 84: Bending moment versus rotation (sample 0-1); red: without out-of-plain support; grey: with out-of-plain support

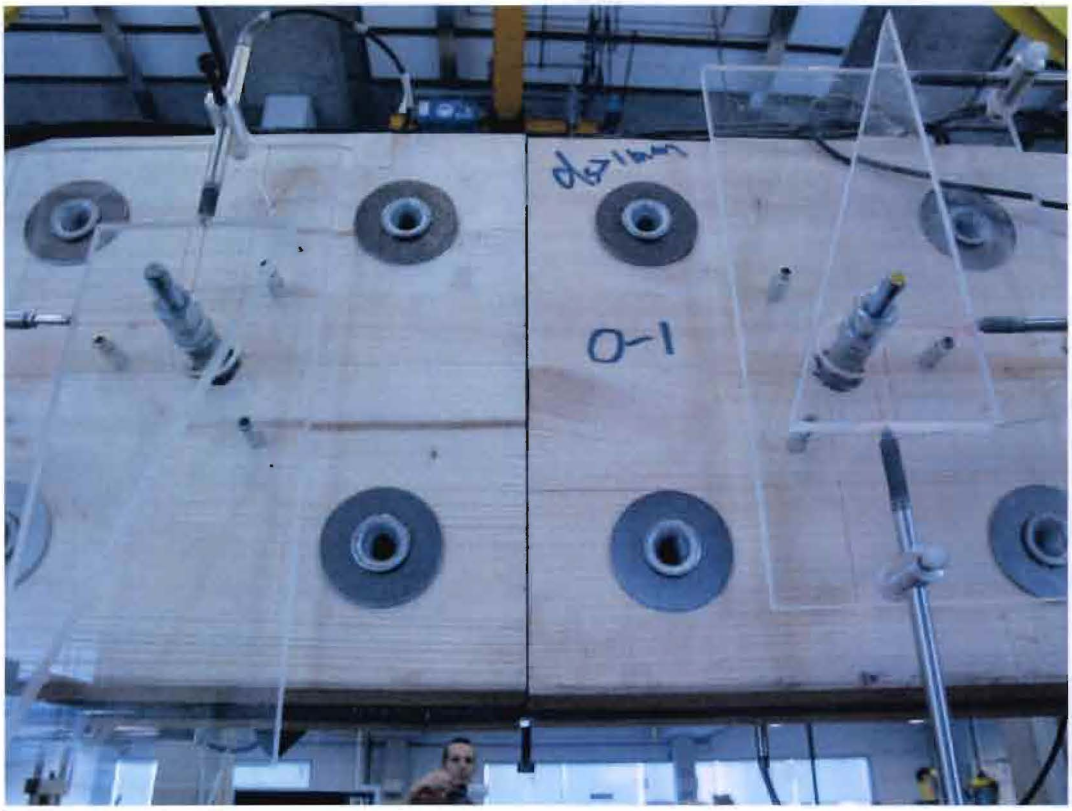

Figure 85: Close-up of initial gap (sample 0-1)

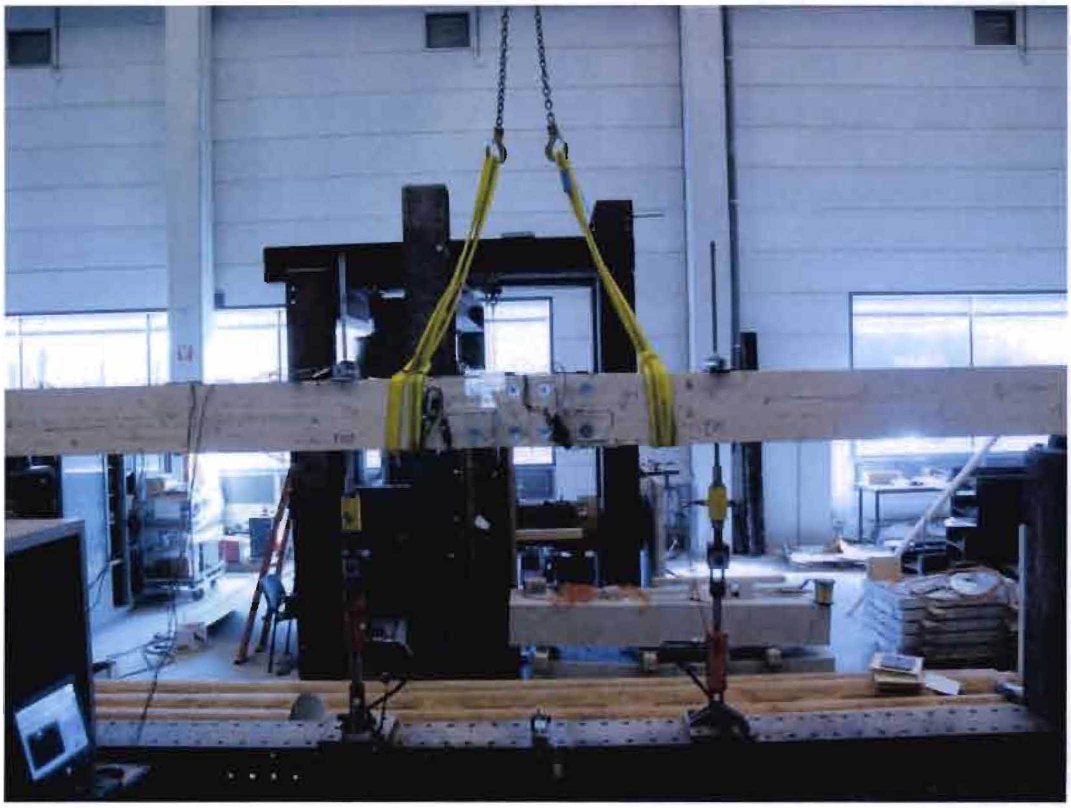

Figure 86: Set-up without out-of-plane support before force initiation (sample 0-1)

Figure 87: Test set-up with out-of-plane support before continuation (sample 0-1)

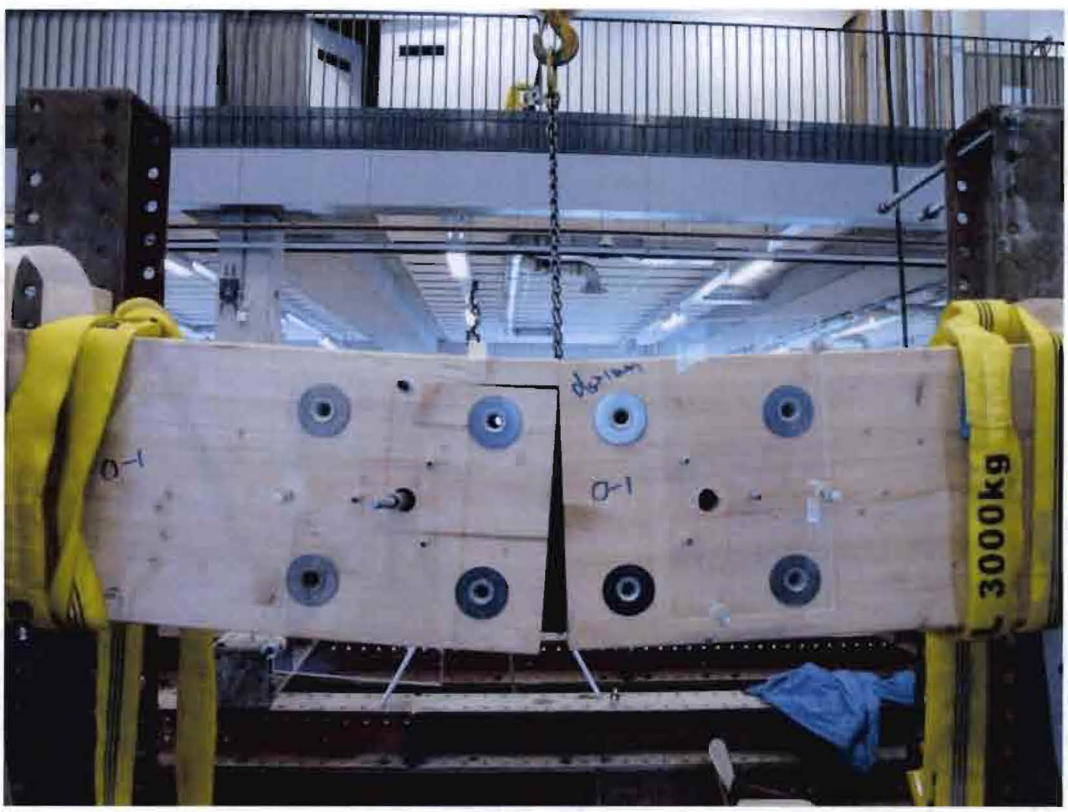

Figure 88: Failed connection due to tube failure (sample 0-1)

Appendix 15 B: sample 0-2

Ultimate bending moment	41.059 kNm
Rotation at ultimate load	0.095 rad
K_s	2270 kNm/rad
K_i	2597 kNm/rad
K_e	7828 kNm/rad
Initial gap width (compressed side)	t_s≈1mm
Type of failure	tube failure
Comments	-

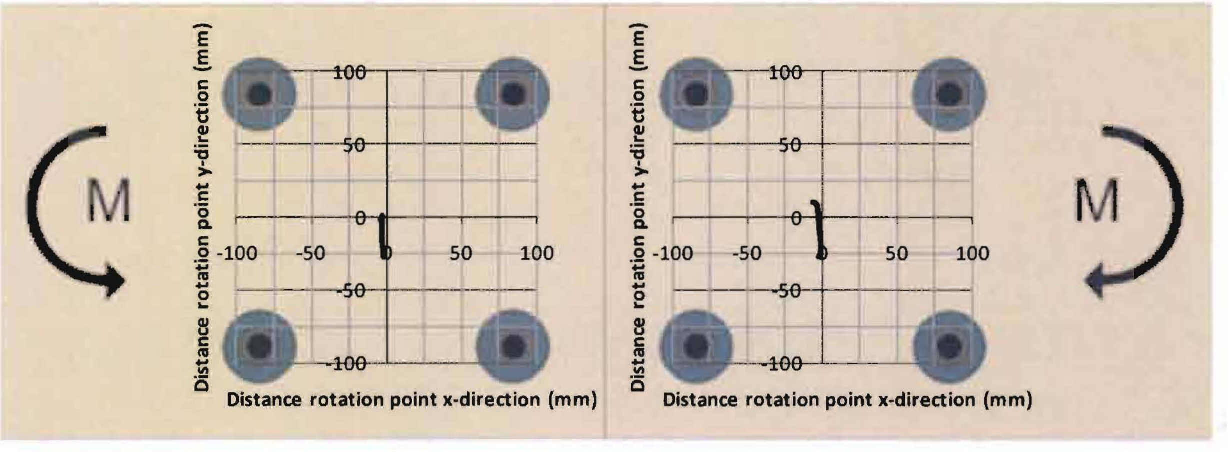

Figure 89: Measured path of rotation point (sample 0-2)

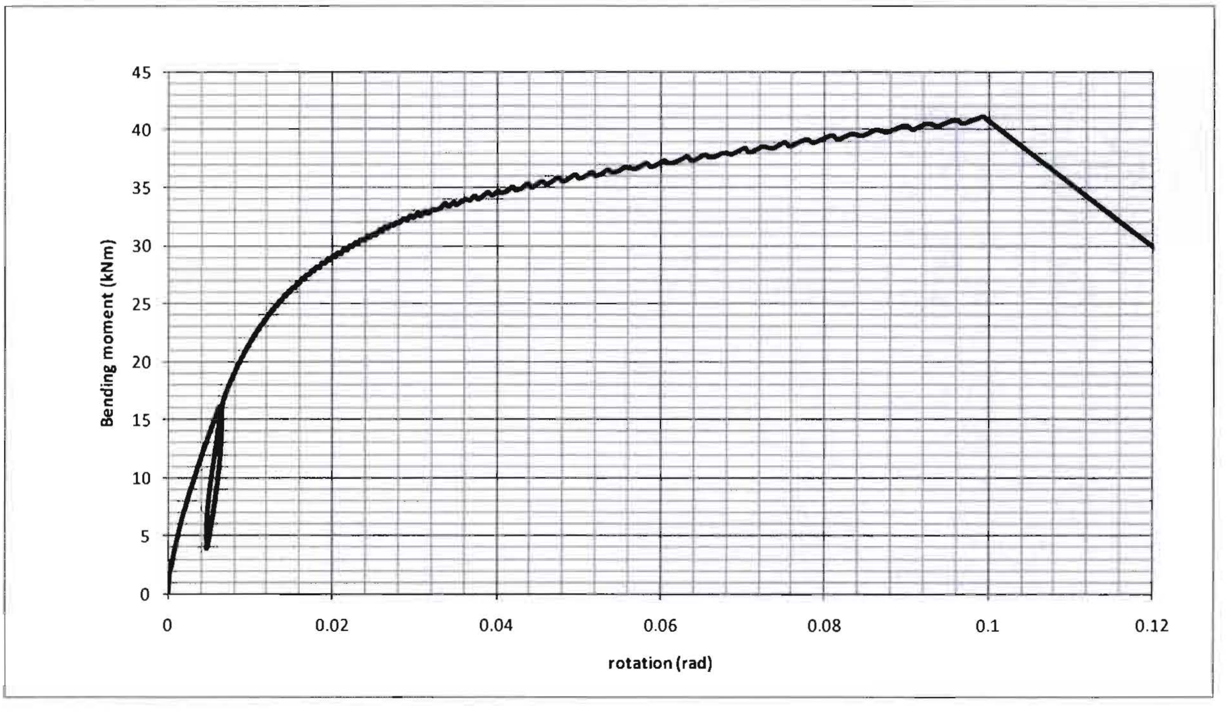

Figure 90: Bending moment versus rotation (sample 0-2)

Figure 91: Close-up of connection before load initiation (sample 0-2)

Figure 92: Test set-up (sample 0-2)

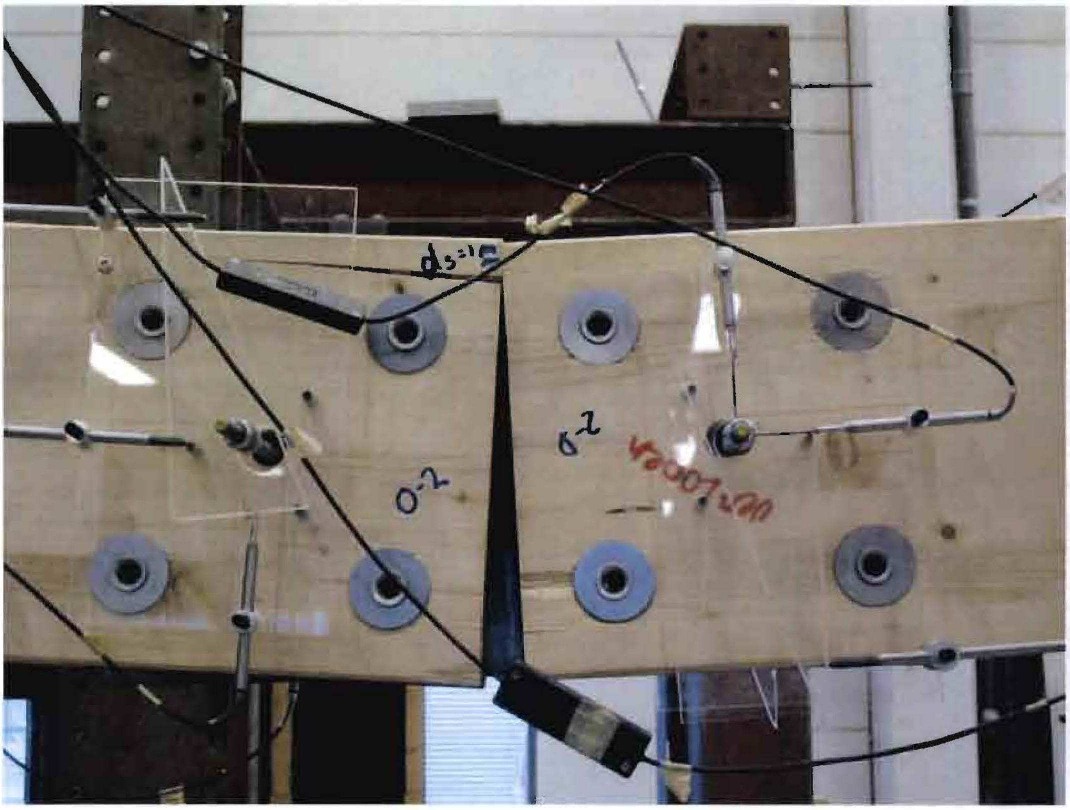

Figure 93: Failed connection (sample 0-2)

Appendix 15 C: sample 0-3

Ultimate bending moment	40.663 kNm
Rotation at ultimate load	0.130 rad
K_s	2258 kNm/rad
K_i	2695 kNm/rad
K_e	7278 kNm/rad
Initial gap width (compressed side)	$t_s \approx 1mm$
Type of failure	tube failure
Comments	-

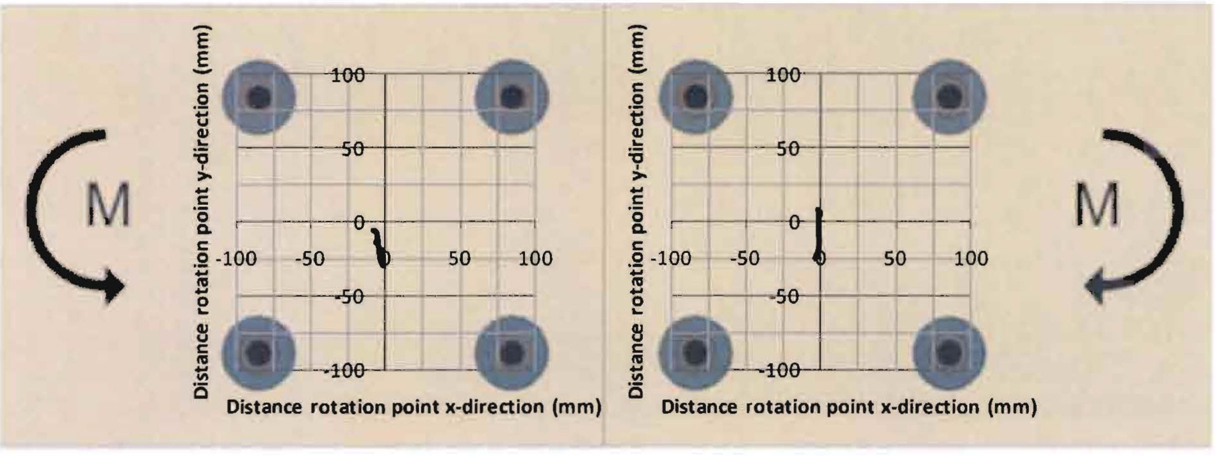

Figure 94: Measured path of rotation point (sample 0-3)

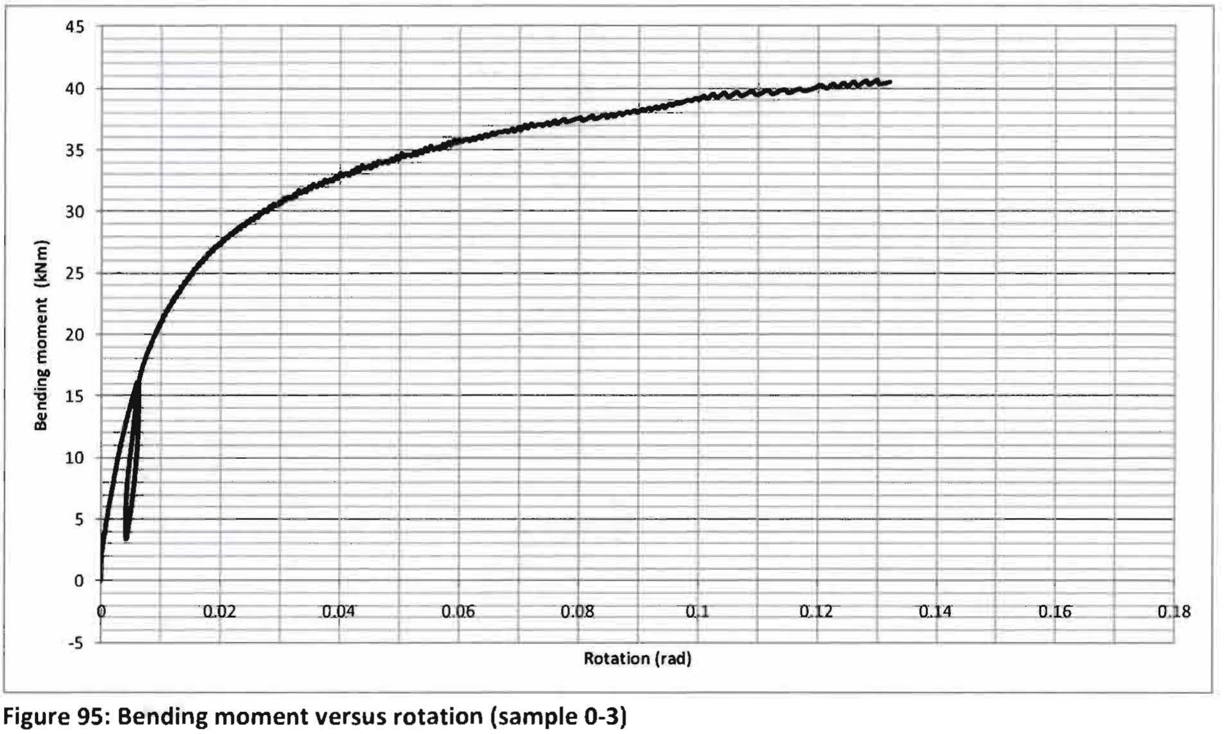

Figure 95: Bending moment versus rotation (sample 0-3)

Figure 96: Compressed zone due to gap closure (sample 0-3)

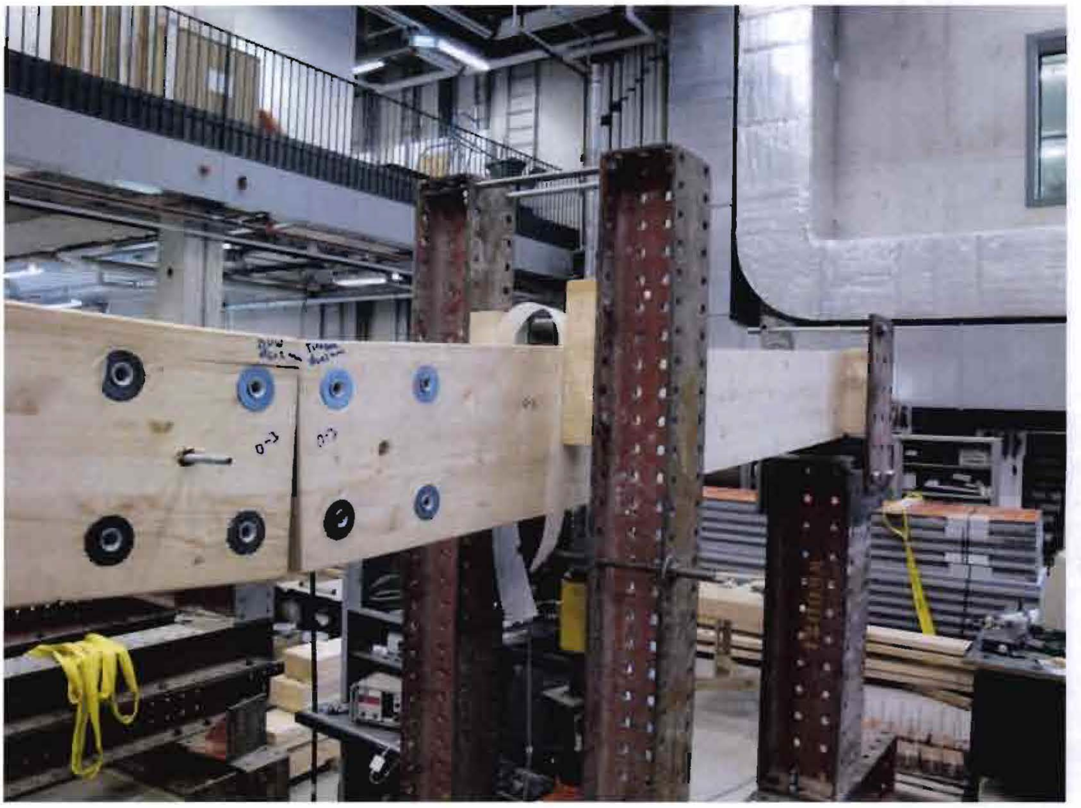

Figure 97: Negligible friction of out-of-plane support due to teflon sheets (sample 0-3)

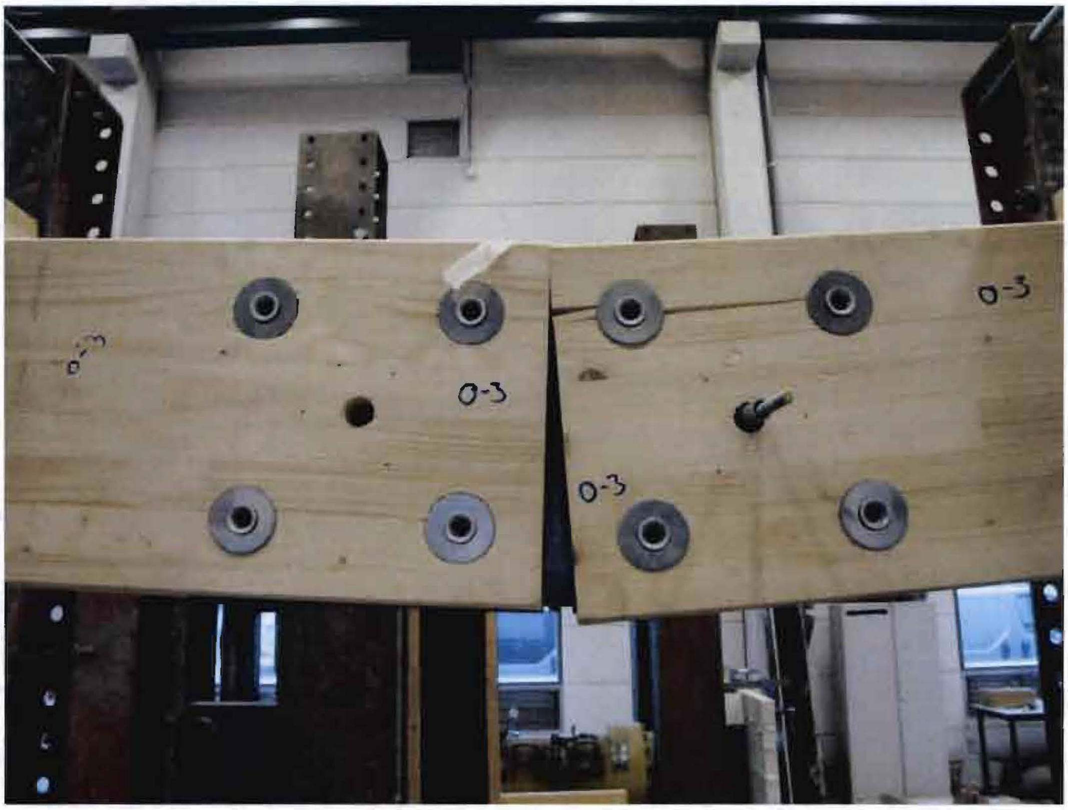

Figure 98: Failed connection (sample 0-3)

Appendix 16: Results of tests of angled connection

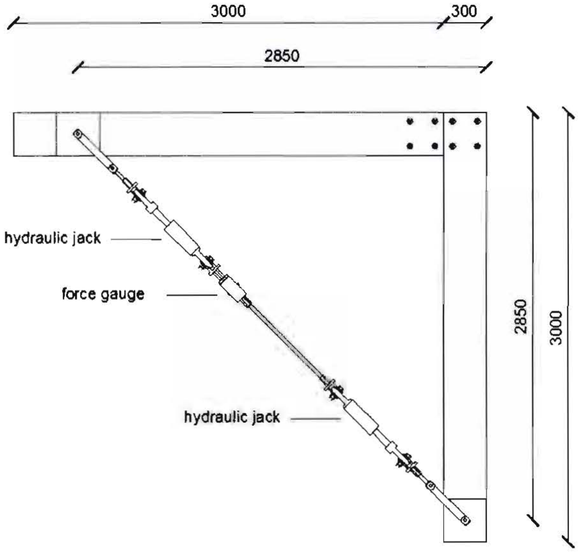

Figure 99: Set-up of test of angled connection

timber beam height	300 mm
timber beam thickness	60 mm
dvw thickness	12 mm
steel thickness	15 mm
adhesive type	Poly-Urethane (DuoCol)
glue line thickness	0,4mm - 0,5mm

Appendix 16 A: sample 90-1

Ultimate bending moment	33.052
Rotation at ultimate load	0.067 rad
K_s	985 kNm/rad
K_i	996 kNm/rad
K_e	3822 kNm/rad
Initial gap width (compressed side)	$t_s \approx 0mm$
Type of failure	timber failure
Comments	10% overlength and only a tube compression of 60 kN applied

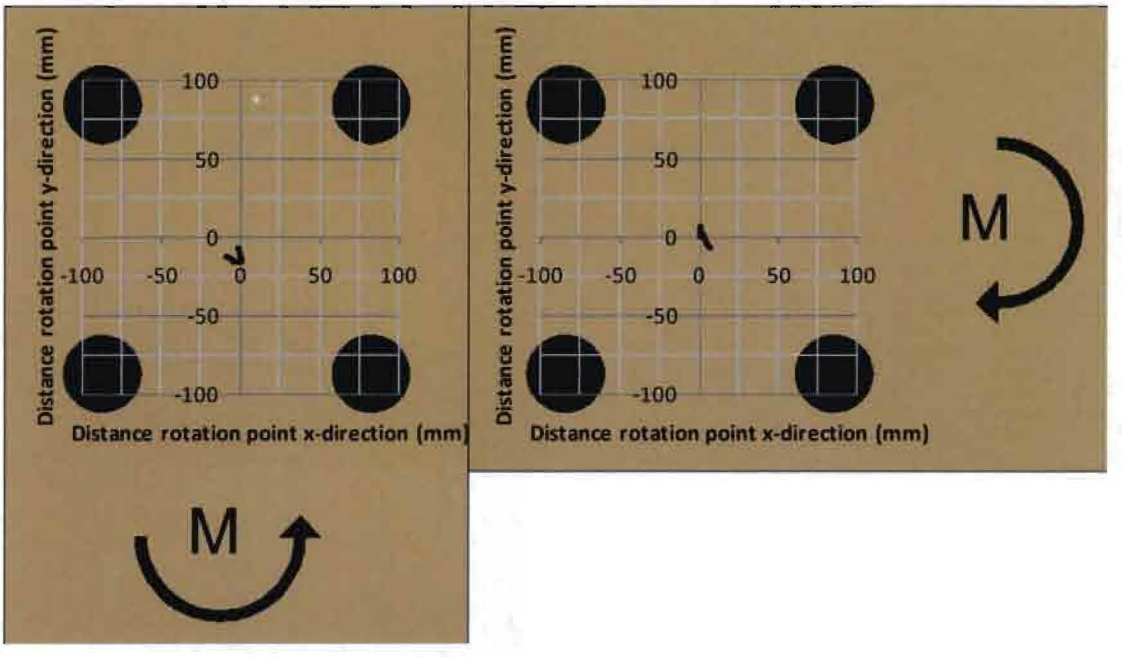

Figure 100: Measured path of rotation point (sample 90-1)

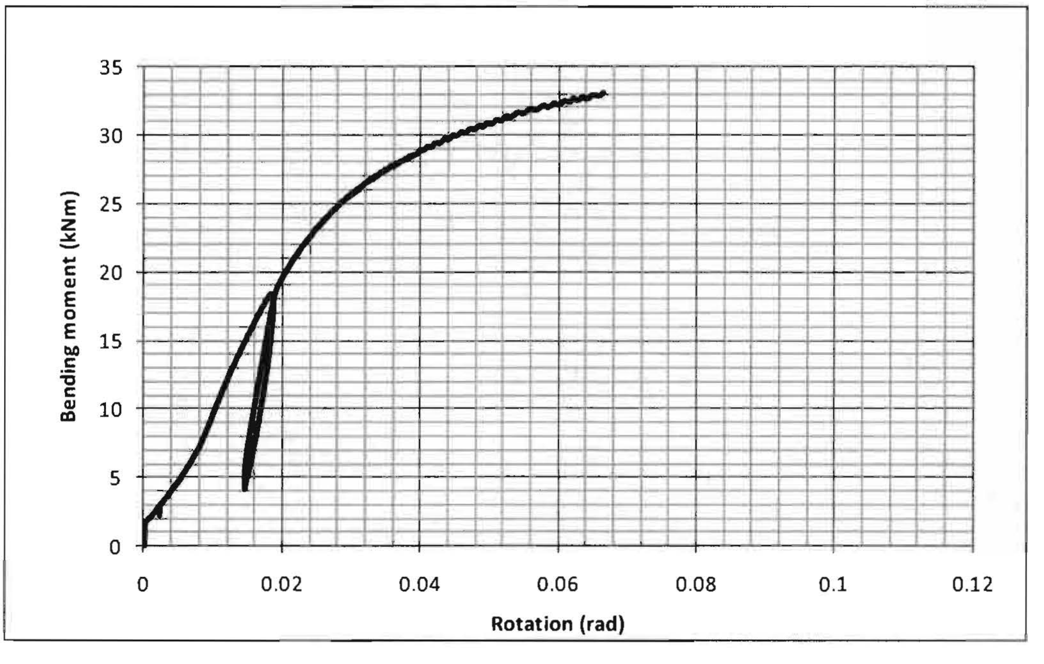

Figure 101: Bending moment versus rotation (sample 90-1)

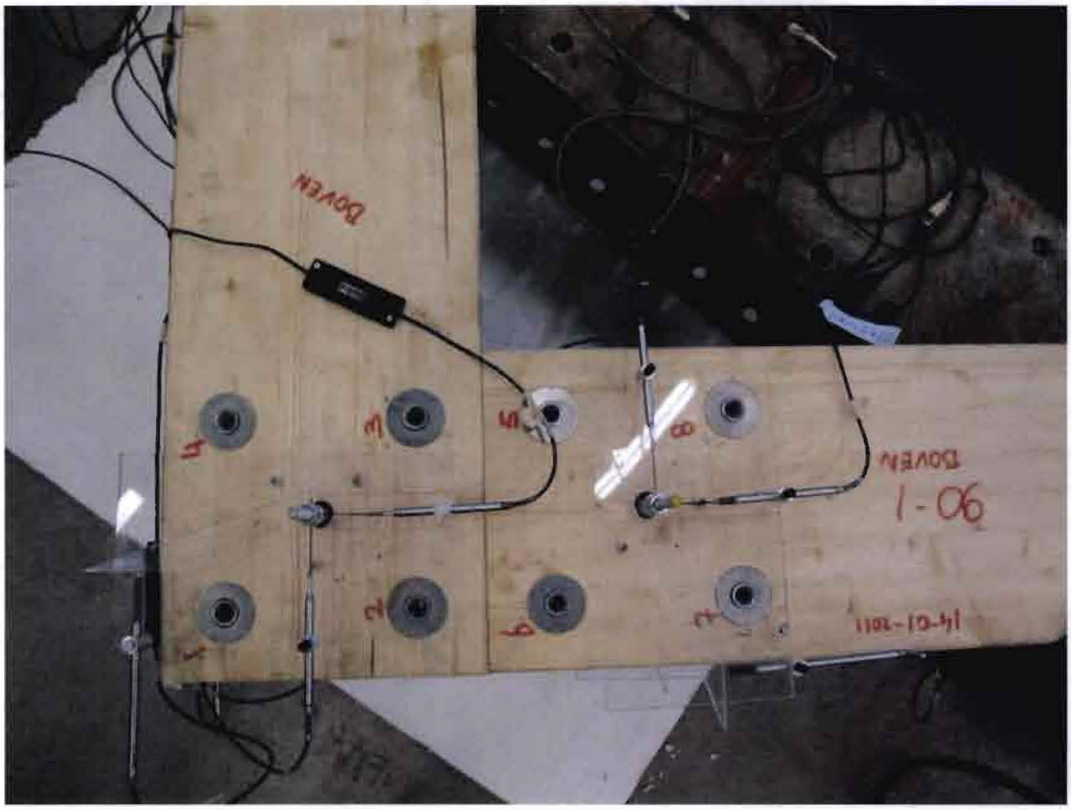

Figure 102: Close-up of connection before load initiation (sample 90-1)

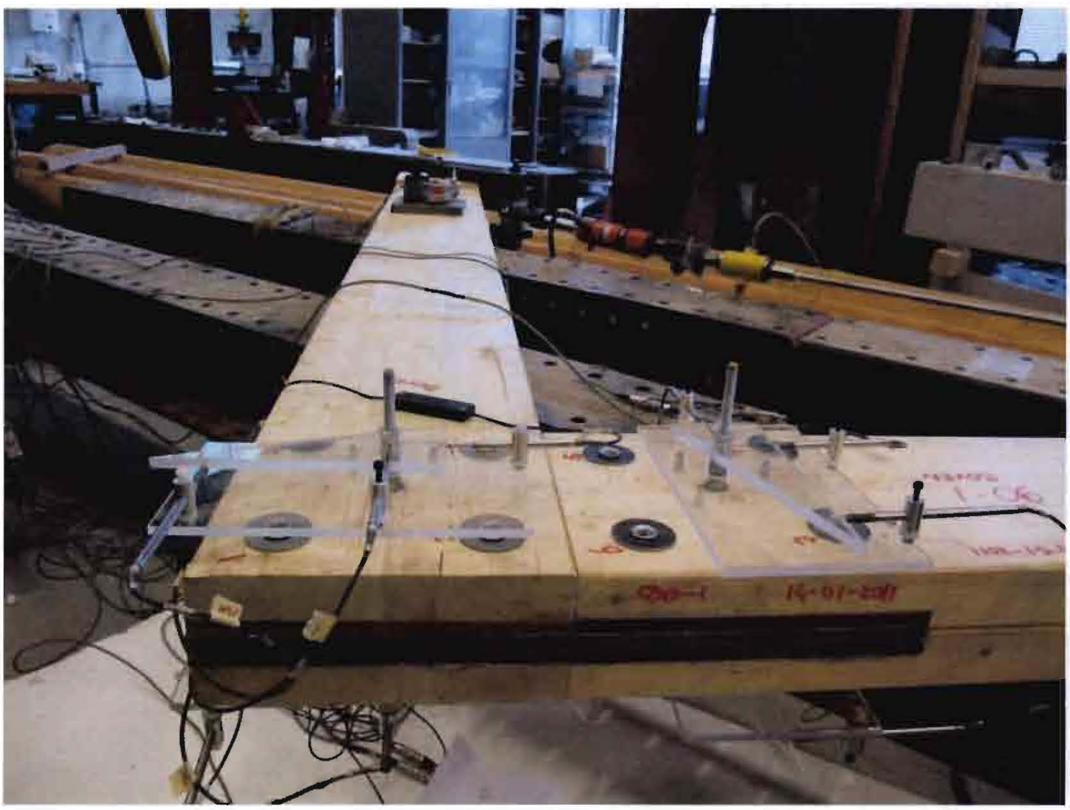

Figure 103: Close-up of connection before load initiation (sample 90-1)

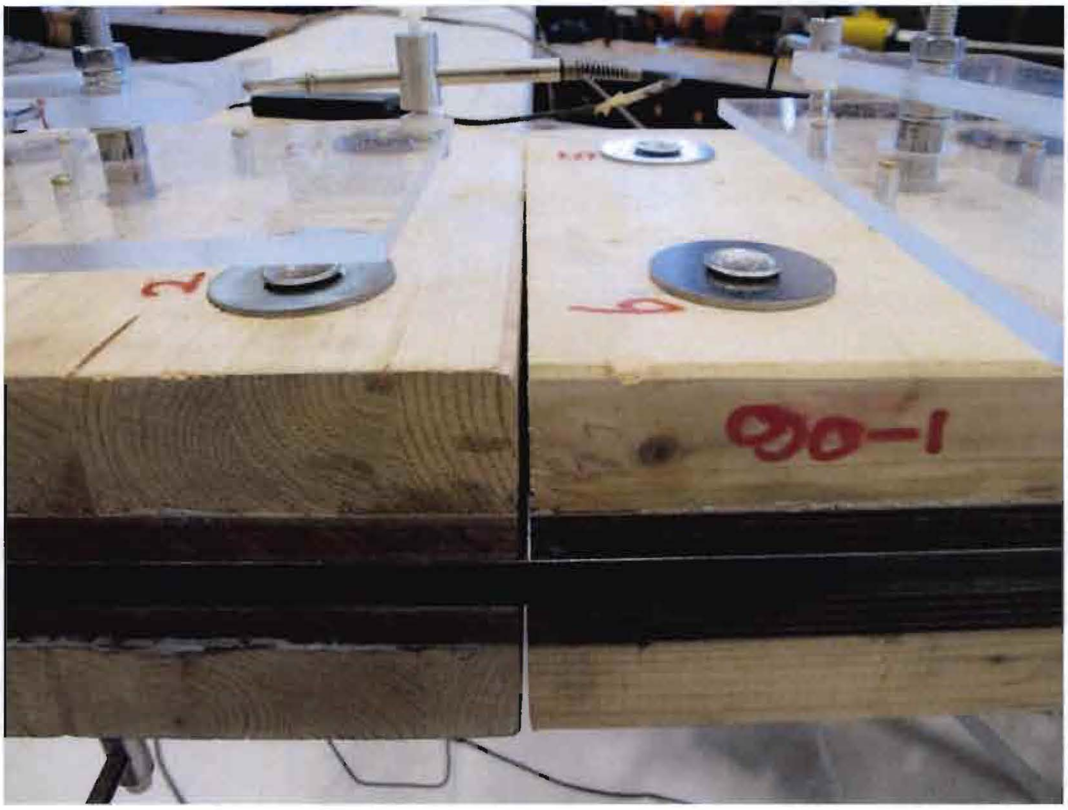

Figure 104: Gap after a small deformation (sample 90-1)

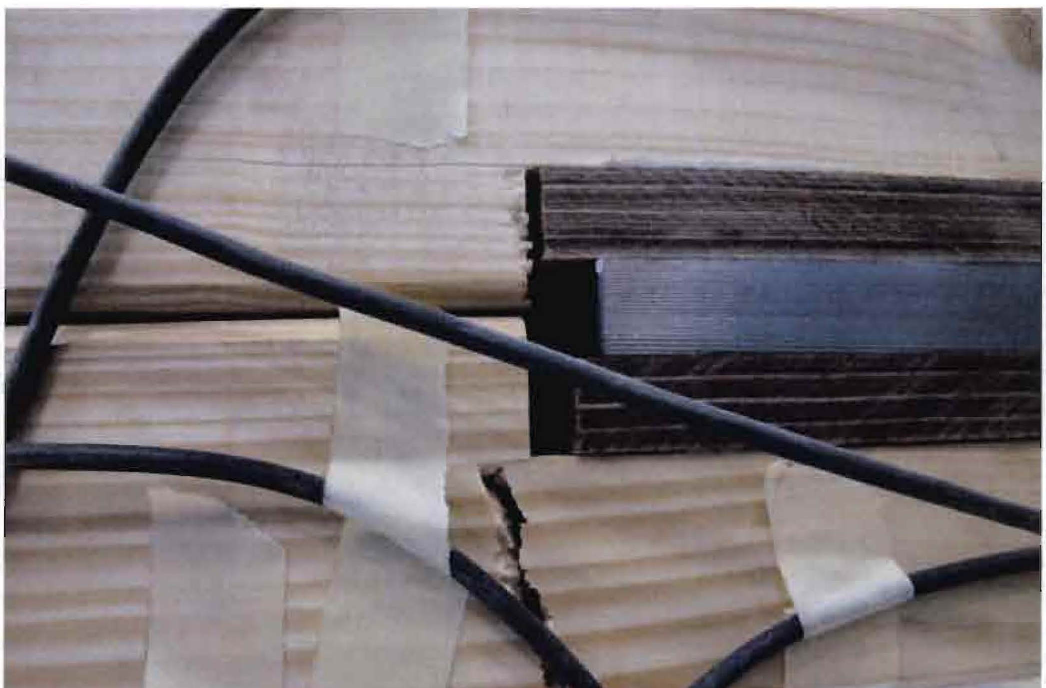

Figure 105: Timber failure of lower beam (sample 90-1)

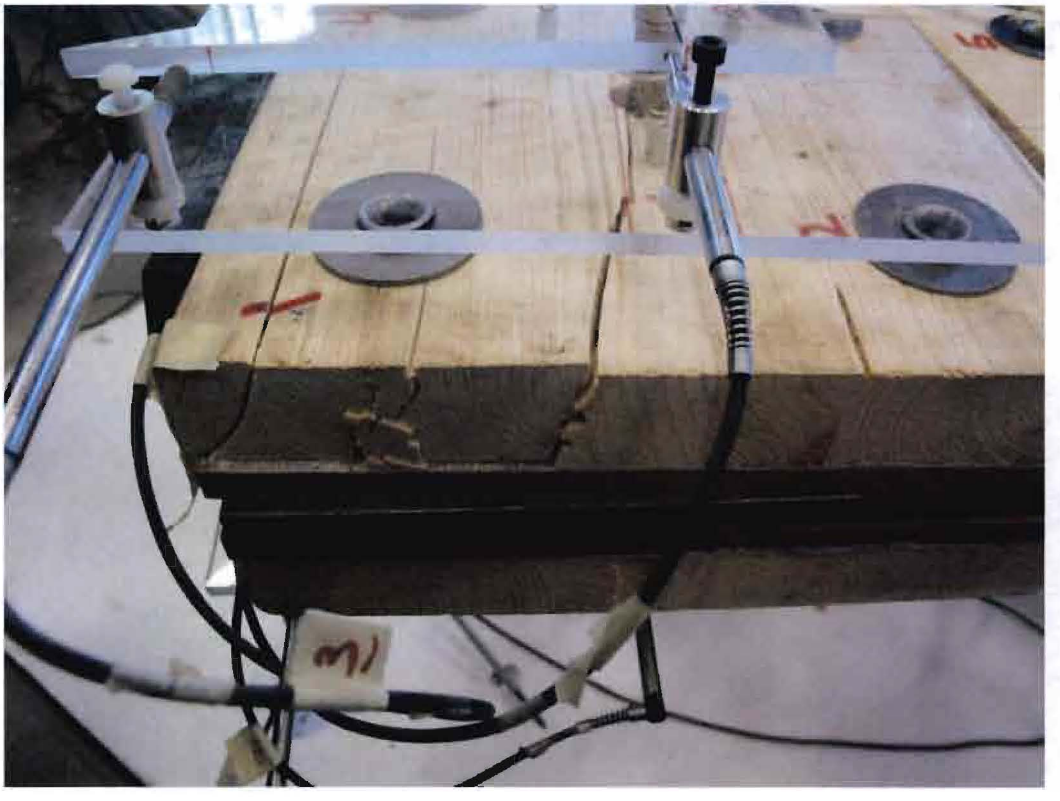

Figure 106: Timber failure and bond line failure of upper beam during continuation after first timber fracture (sample 90-1)

Appendix 16 B: sample 90-2

Ultimate bending moment	34.006
Rotation at ultimate load	0.099 rad
K_s	1843 kNm/rad
K_i	2107 kNm/rad
K_e	4073 kNm/rad
Initial gap width (compressed side)	$t_s \approx 1mm$
Type of failure	bond line failure
Comments	adhesive failed (insufficient amount of glue applied)

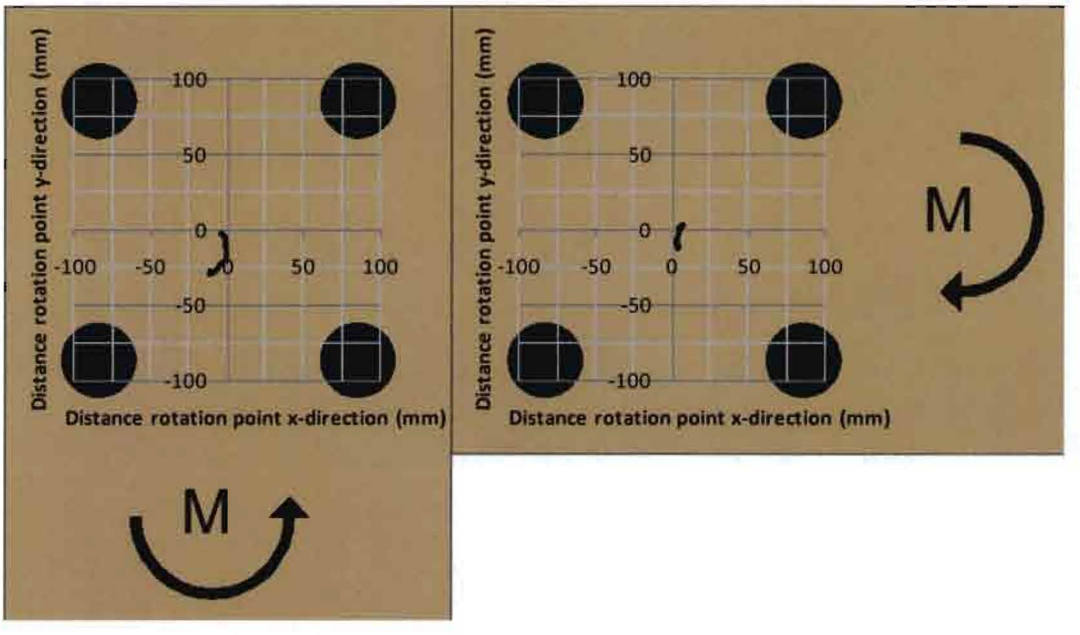

Figure 107: Measured path of rotation point (sample 90-2)

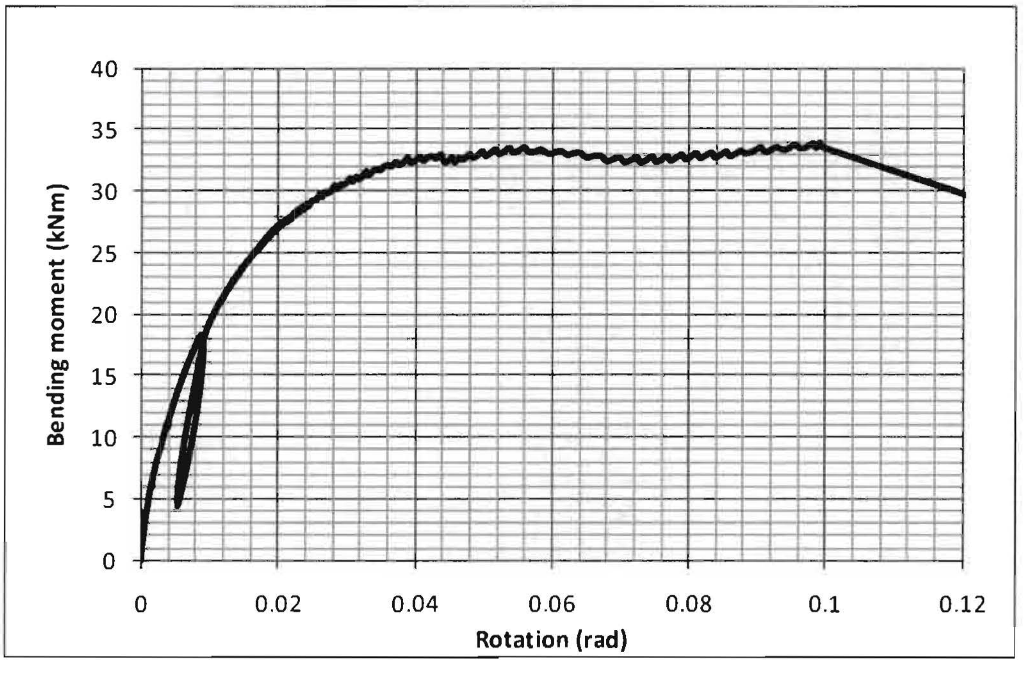

Figure 108: Bending moment versus rotation (sample 90-1)

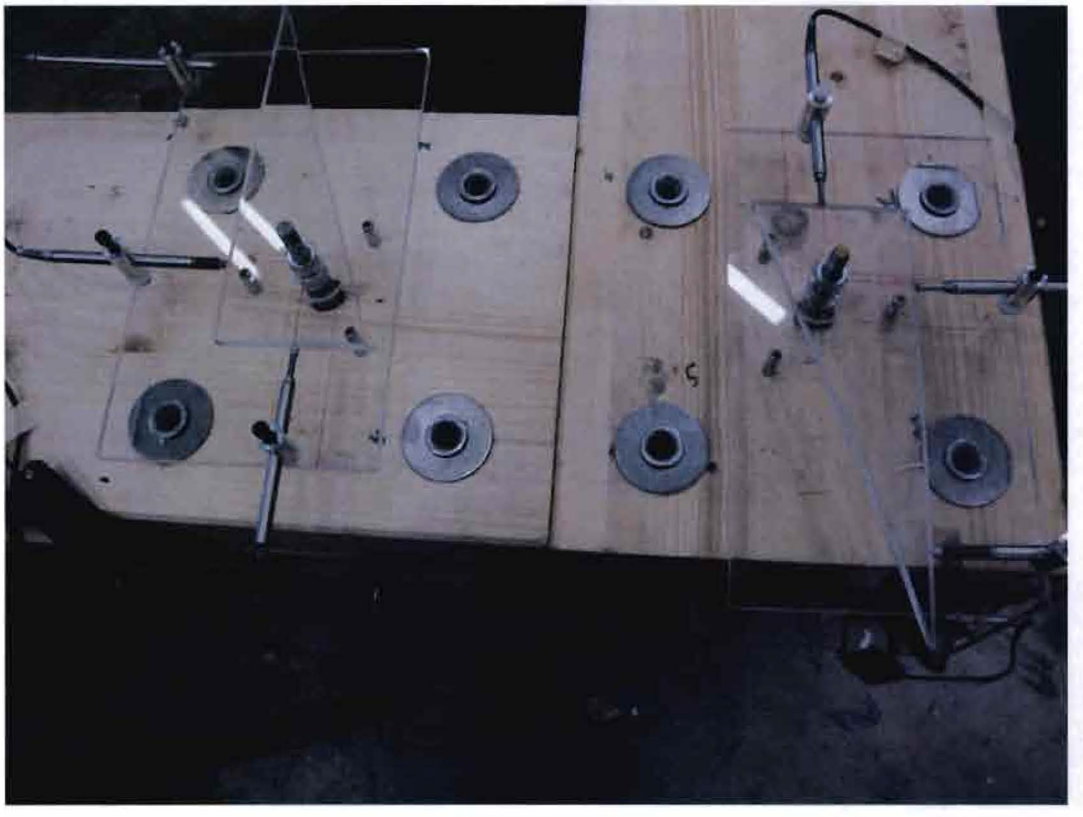

Figure 109: Connection before force initiation (sample 90-2)

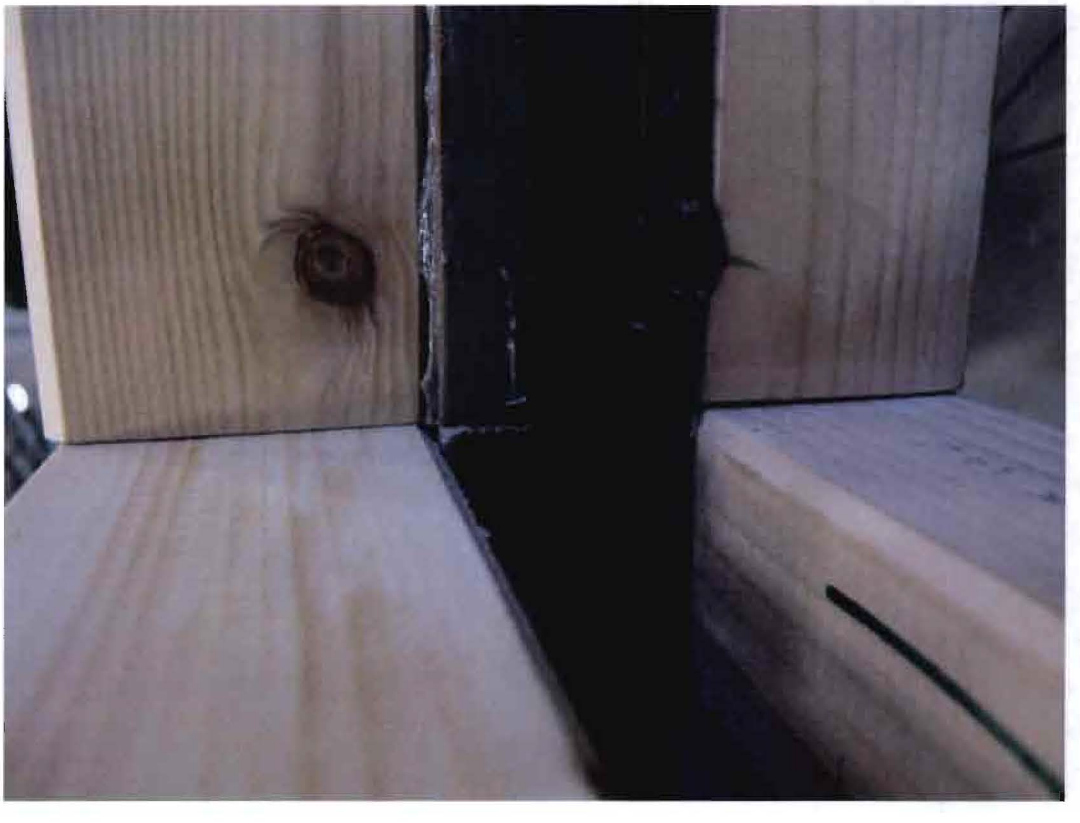

Figure 110: Close-up of gap before force initiation (sample 90-2)

Figure 111: Set-up angled connection (sample 90-2)

Figure 112: Gap after force diminishing; M = 4.6kNm (sample 90-2)

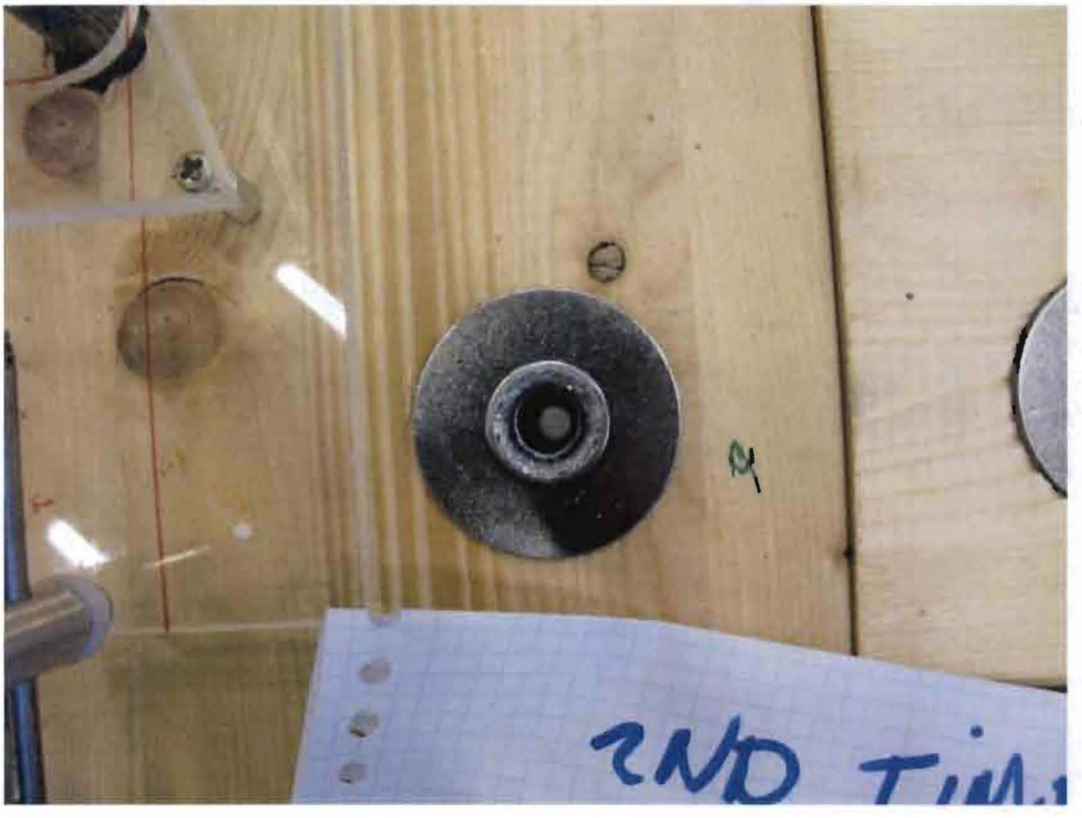

Figure 113: Tube after force diminishing; M = 4.6kNm (sample 90-2)

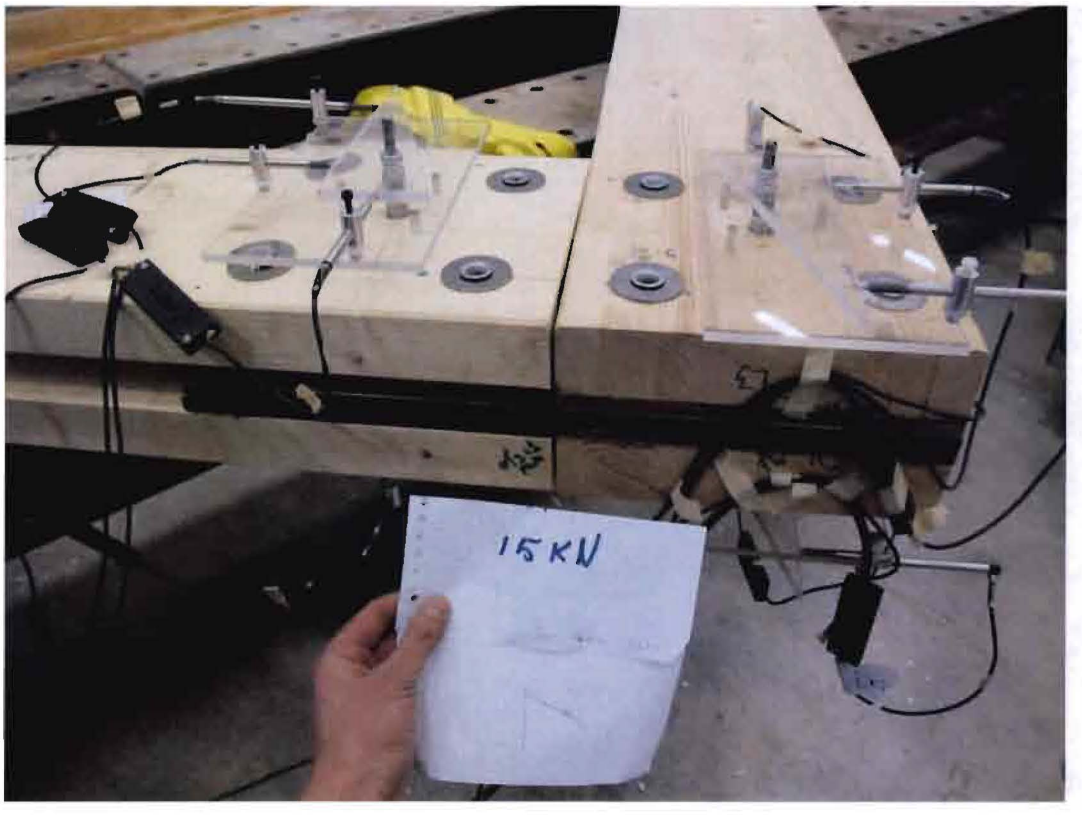

Figure 114: Connection with a bending moment of 28.6 kNm (sample 90-2)

Figure 115: Failed bond line (sample 90-2)

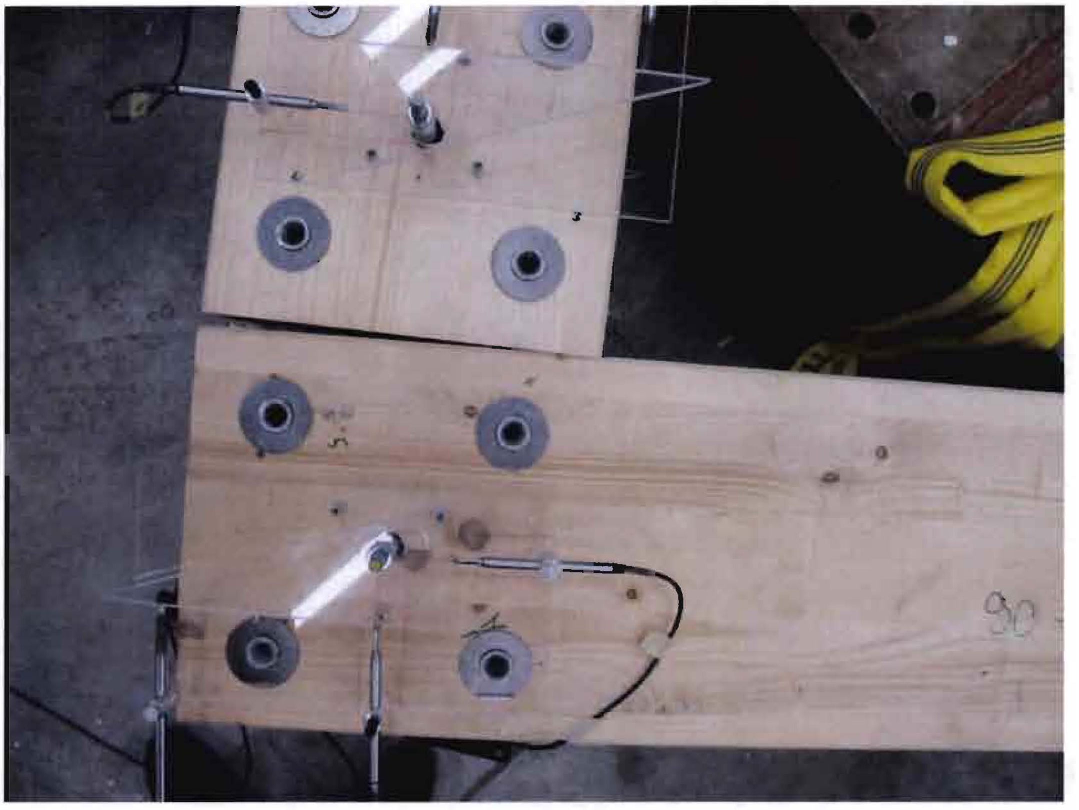

Figure 116: Gap closure (sample 90-2)

Appendix 16 C: sample 90-3

Ultimate bending moment	41.165
Rotation at ultimate load	0.122 rad
K_s	2649 kNm/rad
K_i	3203 kNm/rad
K_e	5408 kNm/rad
Initial gap width (compressed side)	t_s≈0mm
Type of failure	tube failure
Comments	-

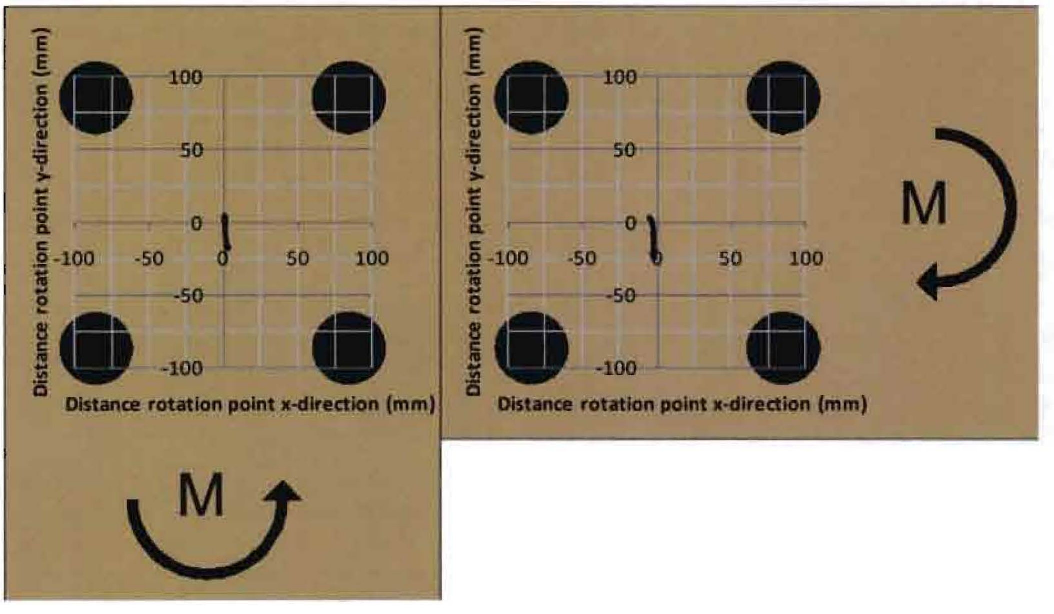

Figure 117: Measured path of rotation point (sample 90-3)

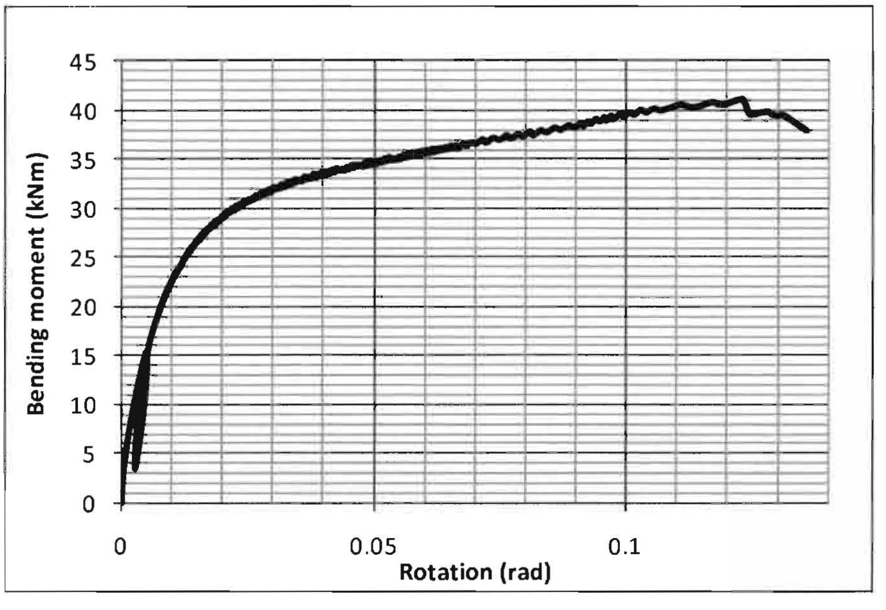

Figure 118: Bending moment versus rotation (sample 90-3)

Figure 119: Connection before force initiation (sample 90-3)

Figure 120: Connection before force initiation (sample 90-3)

Figure 121: Gap after force diminishing; M = 3.8kNm (sample 90-3)

Figure 122: Gap after force diminishing; M = 3.82kNm (sample 90-3)

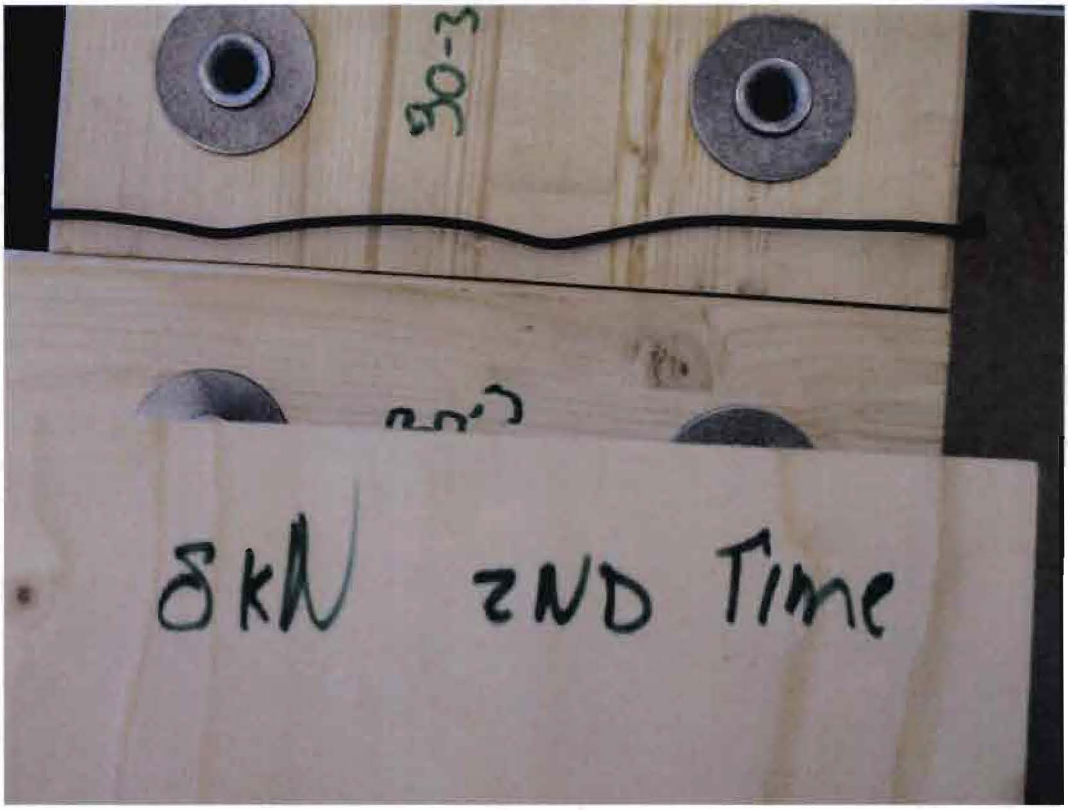

Figure 123: Gap; M = 15.3kNm (sample 90-3)

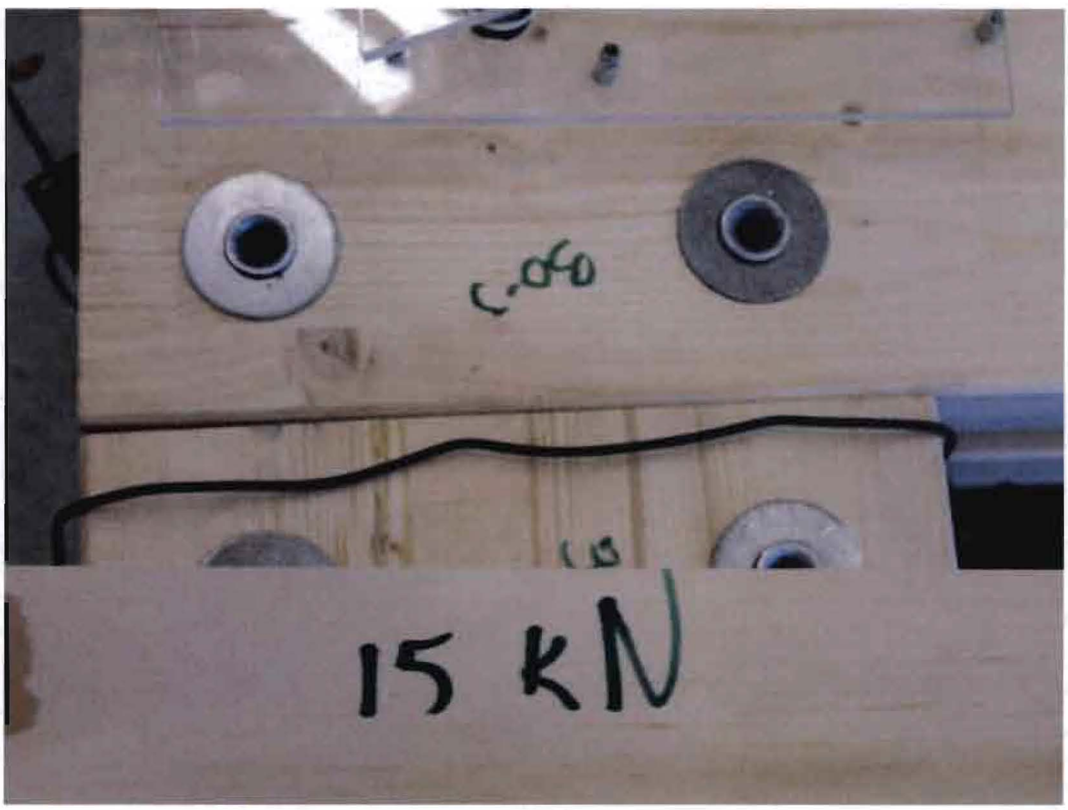

Figure 124: Gap; M = 28.6kNm (sample 90-3)

Figure 125: Gap; M = 38.2kNm (sample 90-3)

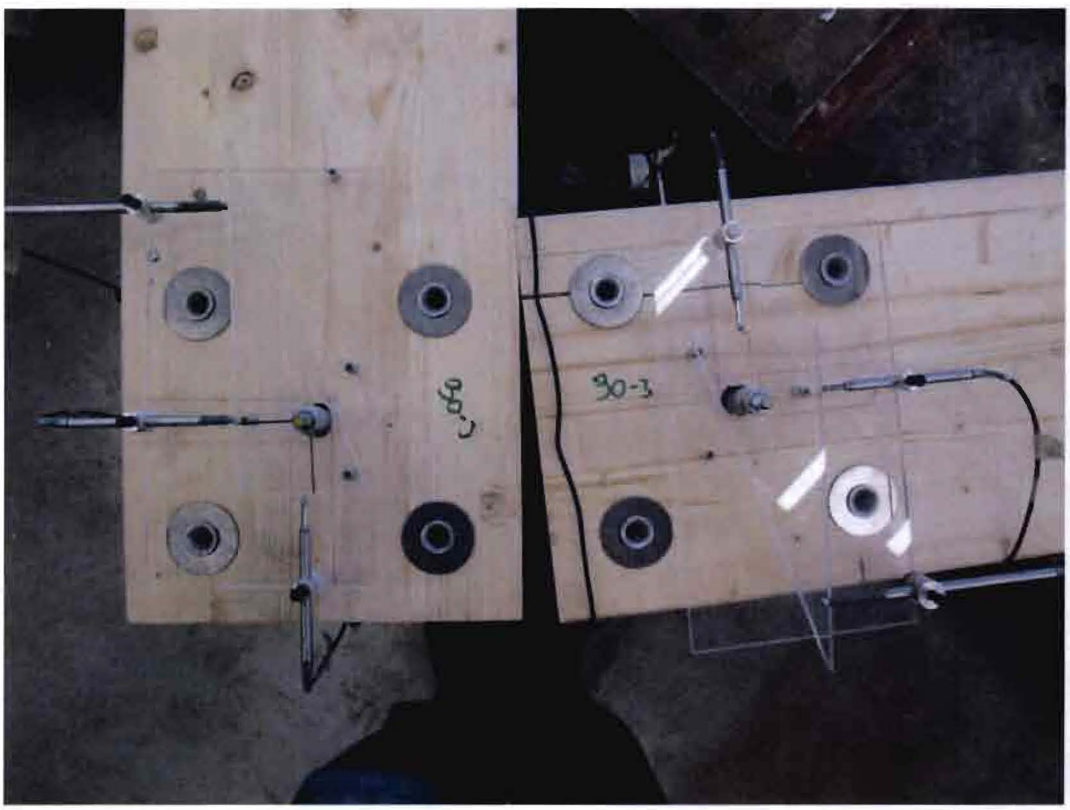

Figure 126: Failed connection (sample 90-3)

Appendix 16 D: sample 90-4

Ultimate bending moment	38.863
Rotation at ultimate load	0.111 rad
K_s	1138 kNm/rad
K_i	1366 kNm/rad
K_e	4080 kNm/rad
Initial gap width (compressed side)	t_s≈0mm
Type of failure	tube failure
Comments	Two tubes are failed. This failure led to the timber failure shown in Figure 130

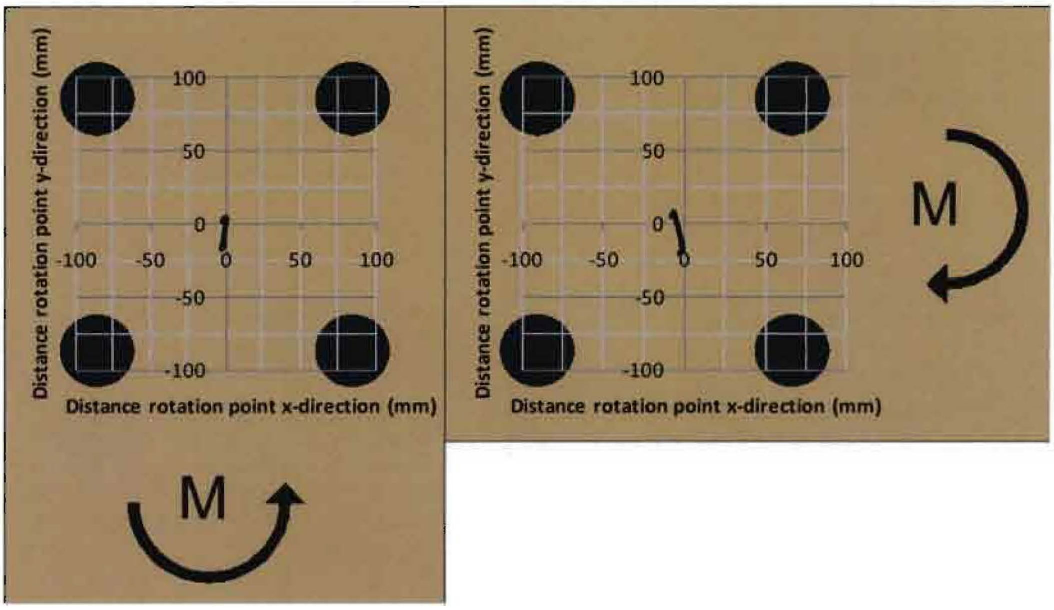

Figure 127: Measured path of rotation point (sample 90-4)

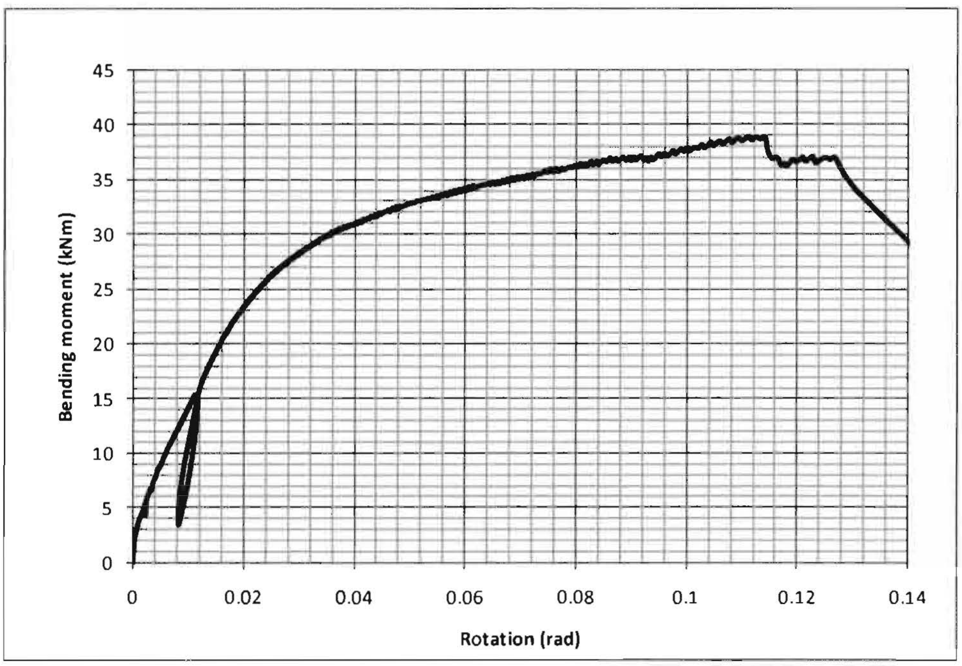

Figure 128: Bending moment versus rotation (sample 90-4)

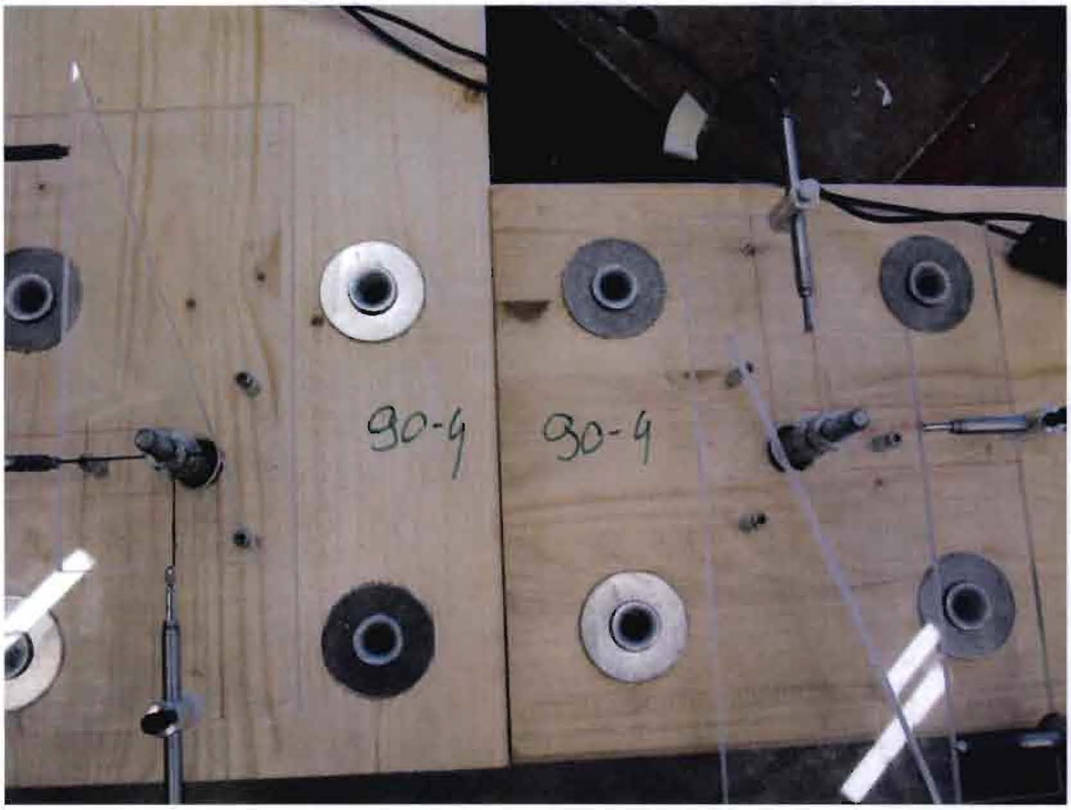

Figure 129: Connection before force initiation (sample 90-4)

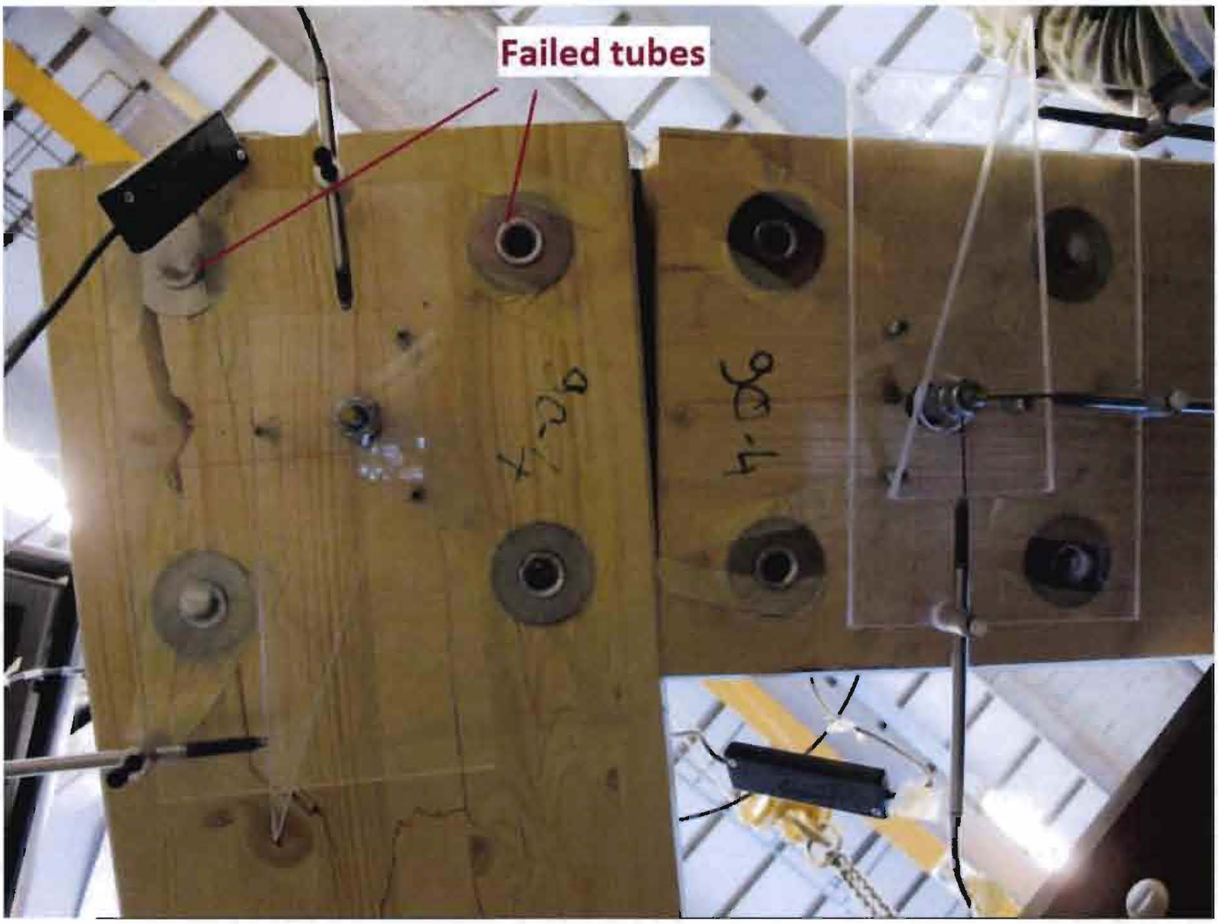

Figure 130: Failed connection (sample 90-4) Timber failed after failure of two tubes

Figure 131: Failed connection (sample 90-4)

Appendix 17:Results tube tests

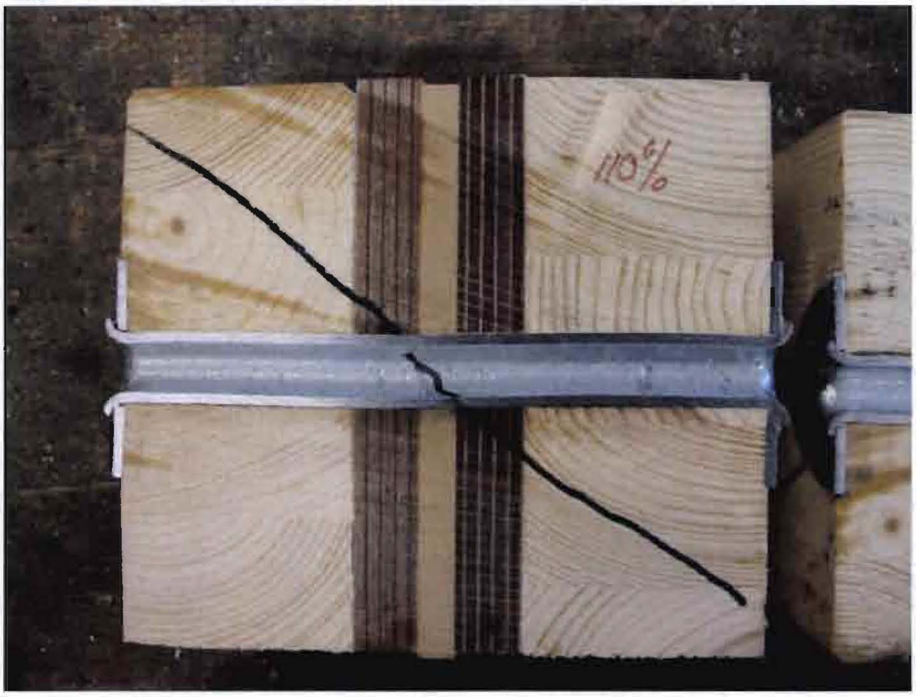

Figure 132: Section of expanded tube with 10% overlength

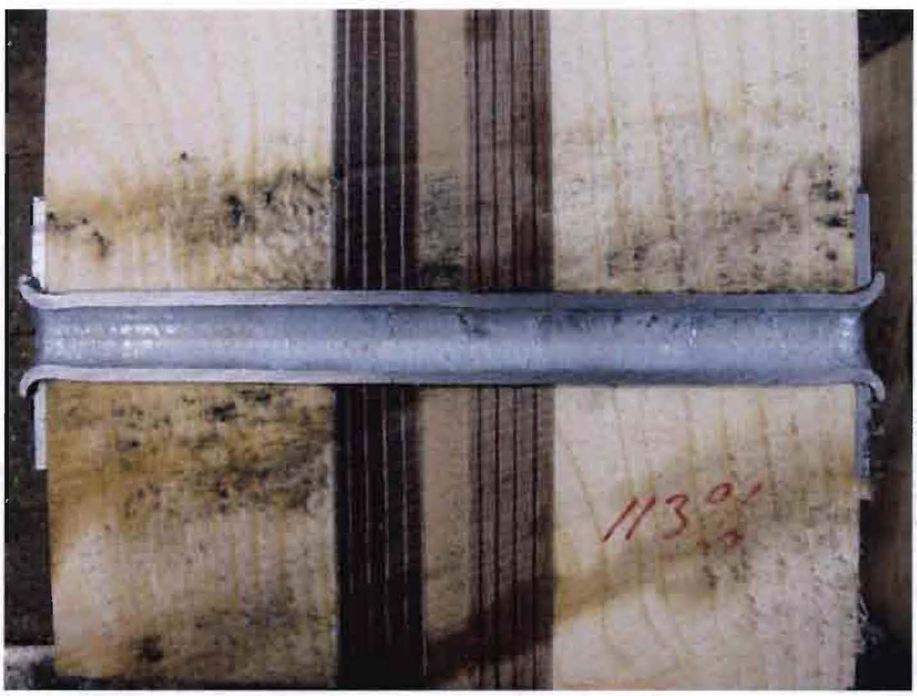

Figure 133: Section of expanded tube with 13% overlength

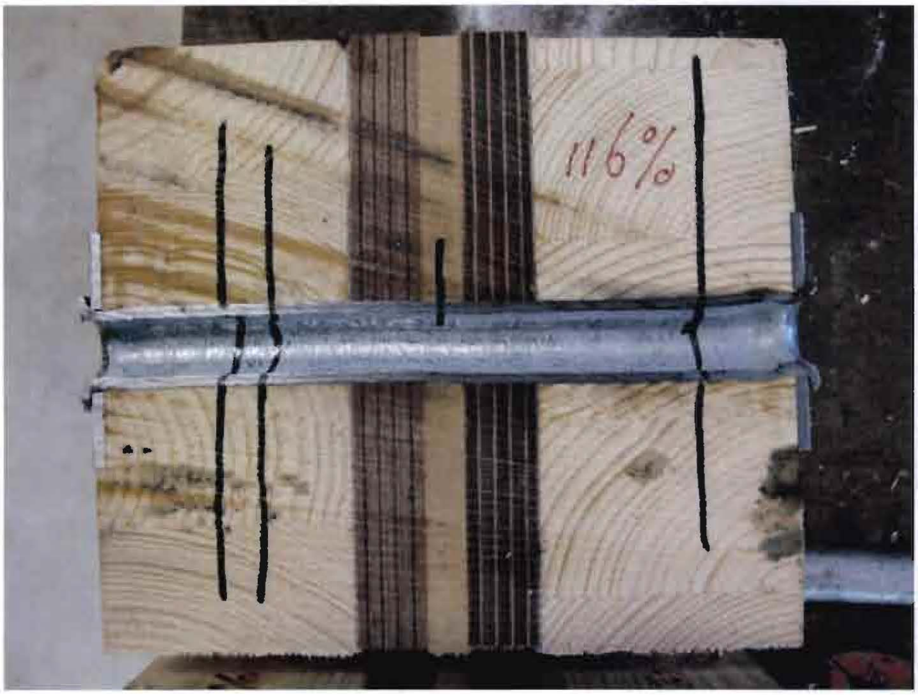

Figure 134: Section of expanded tube with 16% overlength

Figure 135: Section of expanded tube with 16% overlength

Appendix 18: Results dvw tests

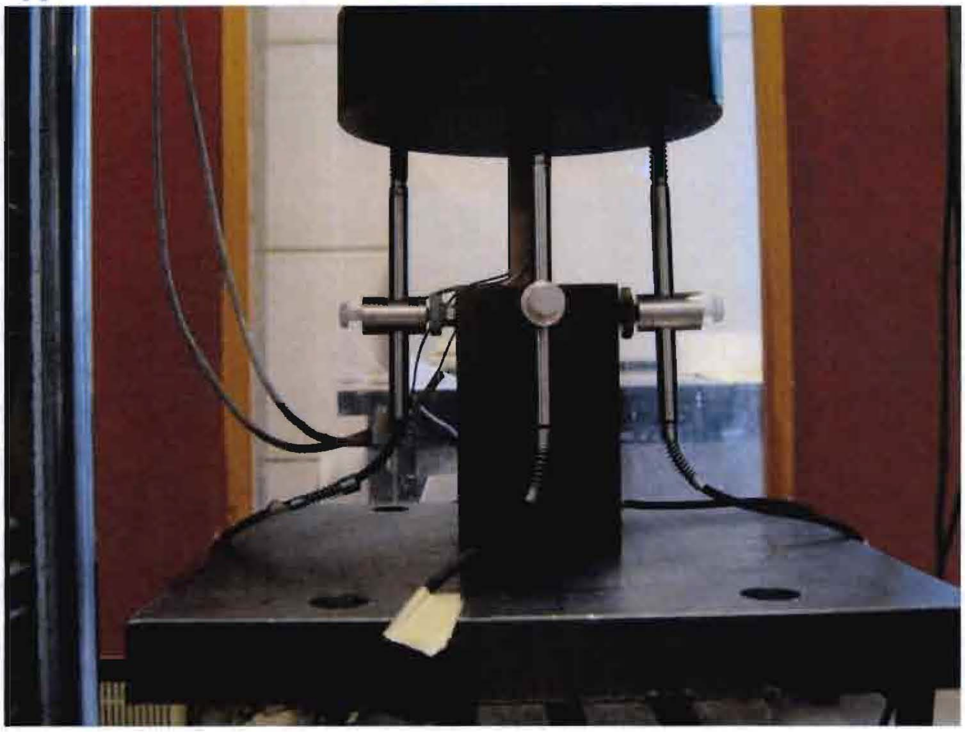

Figure 136: Set-up dvw tests; measurements executed with 4 LDVT's and 2 strain gauges

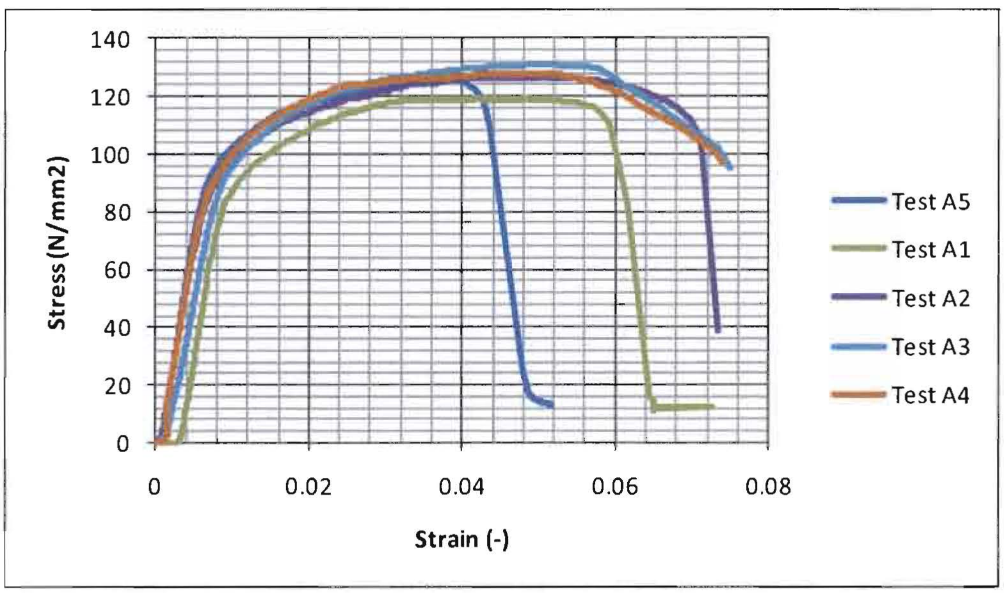

Figure 137: Stress strain results determined with LVDT's

Sample	Width (mm)	Length (mm)	Thickness (mm)	Weight (g)	Density (kg/m^3)	Modulus of elasticity (N/mm^2) Strain gauges	Modulus of elasticity (N/mm^2) LVDT
A1	16.3	64.6	16.3	22.07	1286	20828	16968
A2	16.19	64.62	16.19	21.84	1289	21515	16420
A3	16.09	64.42	16.44	22.19	1302	not applied	14547
A4	16.09	64.61	16.41	22.28	1306	not applied	16668
A5	16.11	64.64	16.58	22.54	1305	not applied	18636
Average	16.16	64.58	16.38	22.18	1298	21172	16648

Table 4: Results of dvw in-plain compression tests

Figure 138: Failed dvw due to compression (sample A1)

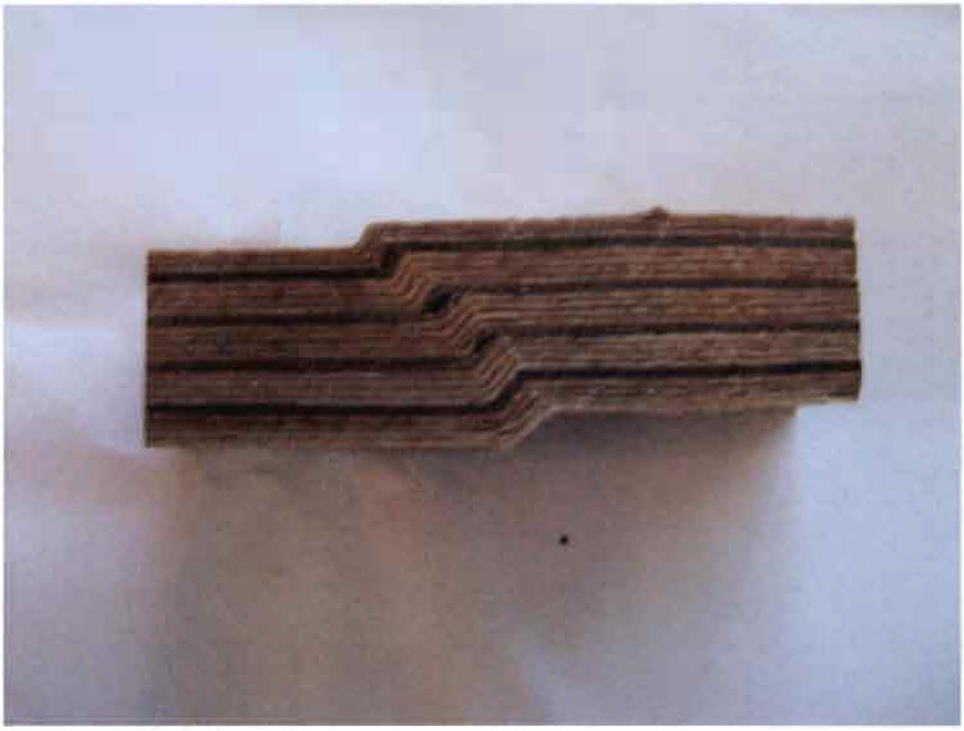

Figure 139: Failed dvw due to compression (sample A2)

Figure 140: Failed dvw due to compression (sample A3)

Figure 141: Failed dvw due to compression (sample A4)

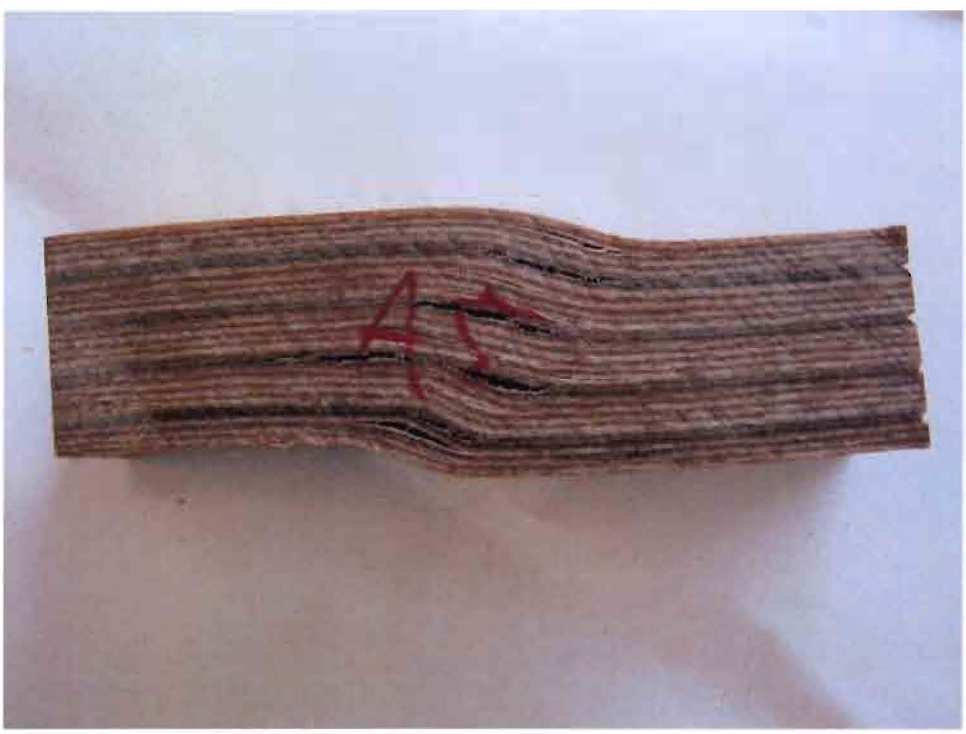

Figure 142: Failed dvw due to compression (sample A5)

Appendix 19: Results adhesive tests

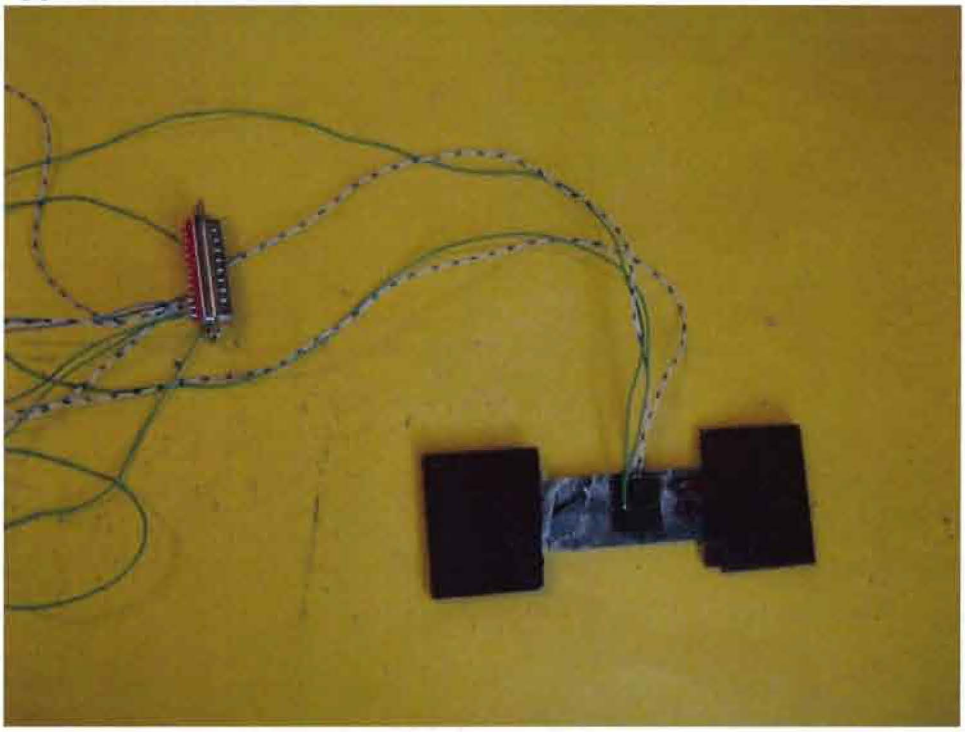

Figure 143: Failed adhesive sample with sandpaper for fixation (sample R6)

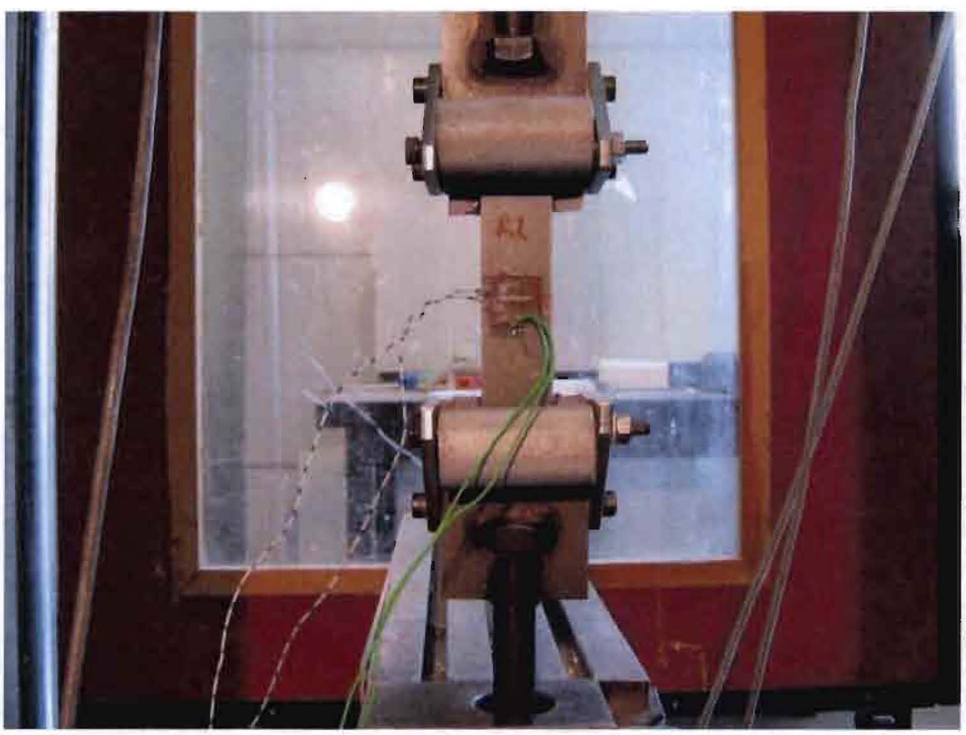

Figure 144: Test set-up for tensile tests of adhesive

Sample	Width (mm)	Thickness (mm)	Modulus of elasicity (N/mm^2)	Poisson-factor v (-)	Shear modulus (N/mm^2)	Ultimate Tensile Strength (N/mm^2)
R1	26.15	4.2	348.04	0.43	121.69	6.56
R2	26.18	4.08	483.00	0.39	173.74	8.54
R3	26.16	4.08	405.55	0.41	143.81	9.19
R4	26.22	4.13	342.51	0.44	118.93	8.27
R5	26.16	4.06	434.22	0.49	145.71	8.63
R6	26.16	4.6	371.55	0.37	135.6	5.08
Average	26.17	4.19	397.48	0.42	139.91	7.71

Table 5: Results of adhesive tensile tests

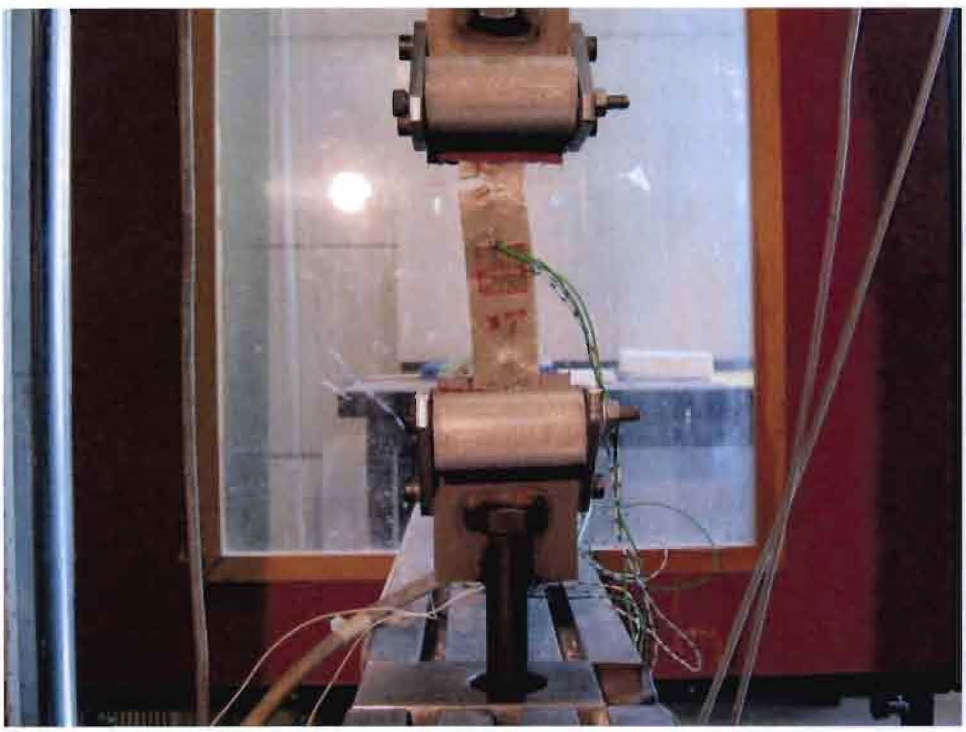

Figure 145: Adhesive failed due to tension (sample R1)

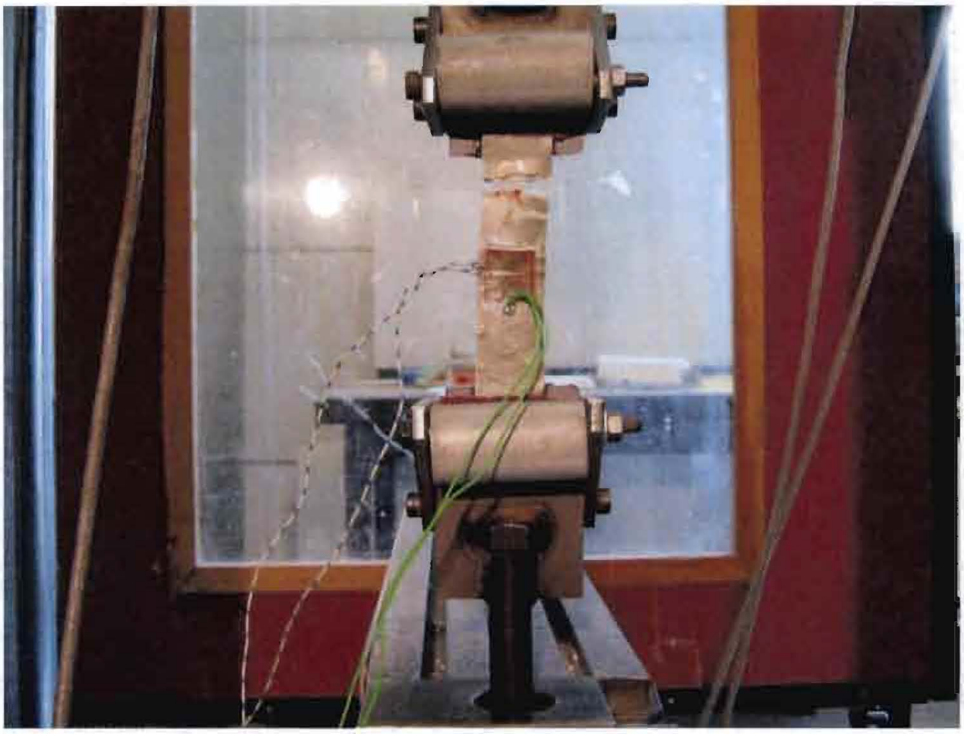

Figure 146: Adhesive failed due to tension (sample R2)

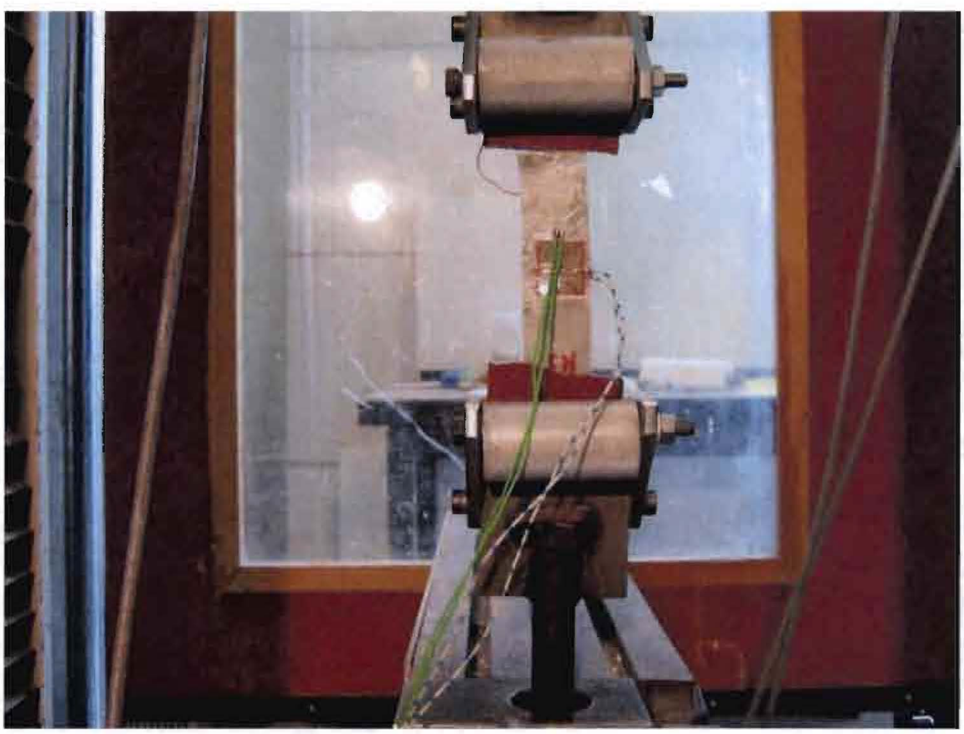

Figure 147: Adhesive failed due to tension (sample R3)

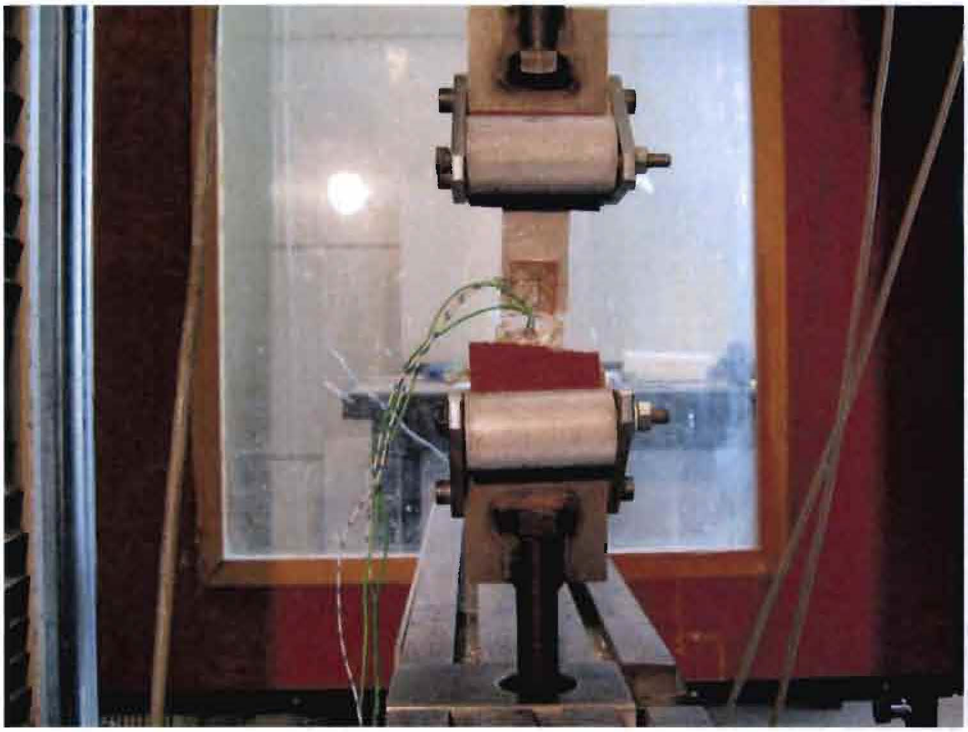

Figure 148: Adhesive failed due to tension (sample R4)

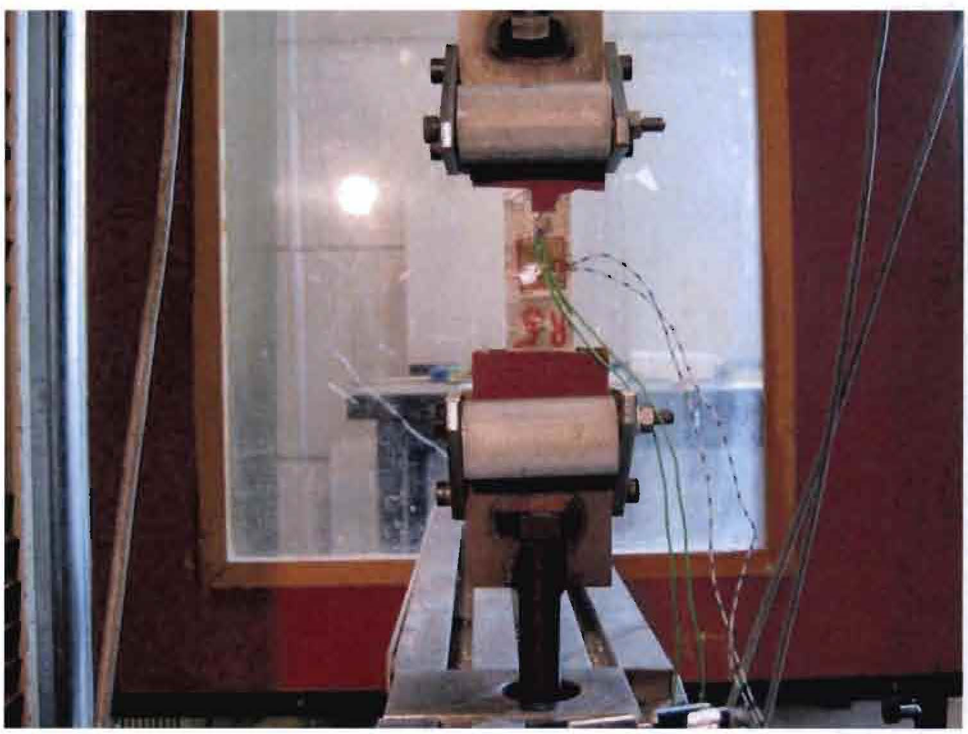

Figure 149: Adhesive failed due to tension (sample R5)

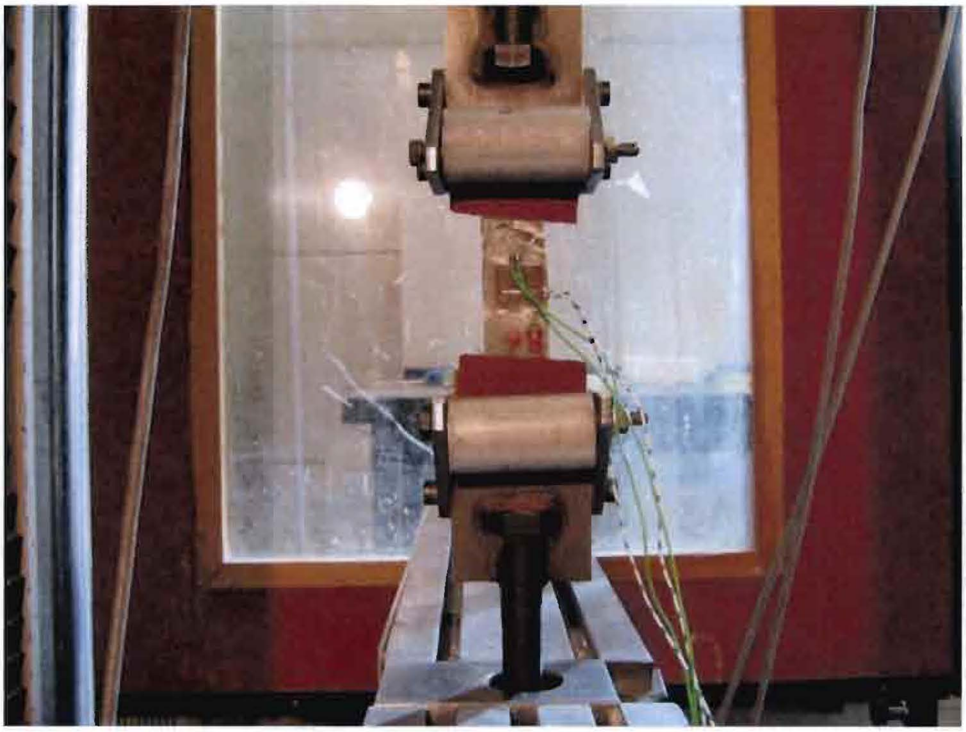

Figure 150: Adhesive failed due to tension (sample R6)

Appendix 20: Analyses of tube deformation with rounded steel plate and 35 mm tube

tube diameter (d)	35 mm
displacement at step time = 1.0 ($\delta_{1.0}$)	18 mm
edge/end distance	3.5d
timber thickness (t_{timber})	55 mm
dvw thickness (t_{dvw})	18 mm

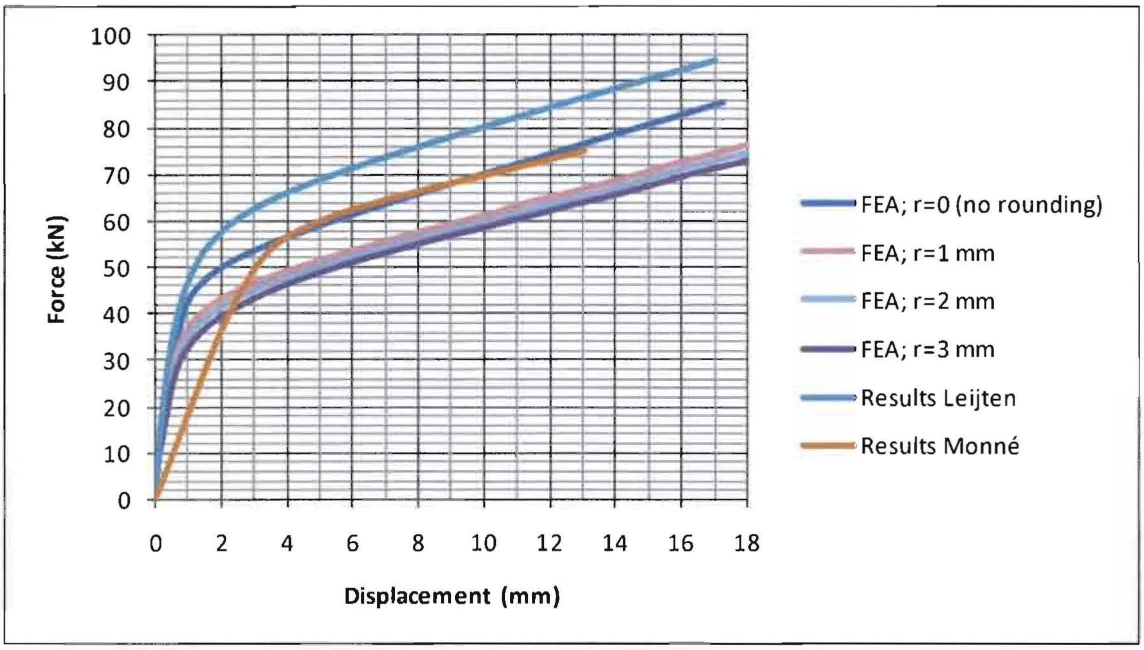

Figure 151: Force-displacement graphs per shear plane with different radii of rounded edge; d=35mm

Appendix 20 A: Rounding radius = 1 mm

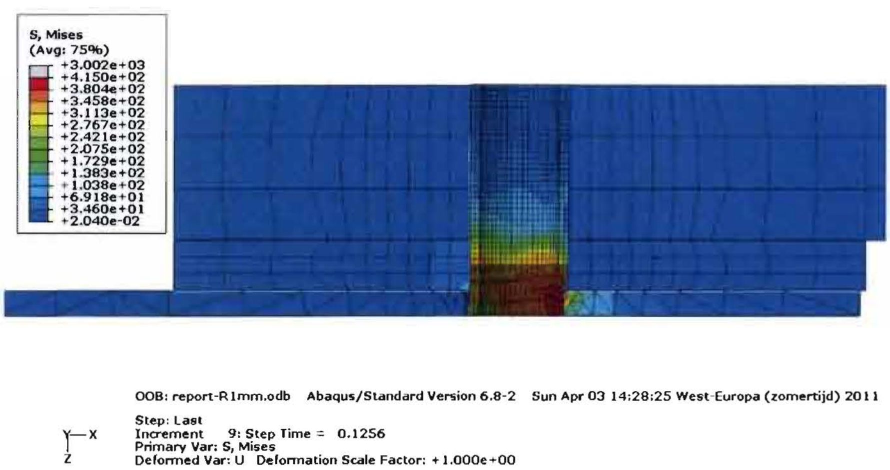

Figure 152: von Mises stress; step time = 0.1256; r=1 mm

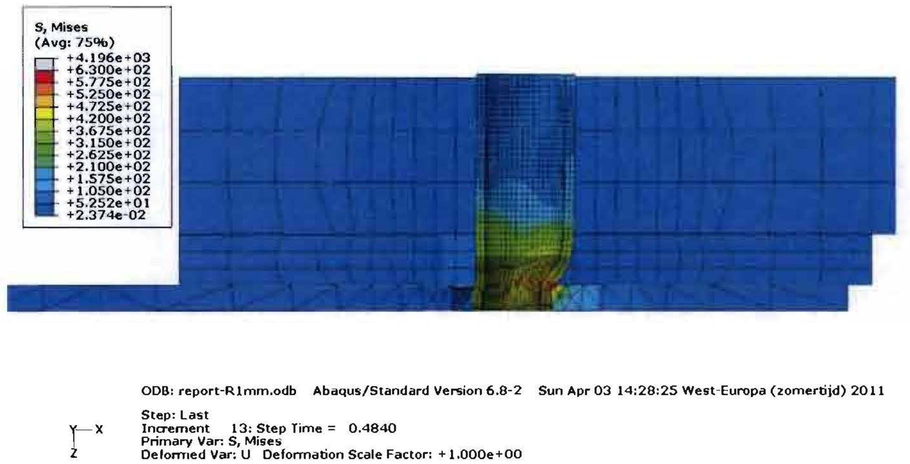

Figure 153: von Mises stress; step time = 0.4840; r=1mm

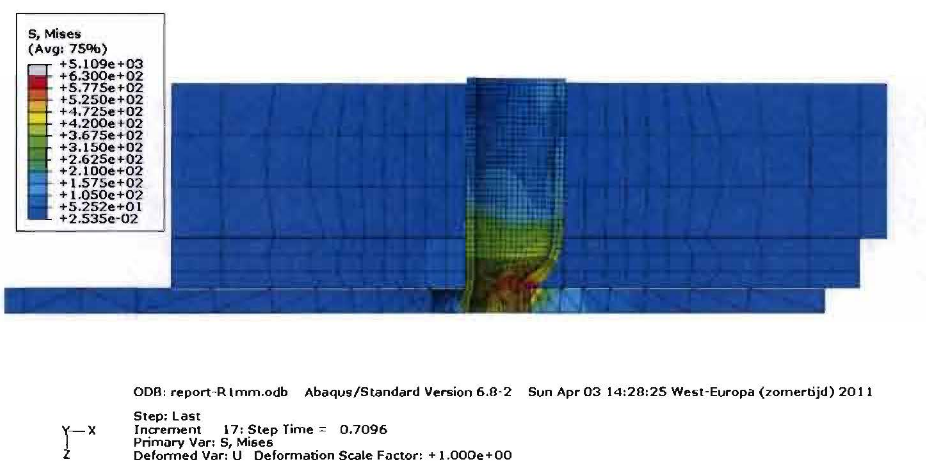

Figure 154: von Mises stress; step time = 0.7096; r=1mm

Figure 155: von Mises stress; step time = 1.000; r=1mm

Appendix 20 B: Rounding radius = 2 mm

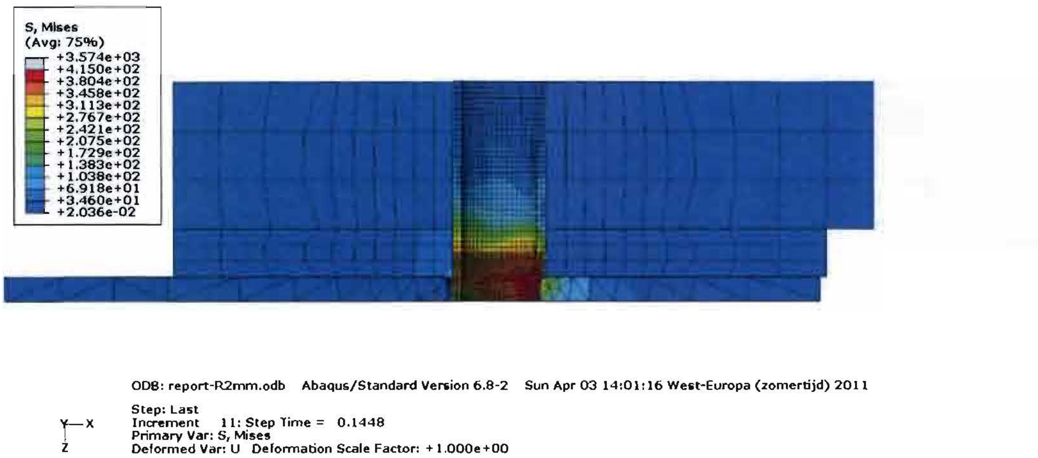

Figure 156: von Mises stress; step time = 0.1448; r=2mm

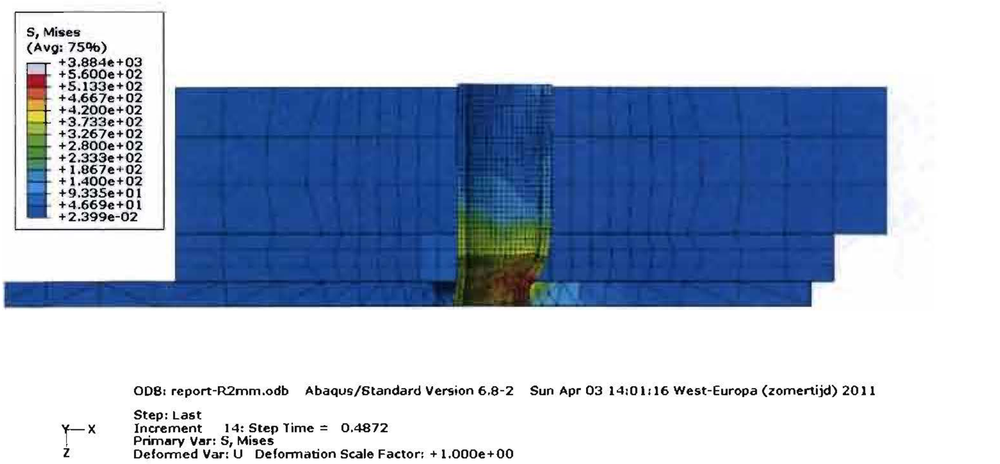

Figure 157: von Mises stress; step time = 0.4872; r=2mm

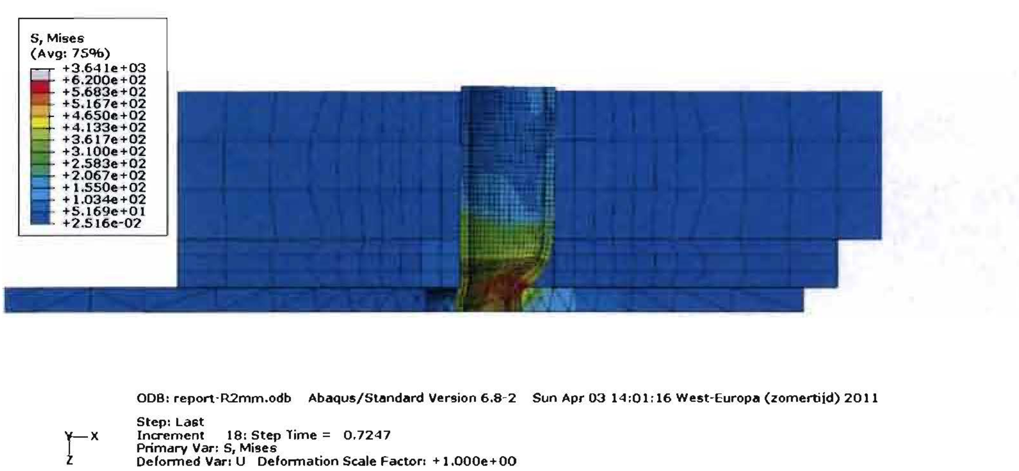

Figure 158: von Mises stress; step time = 0.7247; r=2mm

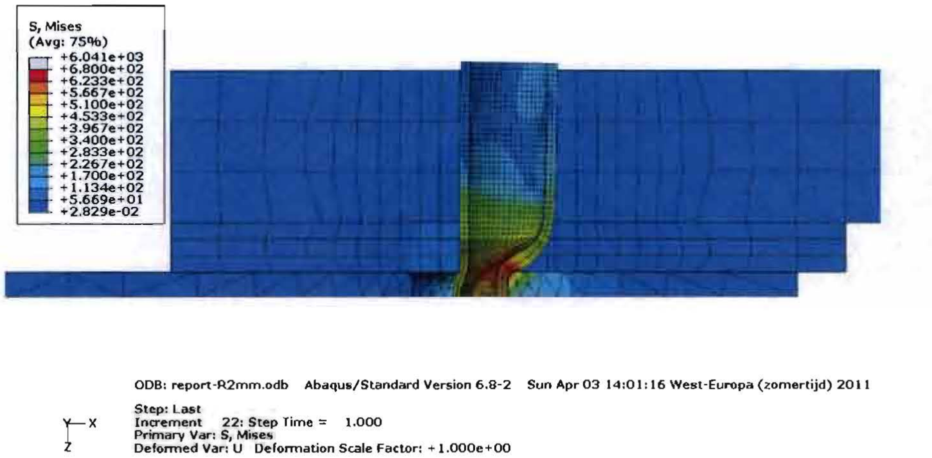

Figure 159: von Mises stress; step time = 1.000; r=2mm

Appendix 20 C: Rounding radius = 3 mm

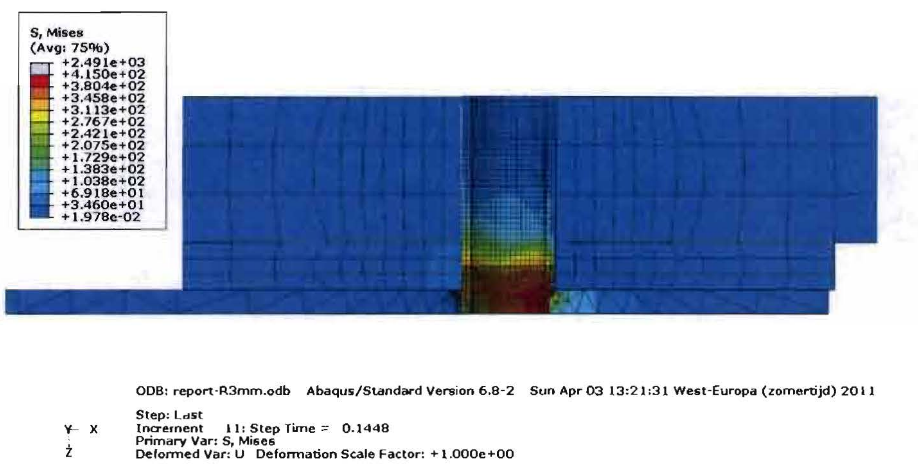

Figure 160: von Mises stress; step time = 0.1448; r=3mm

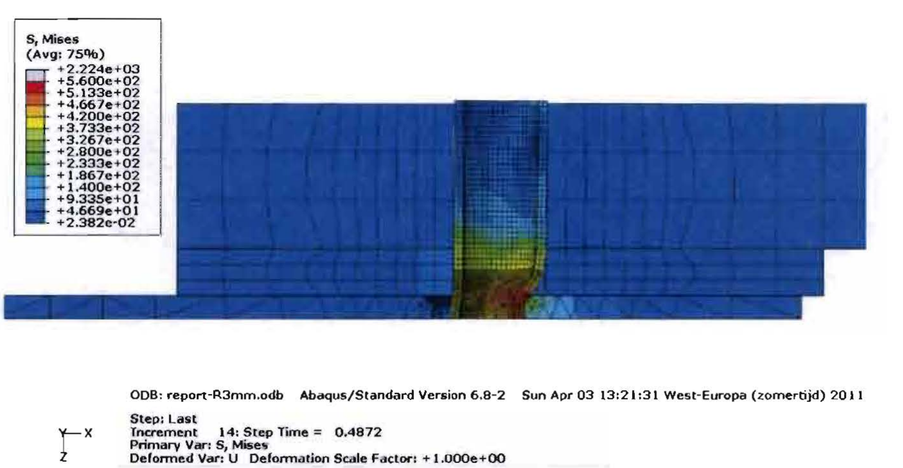

Figure 161: von Mises stress; step time = 0.4872; r=3mm

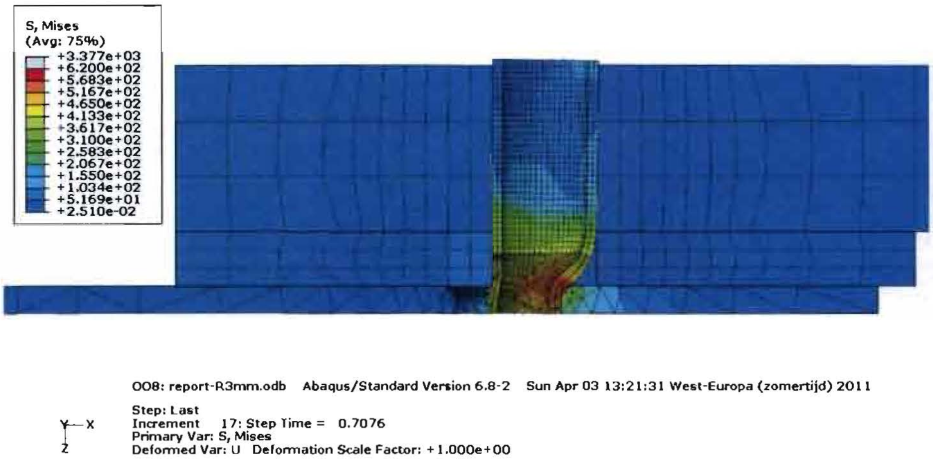

Figure 162: von Mises stress; step time = 0.7076; r=3mm

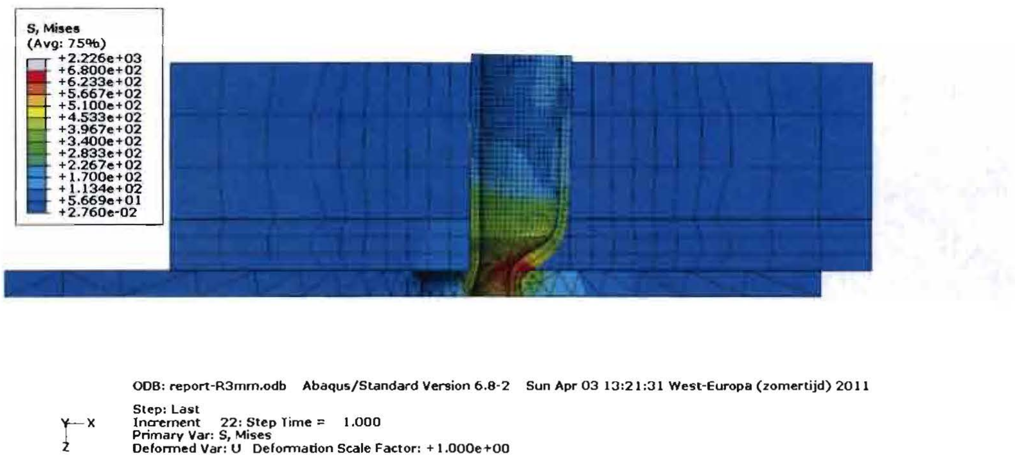

Figure 163: von Mises stress; step time = 1.000; r=3mm

Appendix 21: Parallel to grain shear distribution in bond line (RP-adhesive)

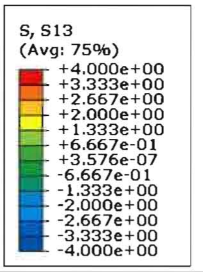

					Tube force per shear plane		
	t_{timber} (mm)	n	b (mm)	h (mm)	30 kN	60 kN	90 kN
	93	8	600	600	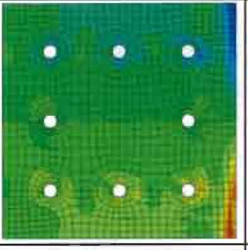	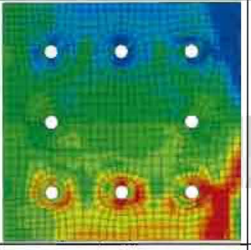	Bond line failed at 77.9 kN tube force per shear plane
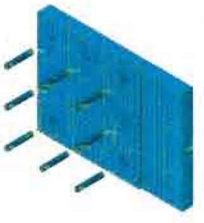	82	8	800	800	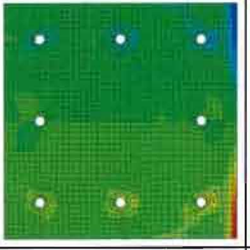	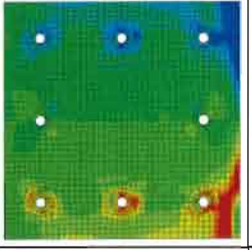	Bond line failed at 87.0 kN tube force per shear plane
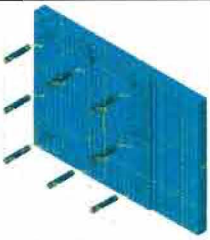	71	8	1000	1000	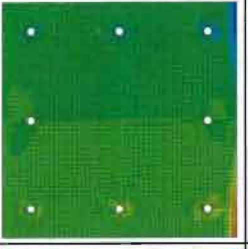	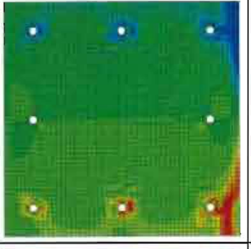	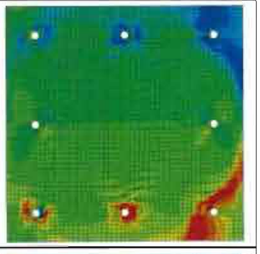
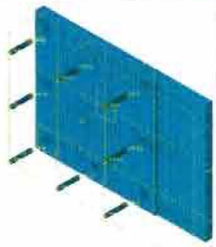	63	8	1200	1200	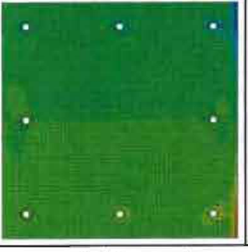	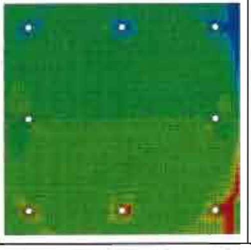	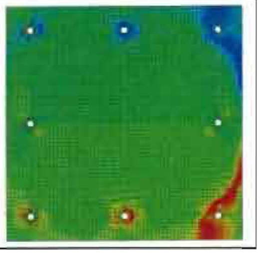

Table 6: Bond line shear stress distribution parallel to grain; arm length=15b; t_{dvw}=18mm; d=35mm; Resorcenol Phenol adhesive

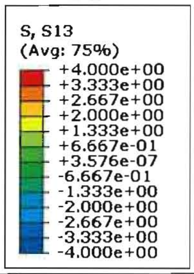

	t_{timber} (mm)	n	b (mm)	h (mm)	Tube force per shear plane 30 kN	60 kN	90 kN
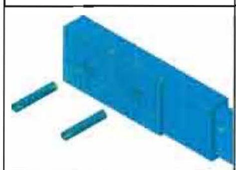	83	2	500	245	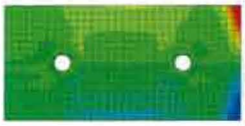	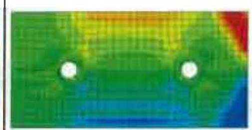	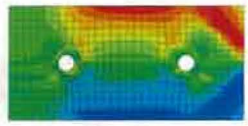
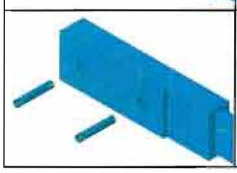	115	2	600	245		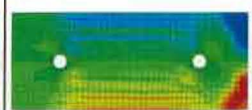	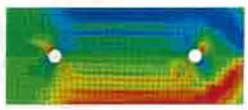

Table 7: Bond line shear stress distribution parallel to grain; arm length=15b; t_{dvw}=18mm; d=35mm; Resorcenol Phenol adhesive

	t_{timber} (mm)	n	b (mm)	h (mm)	Tube force per shear plane 30 kN	60 kN	90 kN
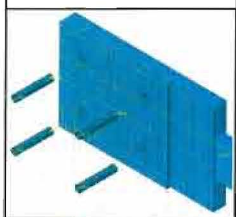	68	4	600	500	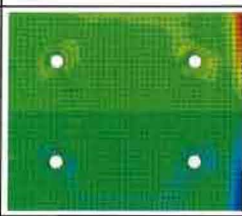	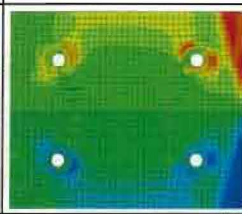	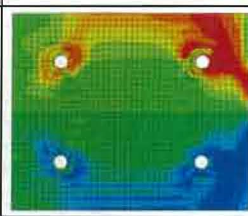
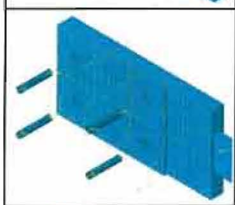	78	4	700	500	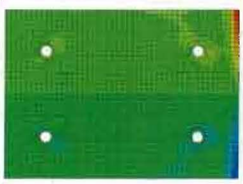	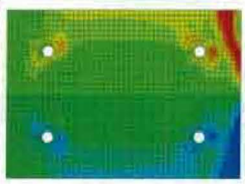	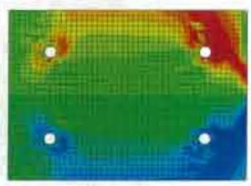
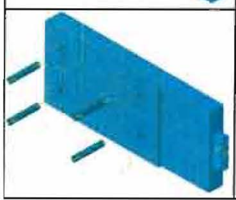	95	4	800	500	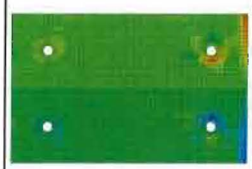	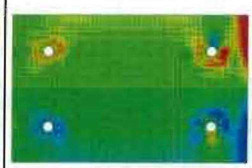	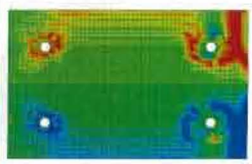

Table 8: Bond line shear stress distribution parallel to grain; arm length=15b; t_{dvw}=18mm; d=35mm; Resorcenol Phenol adhesive

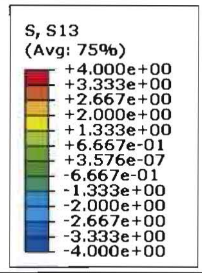

					Tube force per shear plane		
	t_{timber} (mm)	n	b (mm)	h (mm)	30 kN	60 kN	90 kN
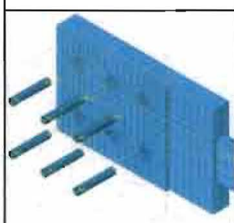	88	6	600	500	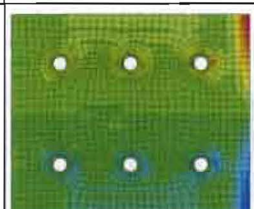	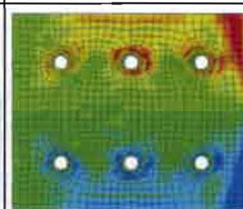	Bond line failed at 89.2 kN tube force per shear plane
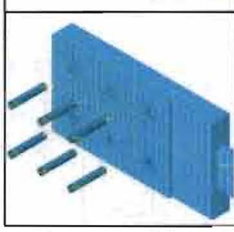	101	4	700	500	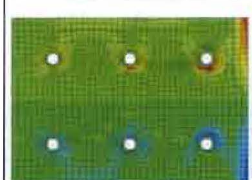	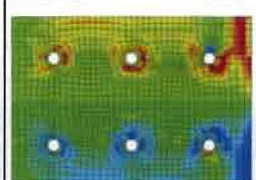	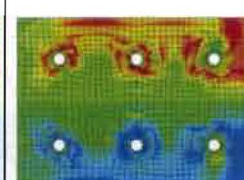

Table 9: Bond line shear stress distribution parallel to grain; arm length=15b; t_{dvw}=18mm; d=35mm; Resorcenol Phenol adhesive

Appendix 22: Numerical predictions of experiments of angled connection

	Material/Member	Criterion	
1	timber compression parallel to grain [9]	σ < -42 N/mm²	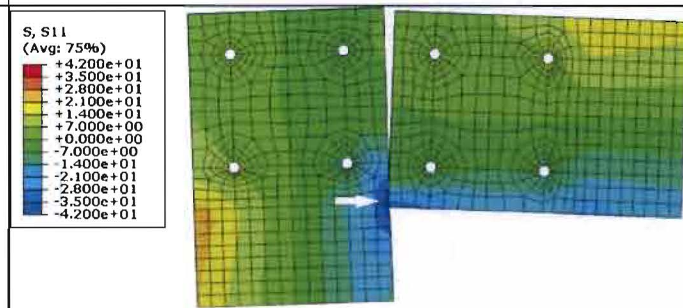
2	timber tension parallel to grain [9]	σ > 42 N/mm²	Not occuring
3	timber compression perpendicular to grain [9**Error! Reference source not found.**]	σ < -3.6 N/mm²	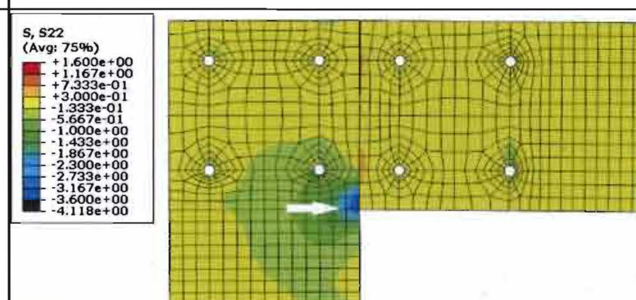
4	timber tension perpendicular to grain [9]	σ > 1.6 N/mm²	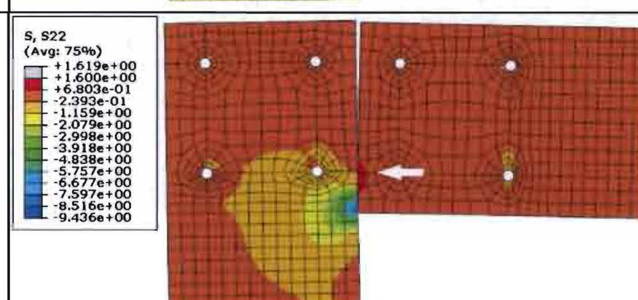
5	dvw failure	ε > 0.07	Not occuring
6	bond line failure	Given by Abaqus	Not occuring
7	first tube failure (d=18 mm) [3]	δ > 8.9mm	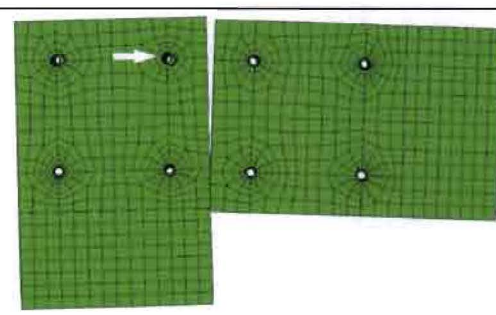

Table 10: Different criteria visualized

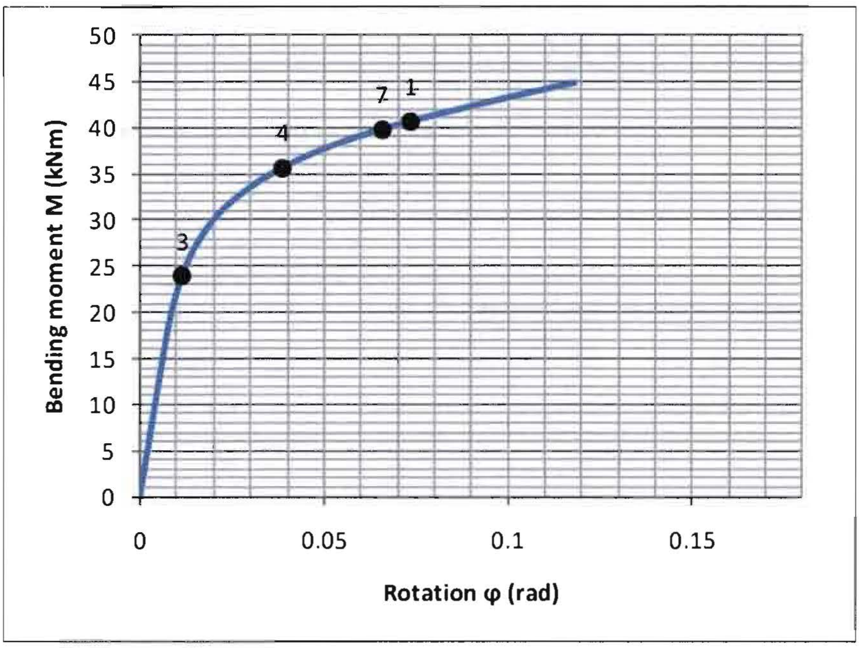

Figure 164: Numerically predicted M-φ curve of angled connection

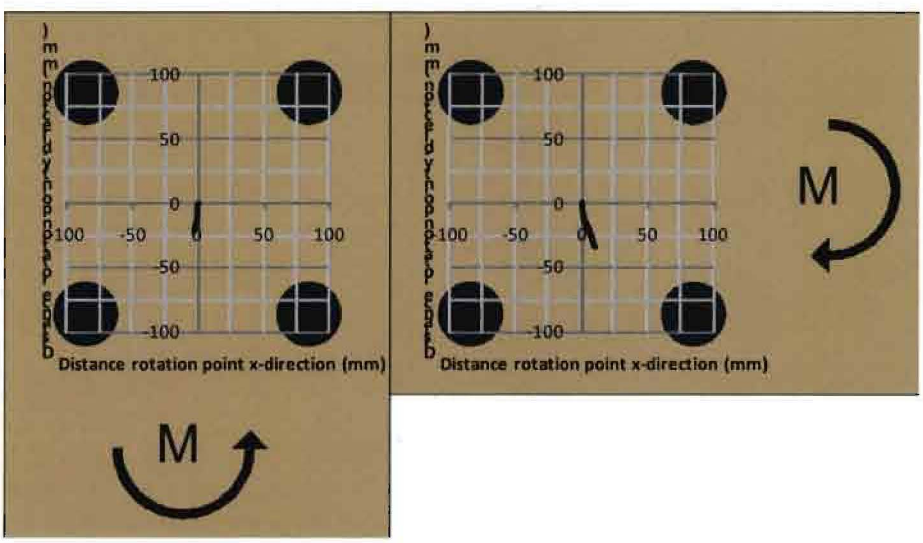

Figure 165: Numerically determined paths of rotation point

Appendix 23: Numerical bond line predictions of angled connection

PU-adhesive (DuoCol) **<u>Thickness = 0.45mm</u>**	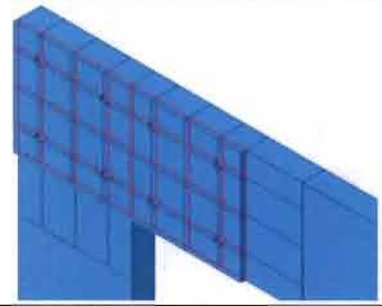		
	shear stress parallel (N/mm^2)	**shear stress perpendicular (N/mm^2)**	**tensile stress (N/mm^2)**
Bending moment	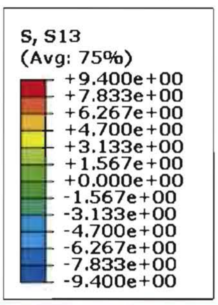	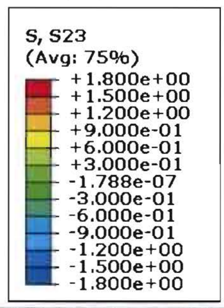	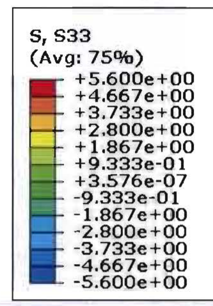
<u>15</u> kNm	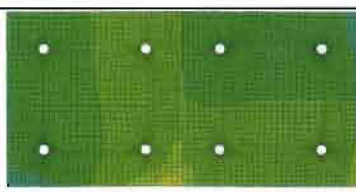	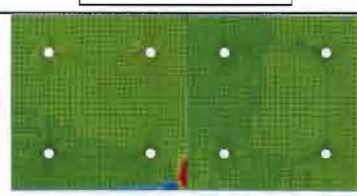	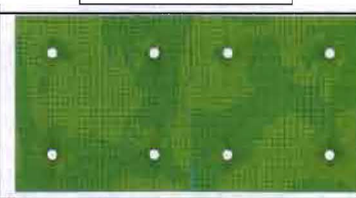
<u>30</u> kNm	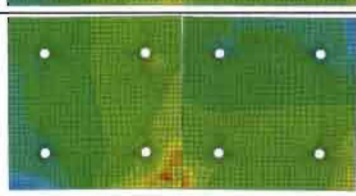		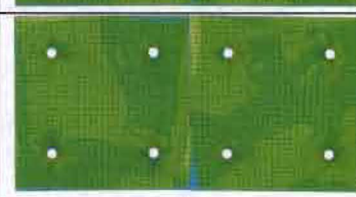
max tube cap.: <u>39.8</u> kNm	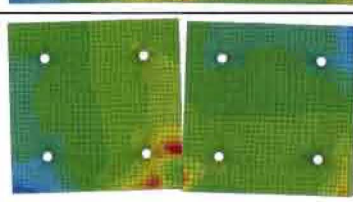		

Table 11: Bond line stress distribution angled connection; t_{timber}=60mm; t_{dvw}=12mm; d=18mm; PU-adhesive

<table>
<tr><td colspan="2">PU-adhesive (DuoCol)
<u>Thickness = 0.2mm</u></td><td colspan="2">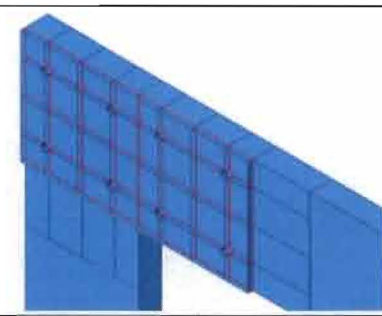</td></tr>
<tr><td>Bending moment</td><td>shear stress parallel (N/mm²)
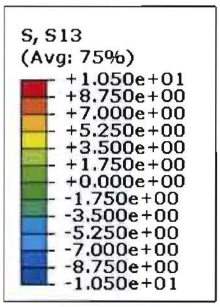
</td><td>shear stress perpendicular (N/mm²)
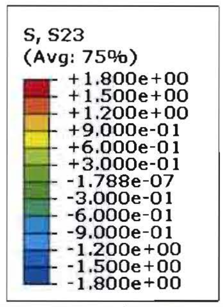
</td><td>tensile stress (N/mm²)
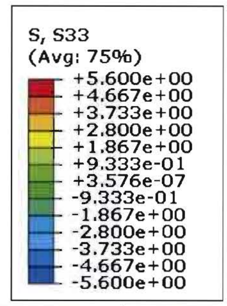
</td></tr>
<tr><td><u>15</u> kNm</td><td>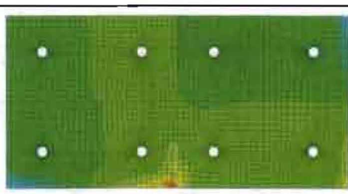</td><td>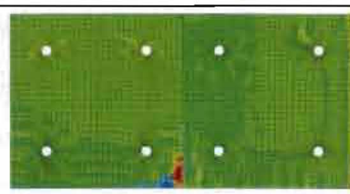</td><td>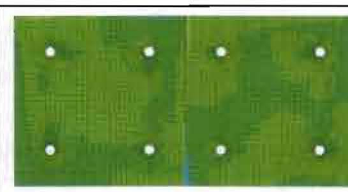</td></tr>
<tr><td><u>30</u> kNm</td><td>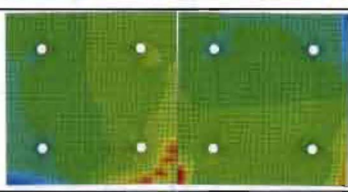</td><td>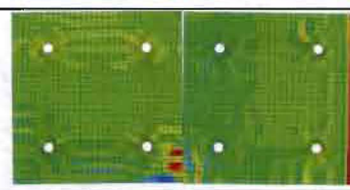</td><td>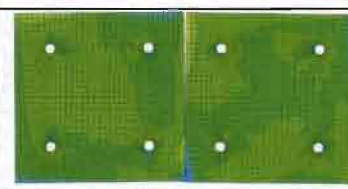</td></tr>
<tr><td>max tube cap.: <u>39.8</u> kNm</td><td>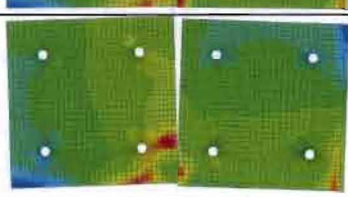</td><td></td><td>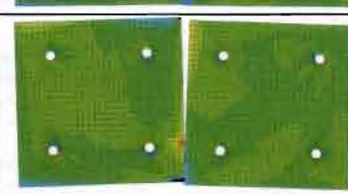</td></tr>
</table>

Table 12: Bond line stress distribution angled connection; t_{timber}=60mm; t_{dvw}=12mm; d=18mm; PU-adhesive

Appendix 24: Numerical predictions of experiments of straight connection

	Material/Member	Criterion	
1	timber compression parallel to grain [9]	σ < -42 N/mm²	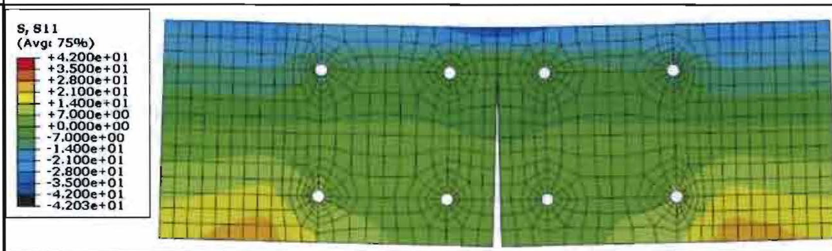
2	timber tension parallel to grain [9]	σ > 42 N/mm²	Not occuring
3	timber compression perpendicular to grain [9**Error! Reference source not found.**]	σ < -3.6 N/mm²	Not occuring
4	timber tension perpendicular to grain [9]	σ > 1.6 N/mm²	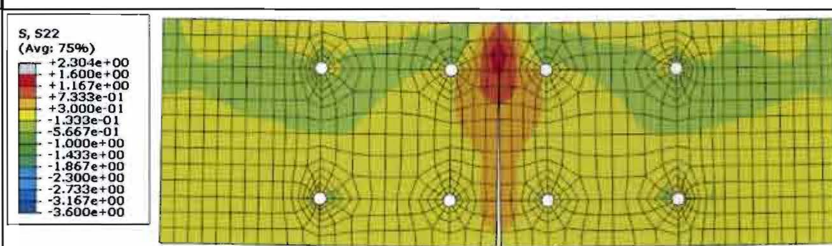
5	dvw failure	ε > 0.07	Not occuring
6	bond line failure	Given by Abaqus	Not occuring
7	first tube failure (d=18 mm) [3]	δ > 8.9mm	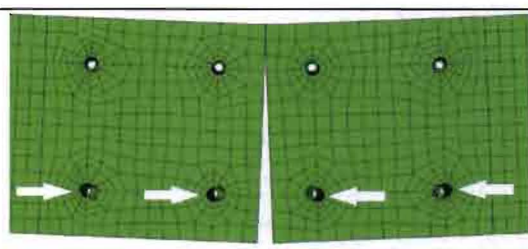

Table 13: Different criteria visualized

Appendix 25: Numerical bond line predictions of straight connection

PU-adhesive (DuoCol) **<u>Thickness = 0.45mm</u>**		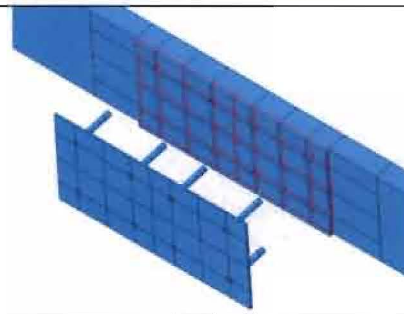	
Bending moment	**shear stress parallel (N/mm²)** S, S13 (Avg: 75%) +9.400e+00 +7.833e+00 +6.267e+00 +4.700e+00 +3.133e+00 +1.567e+00 +0.000e+00 -1.567e+00 -3.133e+00 -4.700e+00 -6.267e+00 -7.833e+00 -9.400e+00	**shear stress perpendicular (N/mm²)** S, S23 (Avg: 75%) +1.800e+00 +1.500e+00 +1.200e+00 +9.000e-01 +6.000e-01 +3.000e-01 -1.788e-07 -3.000e-01 -6.000e-01 -9.000e-01 -1.200e+00 -1.500e+00 -1.800e+00	**tensile stress (N/mm²)** S, S33 (Avg: 75%) +5.600e+00 +4.667e+00 +3.733e+00 +2.800e+00 +1.867e+00 +9.333e-01 +3.576e-07 -9.333e-01 -1.867e+00 -2.800e+00 -3.733e+00 -4.667e+00 -5.600e+00
<u>15</u> kNm	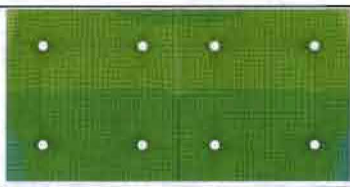	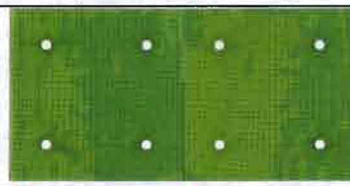	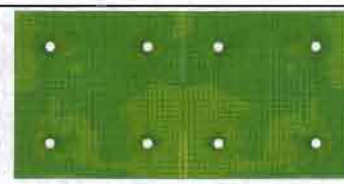
<u>30</u> kNm	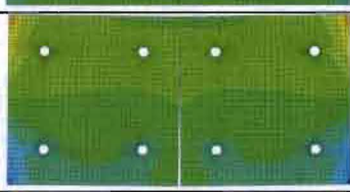	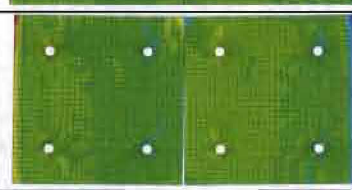	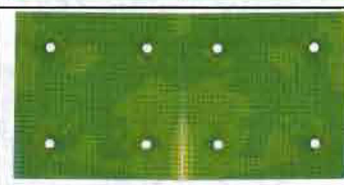
max tube cap.: <u>44.9</u> kNm	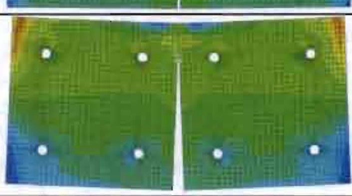	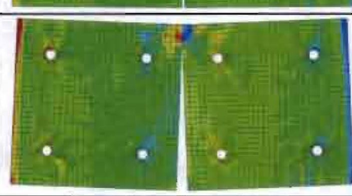	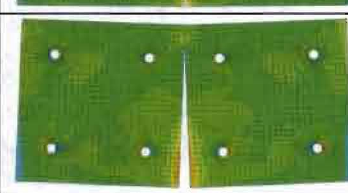

Table 14: Bond line stress distribution straight connection; t_{timber}=60mm; t_{dvw}=12mm; d=18mm; PU-adhesive

	PU-adhesive (DuoCol) **<u>Thickness = 0.2mm</u>**	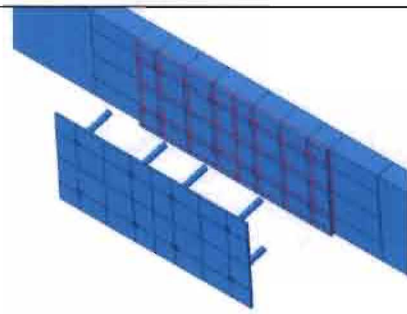	
	shear stress parallel (N/mm²)	**shear stress perpendicular (N/mm²)**	**tensile stress (N/mm²)**
Bending moment	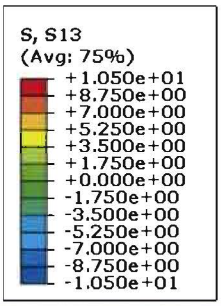	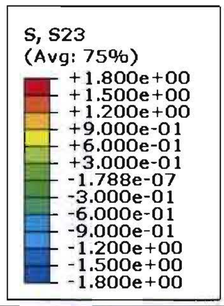	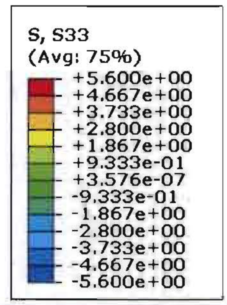
<u>15</u> kNm	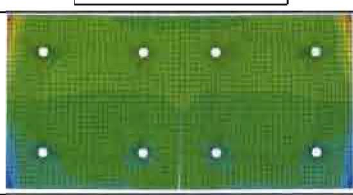	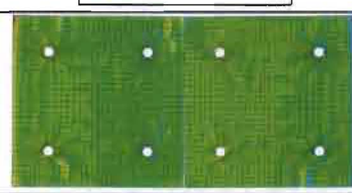	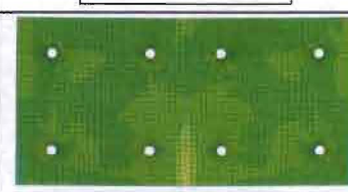
<u>30</u> kNm	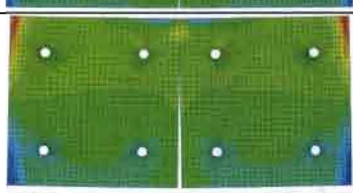	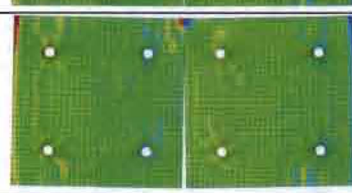	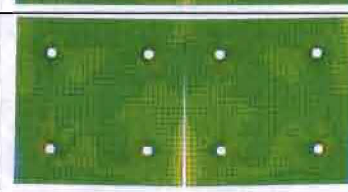
max tube cap.: 44.9 kNm	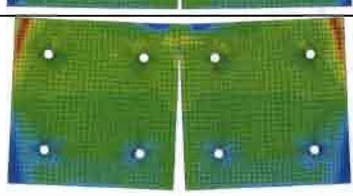		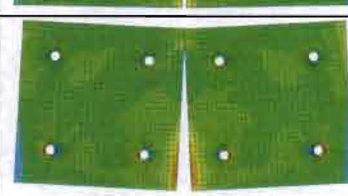

Table 15: Bond line stress distribution straight connection; t_{timber}=60mm; t_{dvw}=15mm; d=35mm; PU-adhesive

Appendix 26: Numerical bond line predictions of angled connection with RP-adhesive

<table>
<tr><td colspan="2">RP-adhesive
<u>Thickness = unknown</u></td><td colspan="2">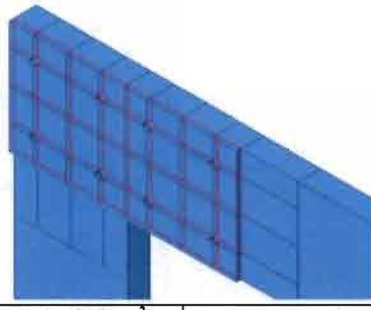</td></tr>
<tr><td>Bending moment</td><td>shear stress parallel (N/mm²)
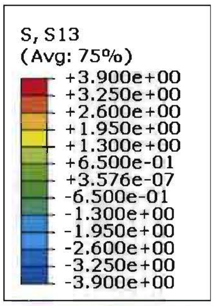
</td><td>shear stress perpendicular (N/mm²)
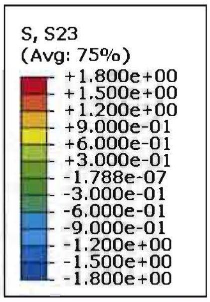
</td><td>tensile stress (N/mm²)
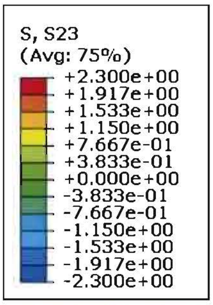
</td></tr>
<tr><td><u>15</u> kNm</td><td>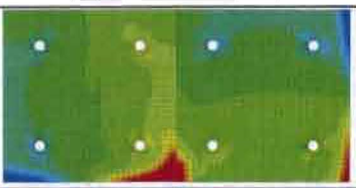</td><td>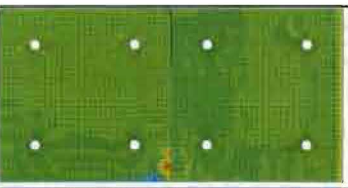</td><td>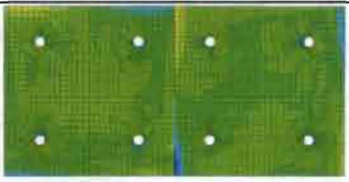</td></tr>
<tr><td><u>30</u> kNm</td><td>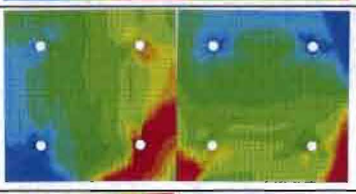</td><td>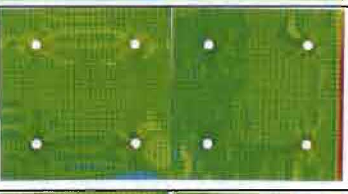</td><td>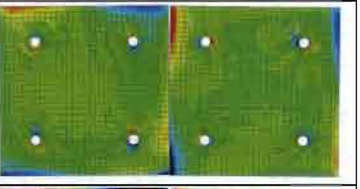</td></tr>
<tr><td>max cap.: <u>36.1</u> kNm</td><td>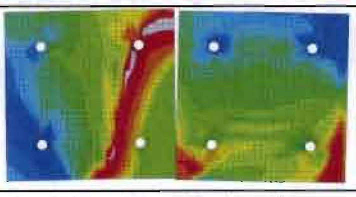</td><td>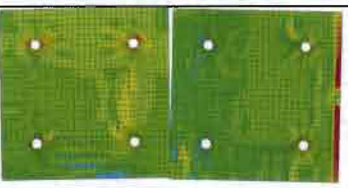</td><td>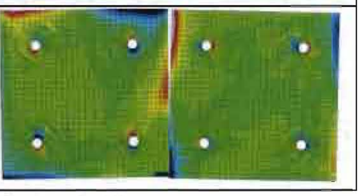</td></tr>
</table>

Table 16: Bond line stress distribution angled connection; t_{timber}=60mm; t_{dvw}=12mm; d=18mm

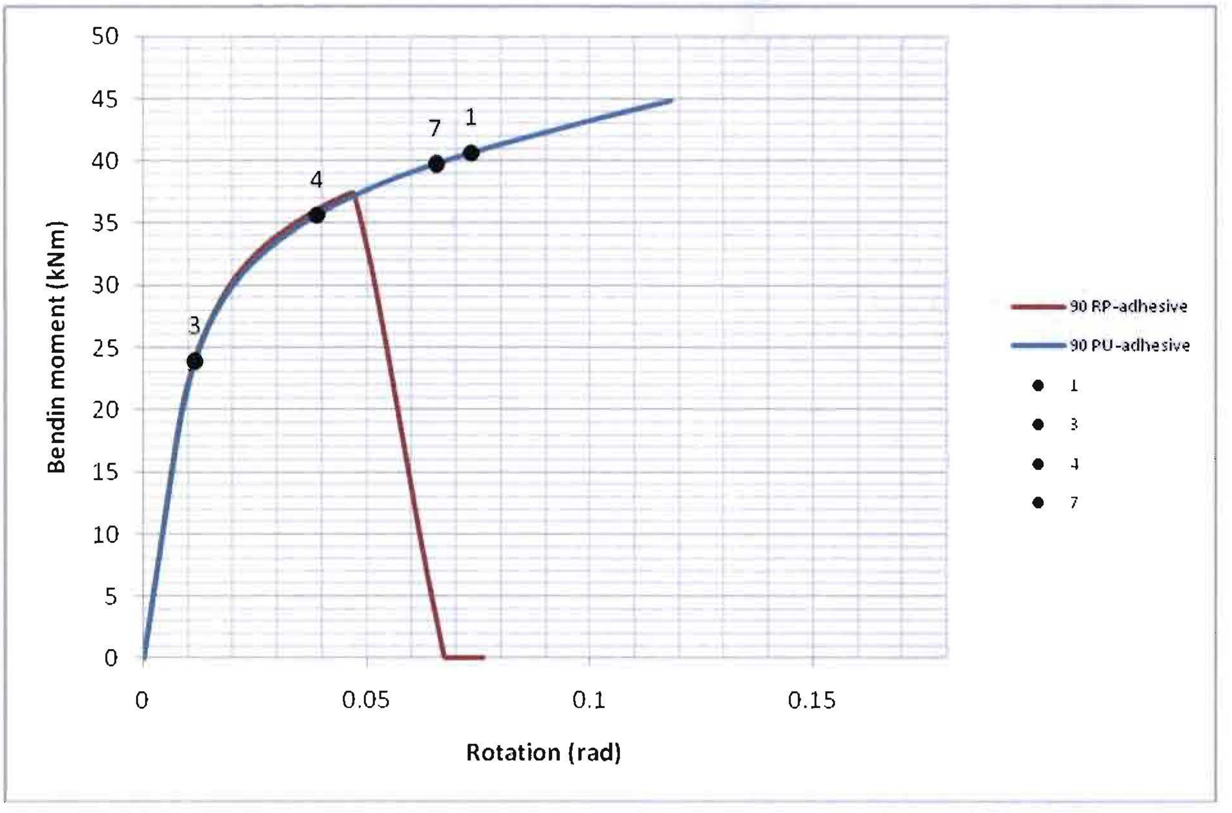

Figure 166: M-φ curve angled connection; t_{timber}=60mm; t_{dvw}=12mm; d=18mm

Appendix 27: Numerical bond line predictions of straight connection with RP-adhesive

RP-adhesive **Thickness = unknown**		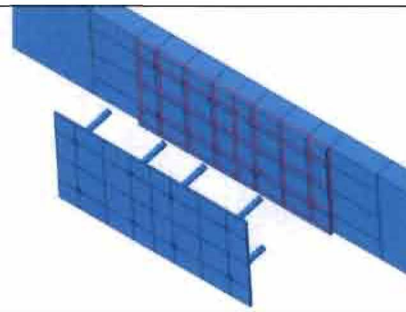	
Bending moment	**shear stress parallel (N/mm²)** 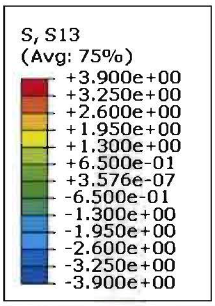	**shear stress perpendicular (N/mm²)** 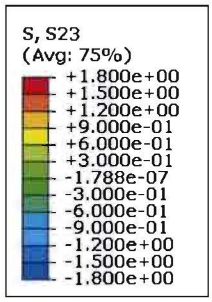	**tensile stress (N/mm²)** 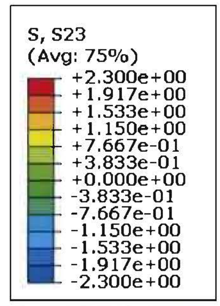
15 kNm	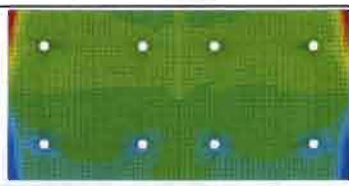	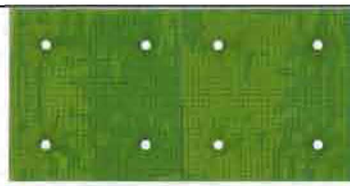	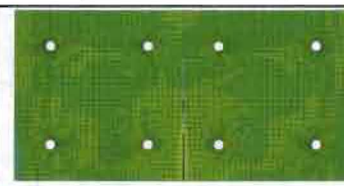
30 kNm	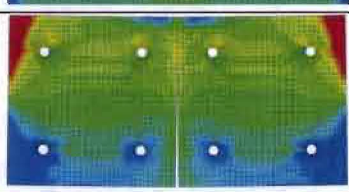	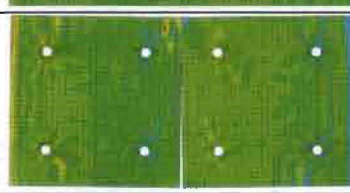	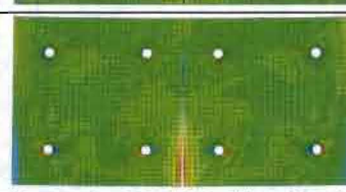
max cap.: 41.9 kNm	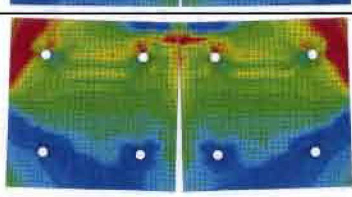	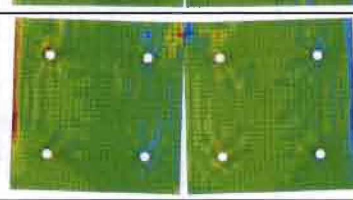	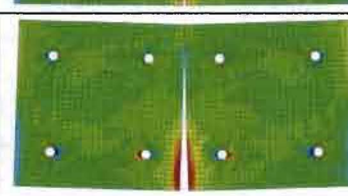

Table 17: Bond line stress distribution straight connection; t_{timber}=60mm; t_{dvw}=12mm; d=18mm

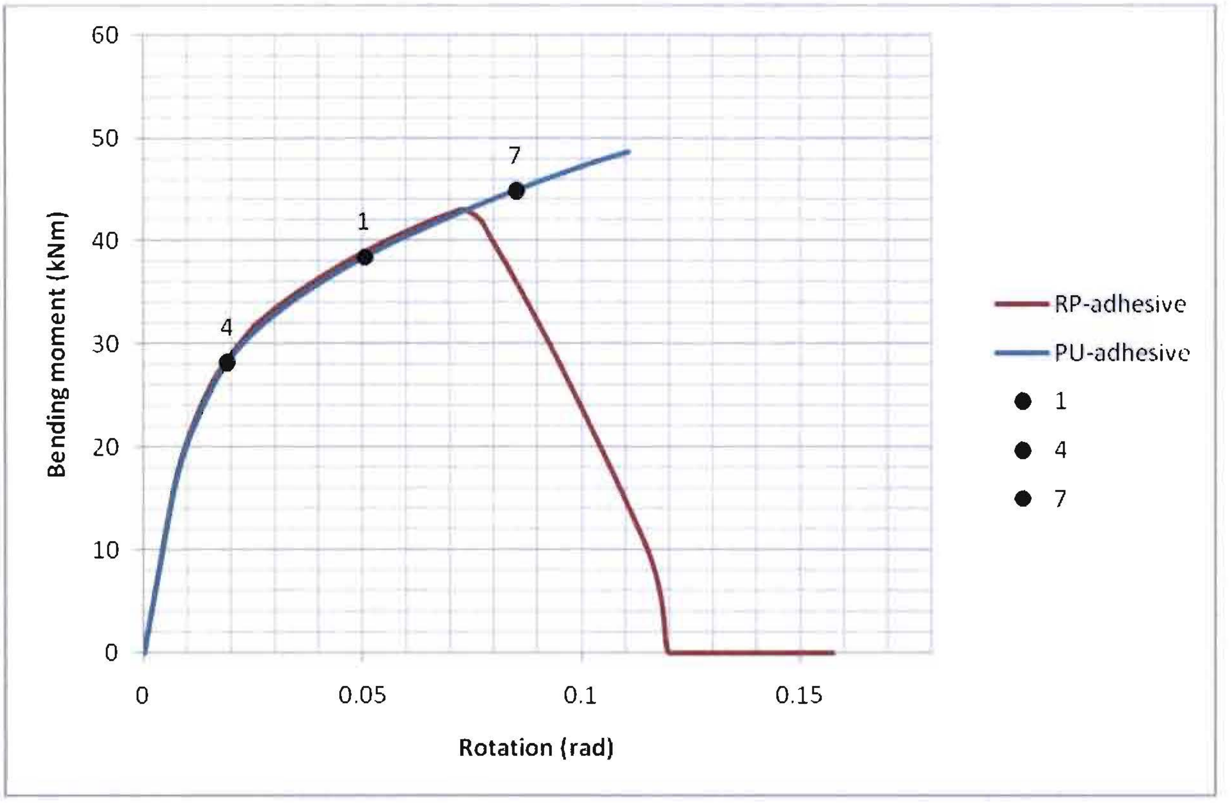

Figure 167: M-φ curve straight connection; t_{timber}=60mm; t_{dvw}=12mm; d=18mm

Appendix 28: Data and material properties of bond line tests at Lund University

			storage duration	
	Relative humidity (%)	Temperature (°C)	Timber	Dvw
Store room	65	20	> 6 months	1 month
Testing room	40	25	4 - 10 days	4 - 10 days

Table 18: Environment properties of the store room and the testing room

North European Spruce

Spruce is the most common wood species used in the Netherlands. Therefore it is useful to choose spruce for the adherent in this research. The average density of the tested spruce is 456 kg/m^3.

Densified Veneer Wood

Densified veneer wood is a plywood of beech veneers, compressed under high temperatures and is available in different densities. The in-plane strength of the product used in these tests is around 110 N/mm^2. Crosswise layed densified veneer has a relatively homogeneous behavior and dependent on the density the material can behave ductile.

Product	Average density (kg/m^3)
Lignostone 1300	1331

Adhesives

In these tests two different adhesives are used with different thicknesses. To accomplish a bond with a high capacity, the adherents should be stronger than the adhesive and the adhesive should behave in a ductile manner. For structural purposes it is recommended to use a 2-component thermosetting adhesive.

Glue type	Product
2-component Epoxy	WEVO spezialharz EP 32 S with WEVO-härter B 22 TS
2-component PU	DuoCol Frencken B.V. Weert

To set the glue line thickness and the size of the glued surface, PTFE distance-sheets of 0.1 mm thickness are used. Dependent on the viscosity of the glue and the amount of pressure on the drying samples, there will be a small volume of glue between the distance sheets and the adherents. As a result the glue line thickness will be bigger than the total thickness of the distance-sheets. The glue dried in the testing room.

Glue type	Sheet thickness (mm)	Average glue line thickness (mm)
PU	0.1	0.23
PU	0.3	0.44
PU	0.5	0.72
Epoxy	0.1	0.16
Epoxy	0.3	0.38
Epoxy	0.5	0.58

Table 19: Distance-sheets thicknesses compared with glue line thicknesses

Appendix 29: Average results of bond line shear tests at Lund University

The deformation measured in the tests includes the deformation of the steel specimen holders and the deformation of the adherents.

Figure 168: Shear tests set-up.

Shear tests average results (parallel to the timber grain)								
Type of adhesive	Separation-sheet tickness (mm)	Actuator speed (mm/min)	Drying time, t (days)	Number of tests	Glue thickness, d_g	Strength, f (N/mm2)	Fracture energy, Gc	Initial stiffness, K (N/mm3)
Poly-urethane	0.1	0.1	t<2	3	0.21	5.80	1829	79
			2<t<4	6	0.23	8.68	3644	323
			t>4	2	0.24	10.20	1858	329
	0.3	0.3	t<2	2	unknown	8.12	2642	7
			2<t<4	10	0.44	8.61	5237	110
	0.5	0.4	t<2	4	0.74	7.14	5882	32
			2<t<4	4	0.73	7.52	6074	91
			t>4	4	0.72	9.24	4939	125
Epoxy	0.1	0.1	-	10	0.16	14.09	3135	379110
	0.3	0.1	-	10	0.4	17.16	3985	32528
	0.5	0.1	-	10	0.58	15.70	2793	541

Table 20: Average results and properties of shear tests

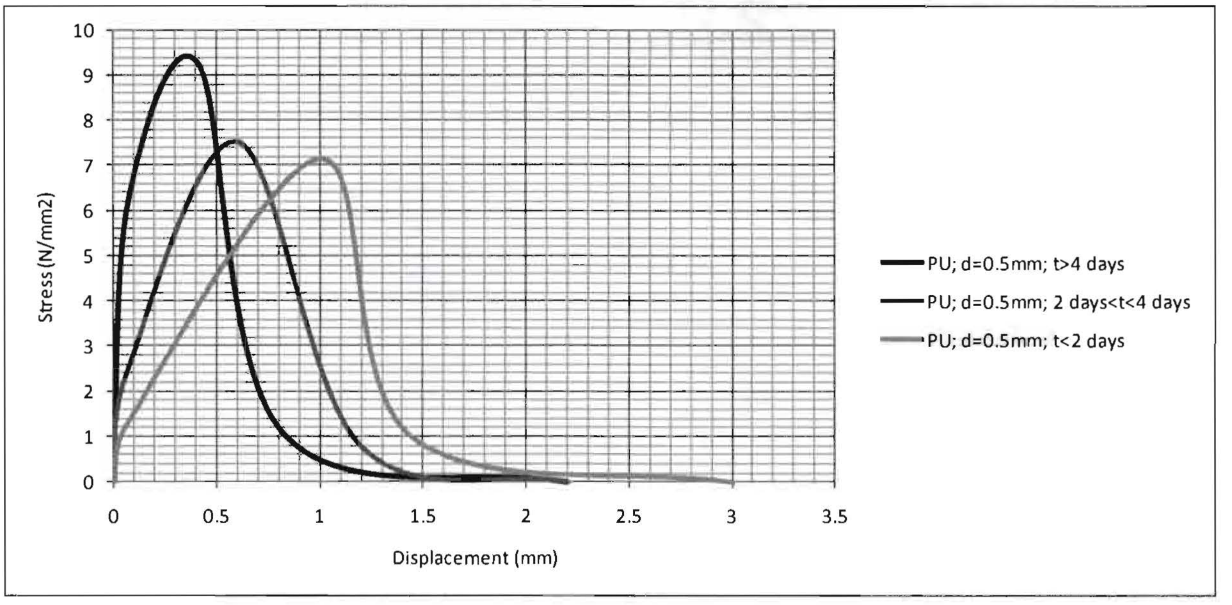

Figure 169: Mean results of shear tests with PU-based adhesive and distance-sheet thickness of 0.1mm and drying time, t

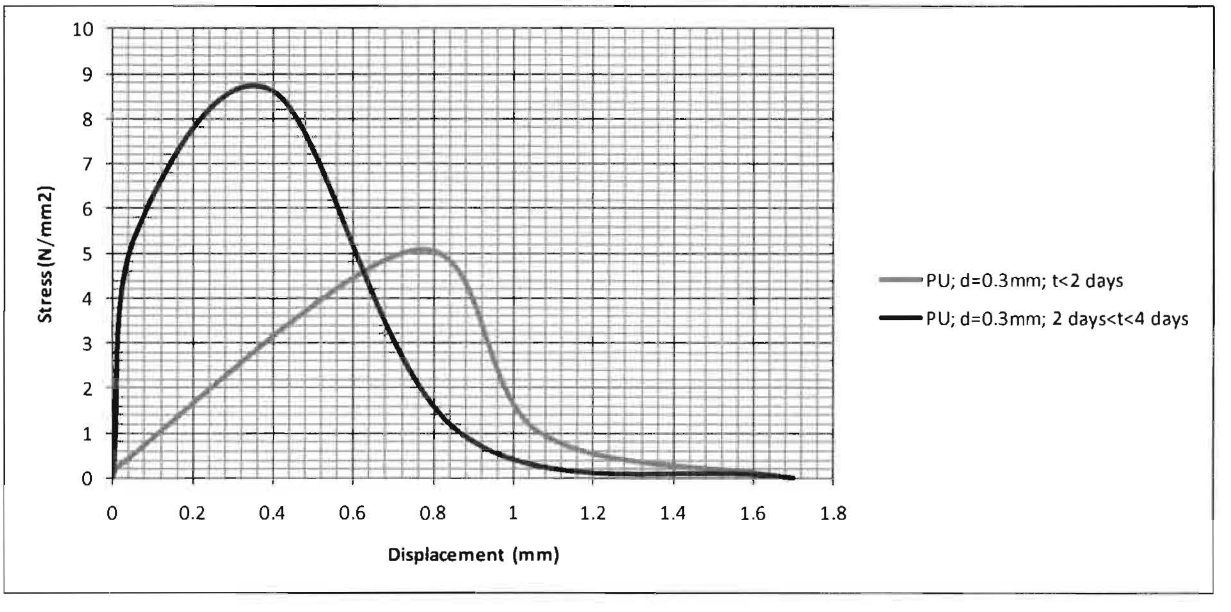

Figure 170: Mean results of shear tests with PU-based adhesive and a distance-sheet thickness of 0.3mm and a drying time, t

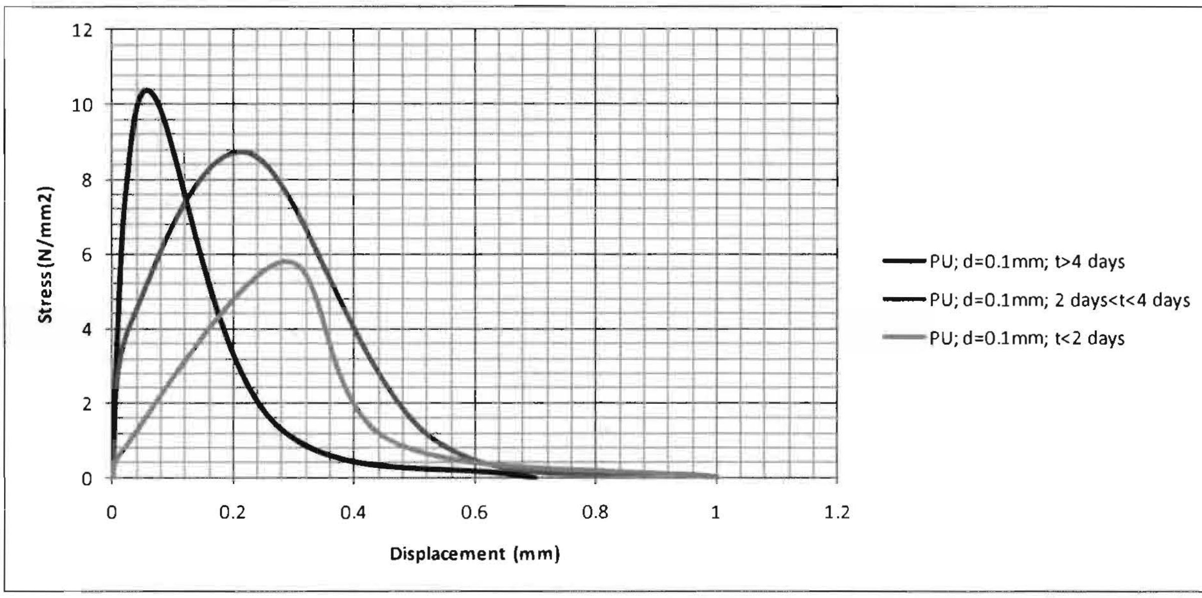

Figure 171: Mean results of shear tests with PU-based adhesive and distance-sheet thickness, d, of 0.5mm and drying time, t

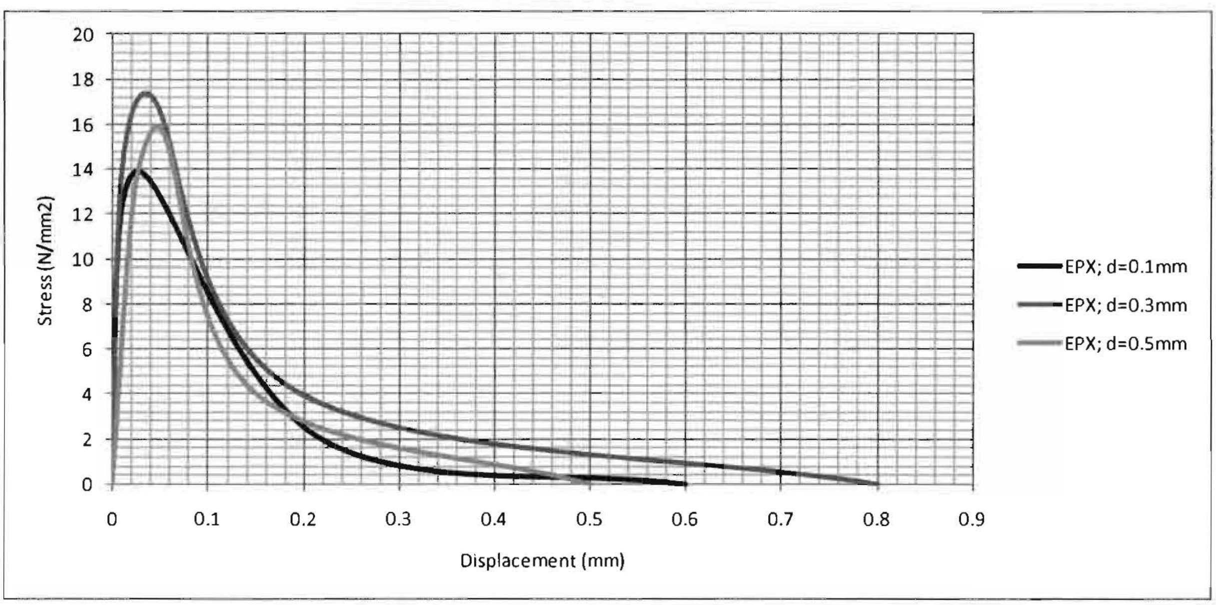

Figure 172: Mean results of shear tests with epoxy-based adhesive and distance-sheet thickness, d

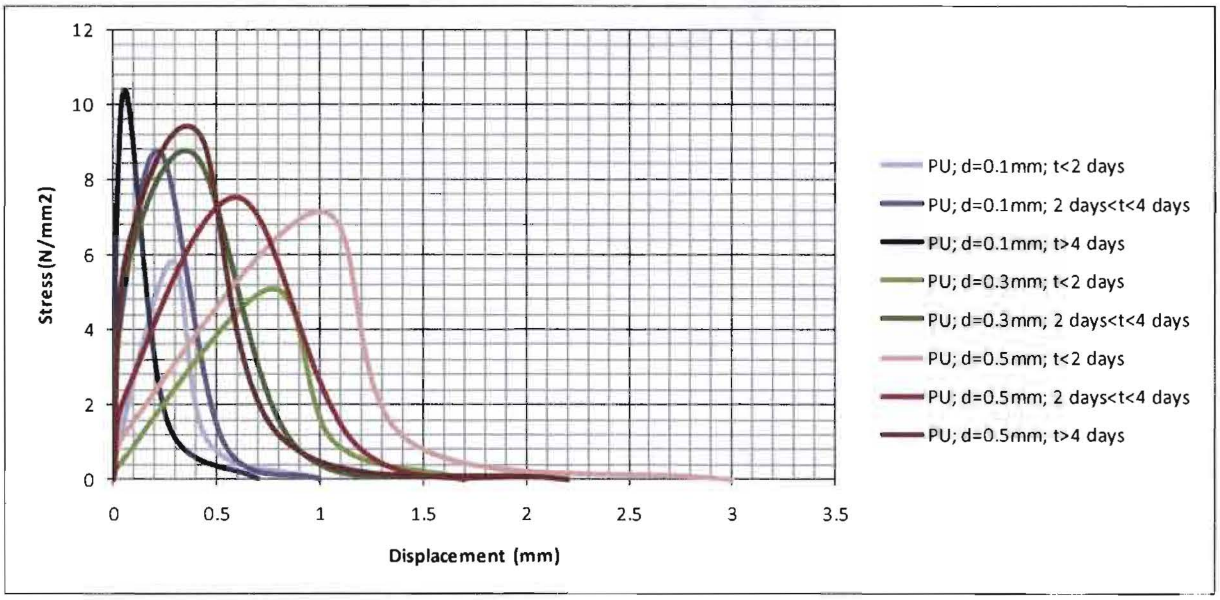

Figure 173: Mean results of shear tests with PU-based adhesive and distance-sheet thicknesses, d, and drying time, t

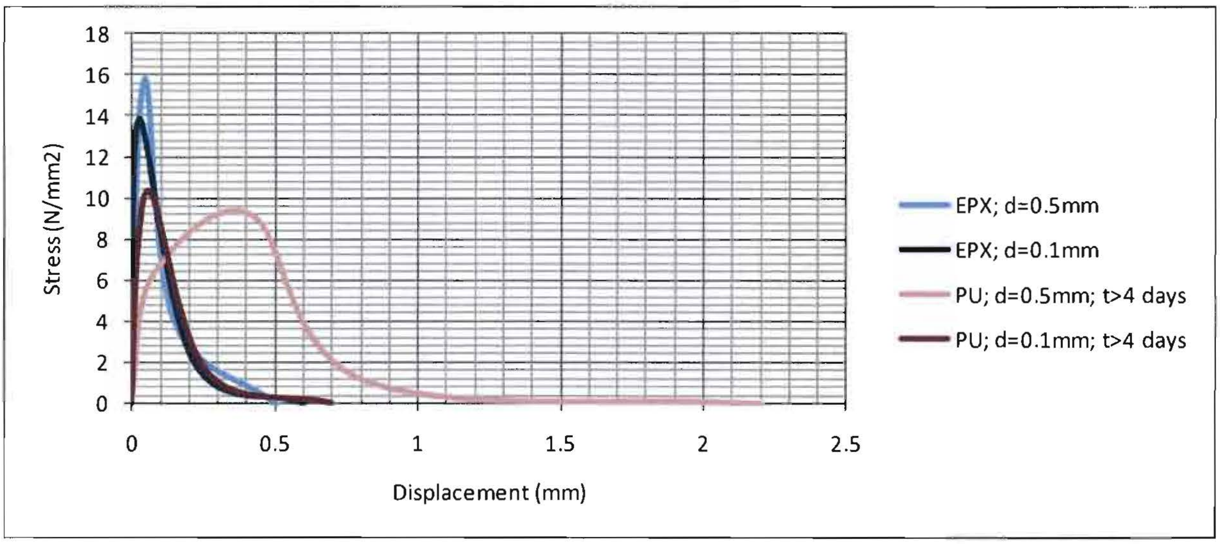

Figure 174: Mean results of shear tests with PU-based and epoxy-based adhesives and distance-sheet thickness, d, and drying time, t

Appendix 30: Average results of bond line tensile tests at Lund University

The thickness of the timber and dvw pieces of the samples is equal to three millimeters. The deformation measured in the test includes the deformation of the timber and the dvw. The strain of the timber is expected to be significantly larger than the strain of the glue. Because of the large scatter in the modulus of elasticity perpendicular to the timber grain, it would be inaccurate to eliminate the strain of the timber the same way it is done with the shear tests. The modulus of elasticity of the glue will be estimated with additional tests. With this E-modulus, it is possible to compare the stiffness of different glue line thicknesses.

Figure 175: Tensile tests set-up.

Tensile tests average results							
Type of adhesive	Separation-sheet tickness (mm)	Actuator speed (mm/min)	Number of tests	Glue thickness, d_g (mm)	Strength, d_g (mm)	Fracture energy, Gc (J/m2)	Initial stiffness, K (N/mm3)
Poly-urethane	0.1	0.2	5	0.26	5.19	1734	72
	0.3	0.2	5	0.47	5.2	1059	59
	0.5	0.2	5	0.66	8.05	1466	111
Epoxy	0.1	0.2	5	0.2	5.03	991	78
	0.3	0.2	5	0.38	5.35	1049	94
	0.5	0.2	4	0.6	4.96	867	59

Table 21 Average results and properties of tensile tests

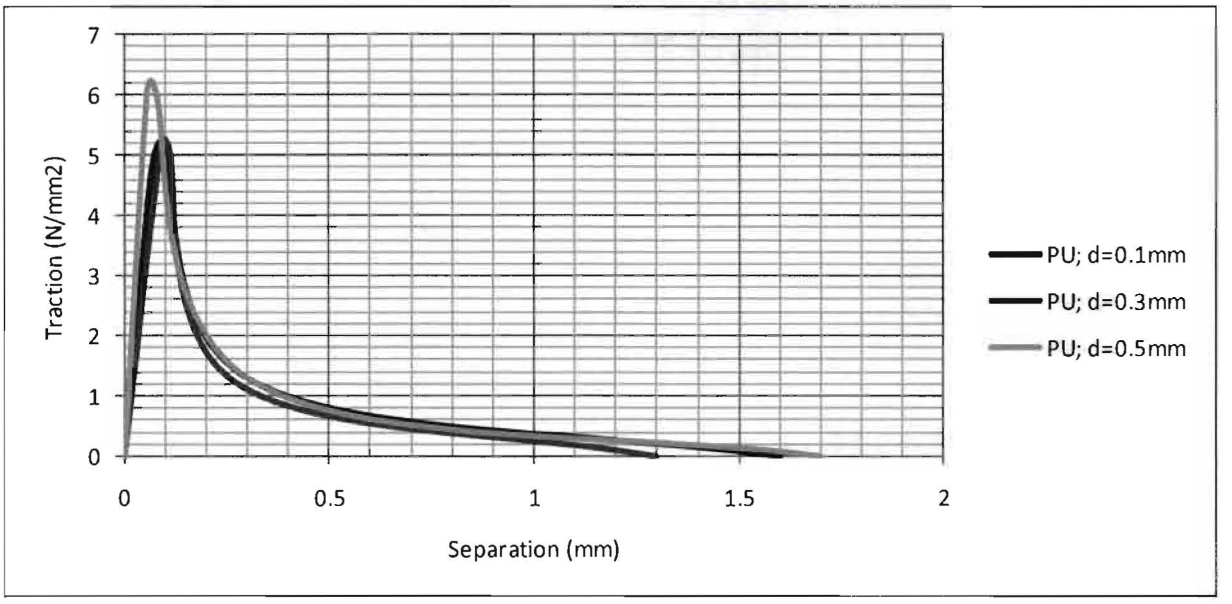

Figure 176 Mean results of tensile tests with PU-based adhesive and distance-sheet thickness, d

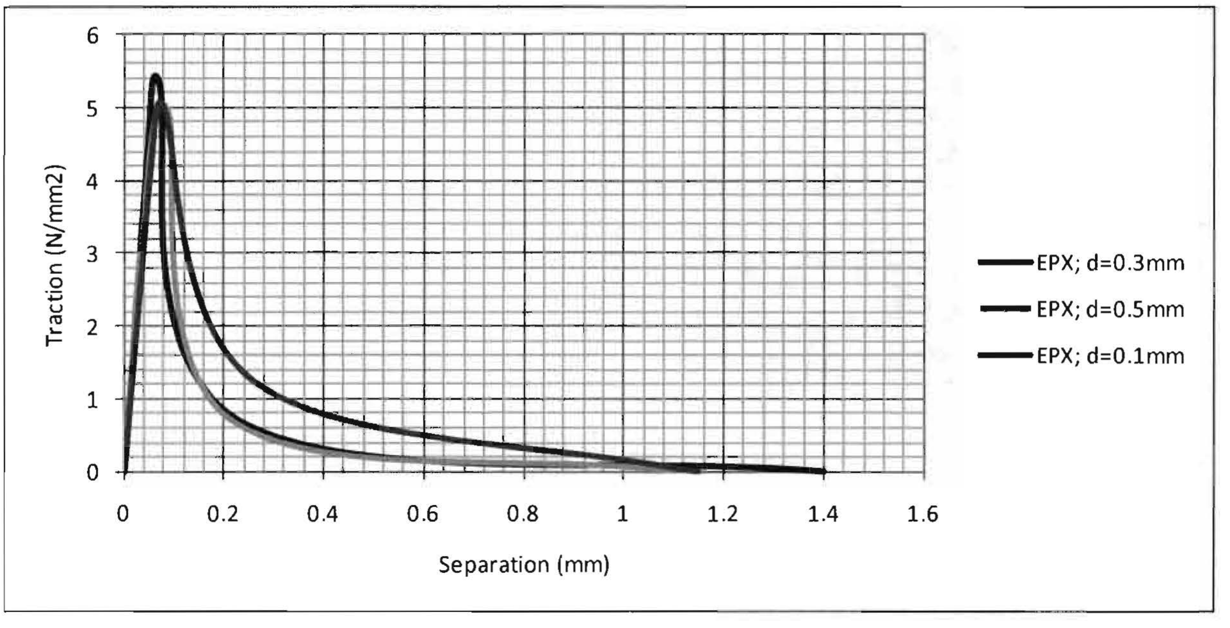

Figure 177: Mean results of tensile tests with epoxy-based adhesive and distance-sheet thickness, d

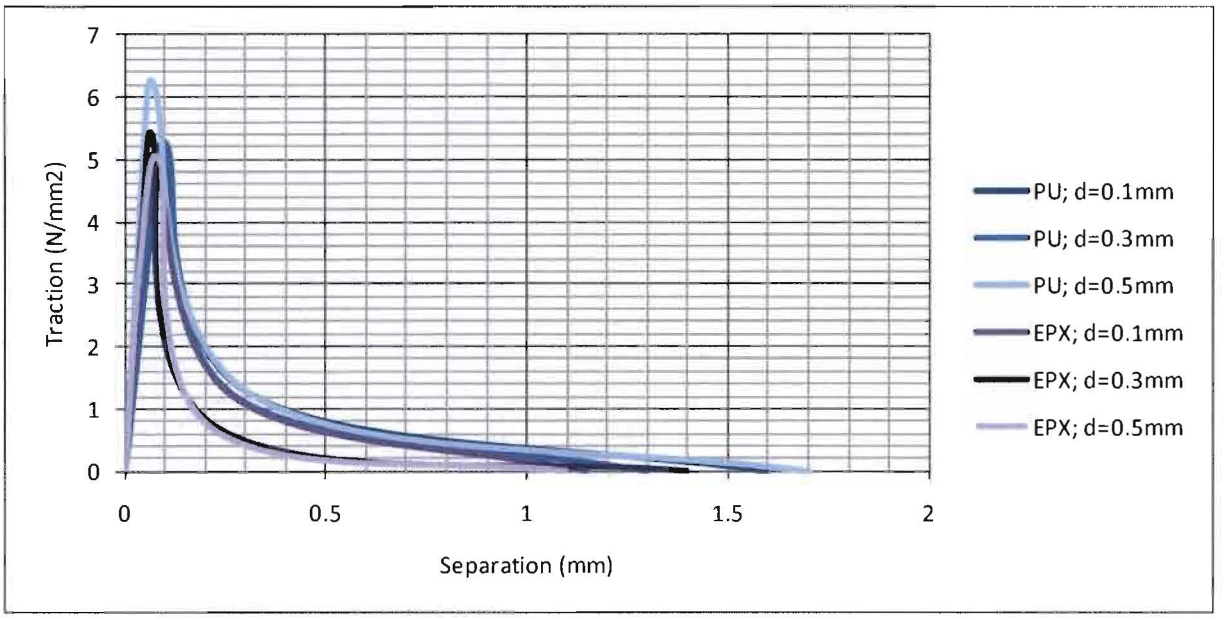

Figure 178: Mean results of tensile tests with PU-based and epoxy-based adhesive and distance-sheet thickness, d

Appendix 31: Detailed results of bond line shear tests at Lund University

Poly-urethane;   d=0,1 mm

							Used for the estimation of:				Percentage of bond surface failed:					
Sample	Angel of anual rings to loaded surface (°)	Fracture energy (J/m2)	Strength (N/mm2)	Initial stiffness (N/mm3)	days of drying	Glue thickness (mm)	Initial stiffness	Strength	Fracture energy	Notes	Timber	Interaction timber-adhesive	Adhesive	Interaction dvw-adhesive	Dvw
PU1-1	unknown	1633	5.48	88	1	0.21	yes	yes	yes				100		
PU2-1	85	1988	6.73		1	0.2	no	yes	yes	1			100		
PU3-1	0	3967	12.39	307	2	0.25	yes	yes	yes		30		70		
PU4-1	10	1876	10.05	361	5	0.28	yes	yes	yes			100			
PU5-1	20	1839	10.34	297	5	0.21	yes	yes	yes		50	50			
PU6-1	55			192	3	0.24	yes	no	no	2	unknown	unknown	unknown	unknown	unknown
PU7-1	30	2876	8.66	198	3	0.19	yes	yes	yes	3	40		60		
PU8-1	5		4.75	217	3	0.28	yes	yes	yes	4	50		50		
PU9-1	0	3642	9.19	848	3	unknown	yes	yes	yes				100		
PU10-1	5	4091	8.39	175	3	unknown	yes	yes	yes				100		
test5	unknown	1867	5.19	70	1	0.22	yes	yes	yes				100		

Notes	
1	Timber part contacted steel holder of dvw part at the beginning
2	X 60* adhesive failed
3	X 60* adhesive between steel holders, but this glue failed short after start of the test
4	Glue line thickness not uniform. Goes from 0,21 mm up to 0,35 mm

* X 60 is a fast drying adhesive, used to attach the samples to the steel holders

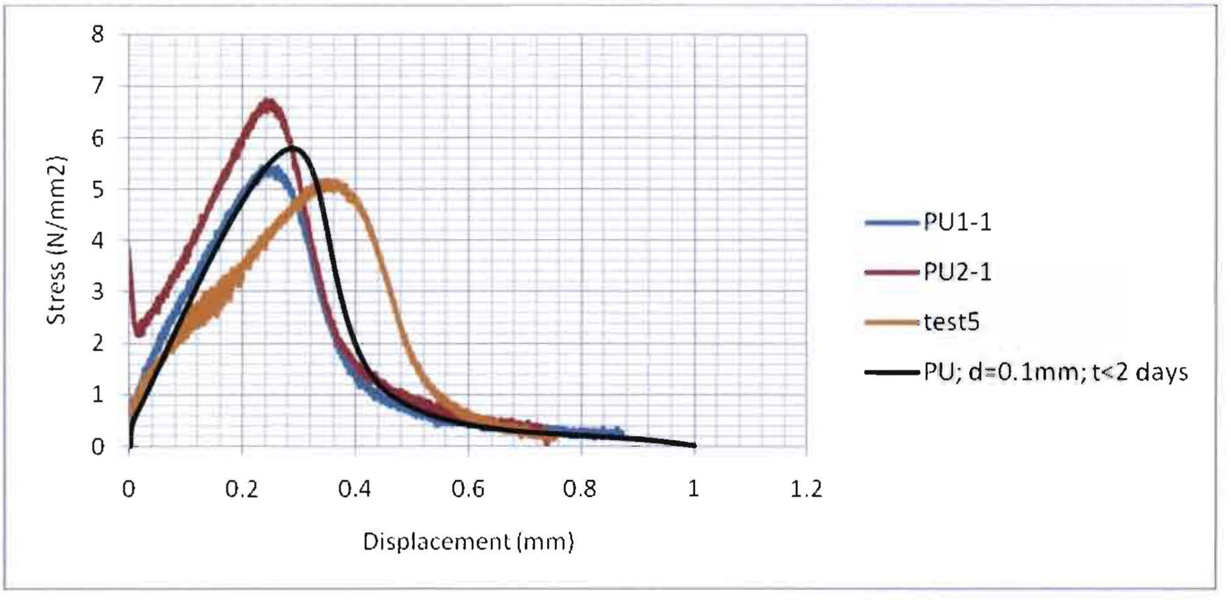

Figure 179: Results of shear tests with PU-based adhesive. d=0.1 mm; t<2 days

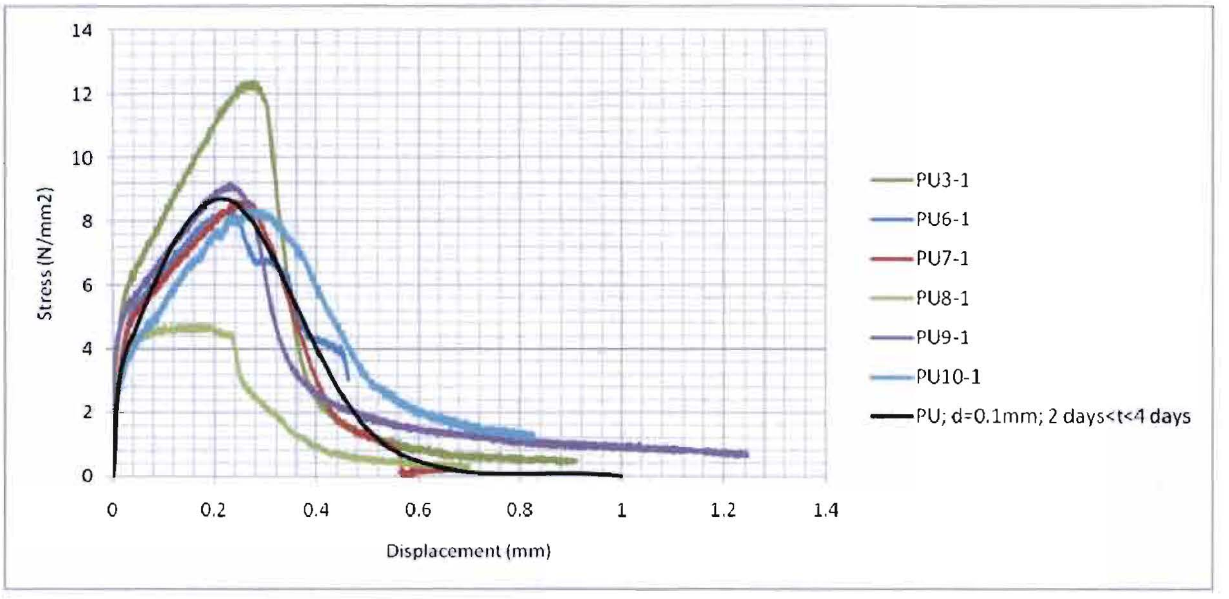

Figure 180: Results of shear tests with PU-based adhesive. d=0.1 mm; 2<t<4 days

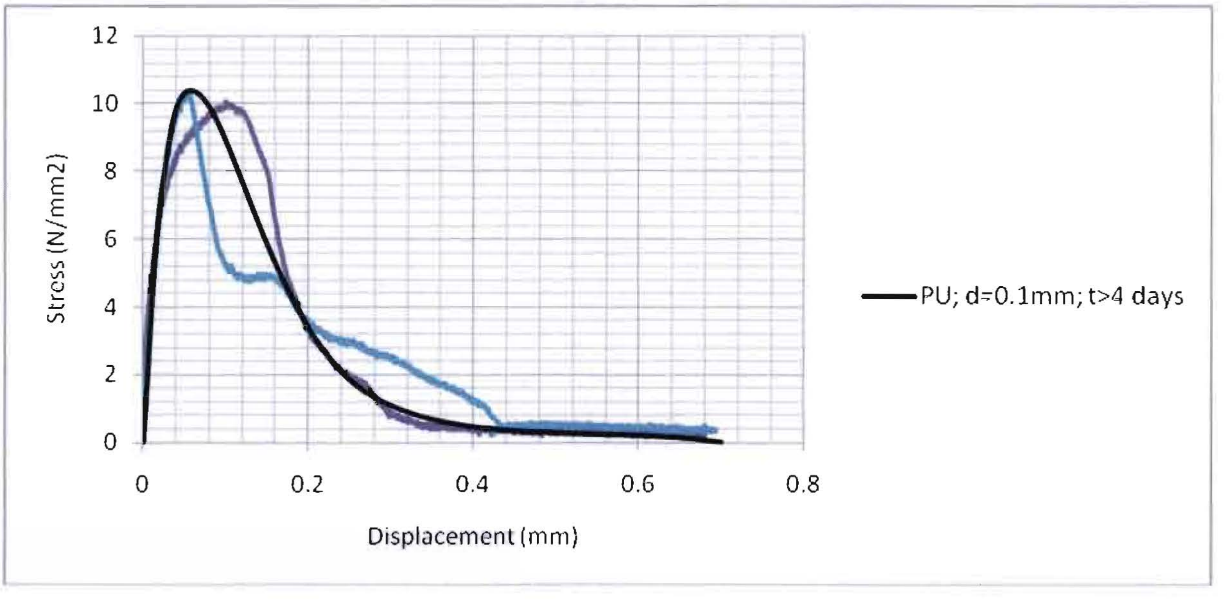

Figure 181: Results of shear tests with PU-based adhesive. d=0.1 mm; t>4 days

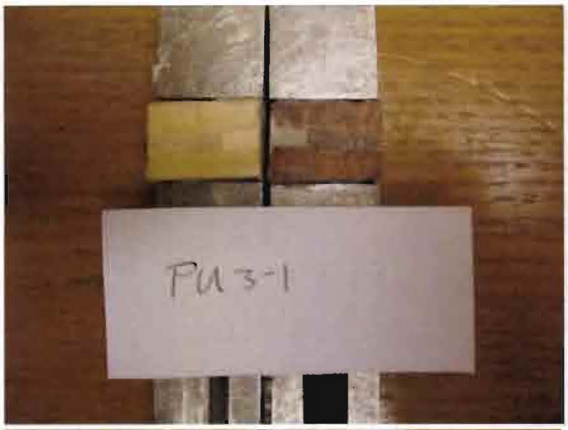
PU 3-1

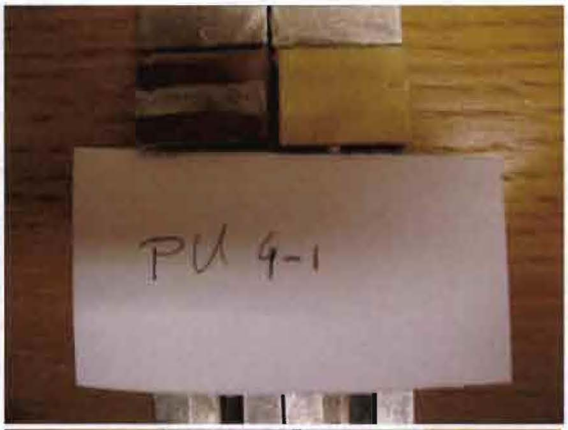
PU 4-1


PU 5-1


PU 6-1


PU 7-1

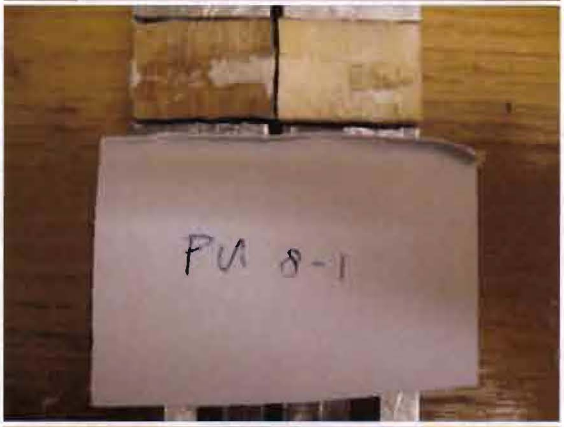
PU 8-1

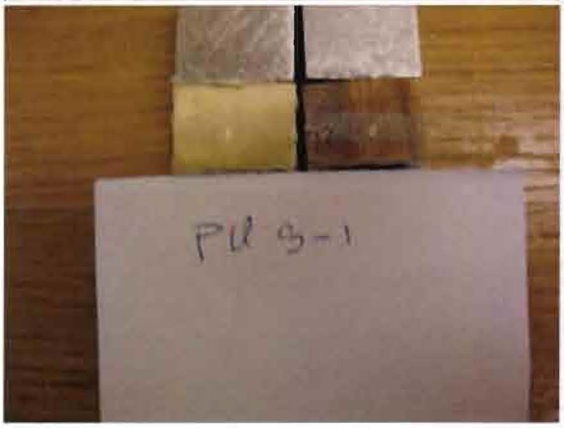
PU 9-1

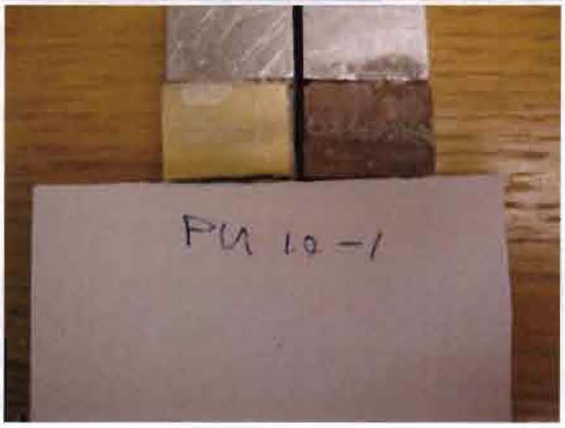
PU 10-1

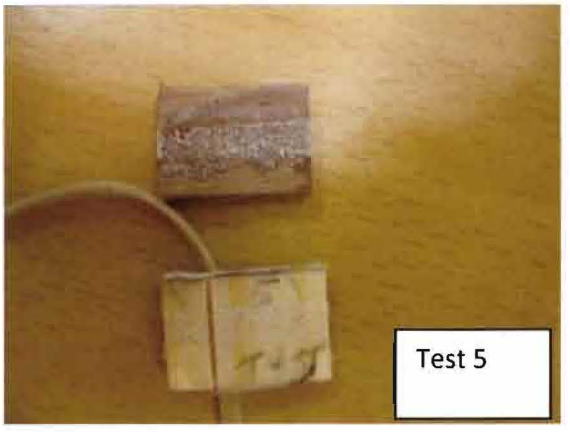
Test 5

Poly-urethane;   d=0,3 mm

							Used for the estimation of:				Percentage of bond surface failed:				
Sample	Angel of anual rings to loaded surface (°)	Fracture energy (J/m2)	Strength (N/mm2)	Initial stiffness (N/mm3)	days of drying	Glue thickness (mm)	Initial stiffness	Strength	Fracture energy	Notes	Timber	Interaction timber-adhesive	Adhesive	Interaction dvw-adhesive	Dvw
PU1-3	10			69	2	0.35	yes	no	no	1			20		80
PU2-3	unknown				2	0.45	no	no	no	2	-	-	-	-	-
PU3-3	5	3981	6.08	104	2	0.48	yes	yes	yes	3			100		
PU4-3	45	8587	11.99	107	2	0.49	yes	yes	yes	3			100		
PU5-3	20	6272	10.34	128	2	0.51	yes	yes	yes				100		
PU6-3	unknown	3698	7.73	110	3	0.35	yes	yes	yes		25		75		
PU7-3	45	4235	6.94	151	3	0.54	yes	yes	yes	4			100		
PU8-3	30	4133	8.56	79	3	0.37	yes	yes	yes				95		5
PU9-3	close to center		9.59	105	3	unknown	yes	yes	no	5	-	-	-	-	-
PU10-3	unknown	5755	7.64	136	3	unknown	yes	yes	yes				100		
test 4	unknown	3365	5.60	8	1	unknown	yes	yes	yes				100		
test 7	unknown	3118	4.53	7	1	unknown	yes	yes	yes				100		

Notes	
1	X 60* adhesive failed
2	test failed completely
3	X 60* adhesive between steel holders, but this glue failed short after start of the test
4	Glue line thickness is large
5	Timber failed due to tension perpendicular to the grain caused by the bending moment

* X 60 is a fast drying adhesive, used to attach the samples to the steel holders

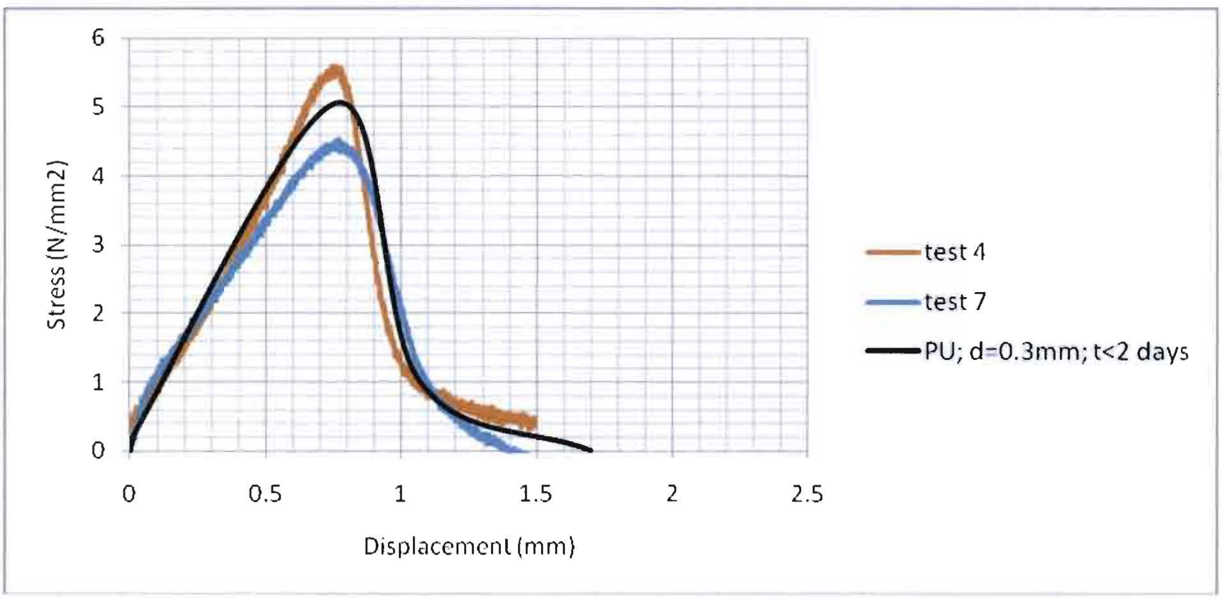

Figure 182: Results of shear tests with PU-based adhesive. d=0.3 mm; t<2 days

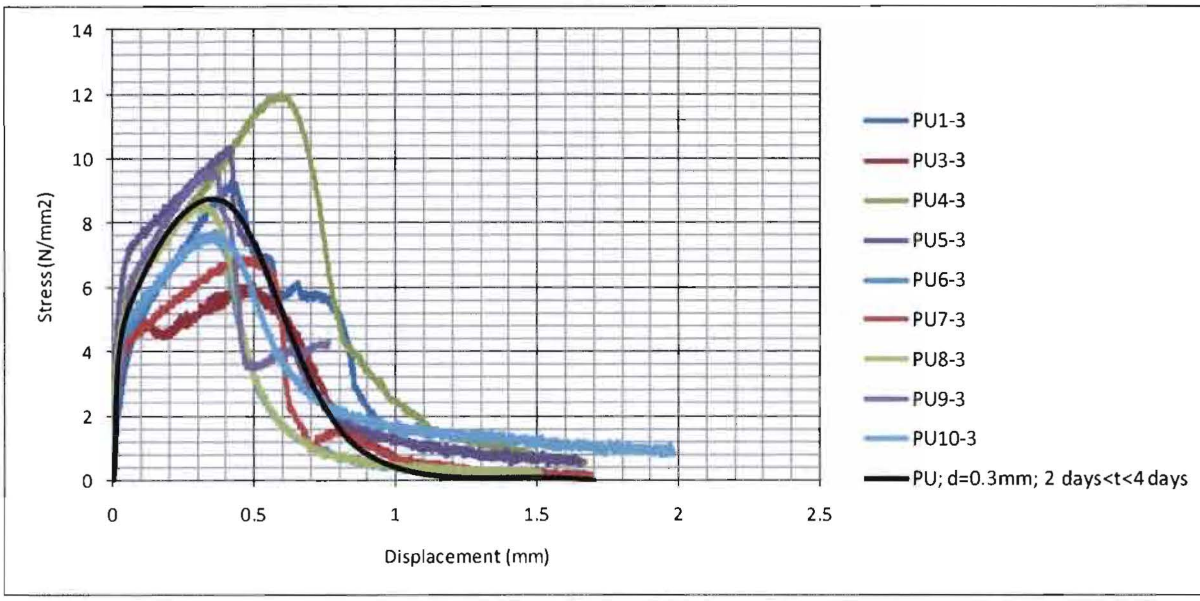

Figure 183: Results of shear tests with PU-based adhesive. d=0.3 mm; 2<t<4 days


PU 6-3


PU 7-3

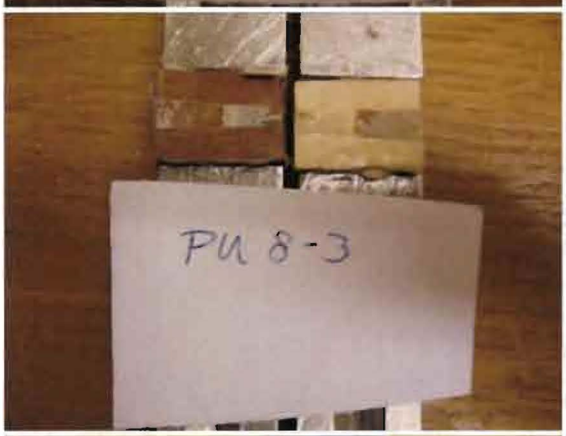
PU 8-3

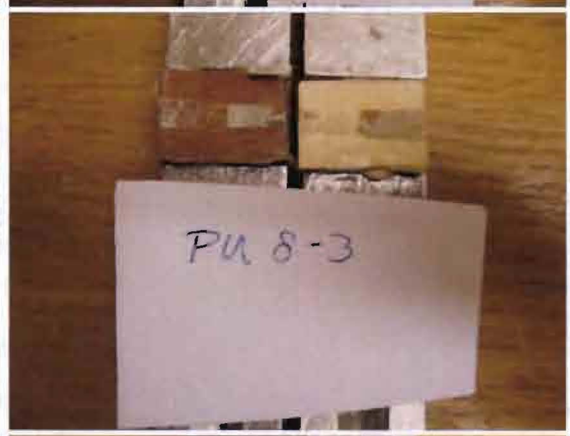
PU 8-3


PU 9-3

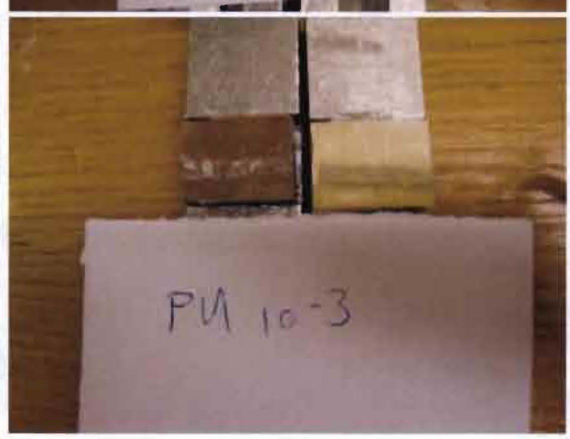
PU 10-3

Poly-urethane; d=0,5 mm

							Used for the estimation of:				Percentage of bond surface failed:				
Sample	Angel of anual rings to loaded surface (°)	Fracture energy (J/m2)	Strength (N/mm2)	Initial stiffness (N/mm3)	days of drying	Glue thickness (mm)	Initial stiffness	Strength	Fracture energy	Notes	Timber	Interaction timber-adhesive	Adhesive	Interaction dvw-adhesive	Dvw
PU1-5	50	4915	6.75	27	1	0.69	yes	yes	yes				100		
PU2-5	30	9507	9.02	33	1	0.79	yes	yes	yes				100		
PU3-5	5	7562	8.75	59	2	0.72	yes	yes	yes		50	40	10		
PU4-5	5			88	2	0.76	yes	no	no	1	unknown	unknown	unknown	unknown	unknown
PU5-5	0			110	2	0.7	yes	no	no	1	100				
PU7-5	0	4585	6.29	107	3	0.69	yes	yes	yes		55		45		
PU8-5	close to center	4540	7.62	161	4	0.76	yes	yes	yes	2			100		
PU6-5	unknown	5038	8.92	154	4	0.68	yes	yes	yes	3			100		
PU9-5	5	5241	7.74	68	4	unknown	yes	yes	yes		50		50		
PU10-5	40		12.67	119	4	unknown	yes	yes	no	4	-	-	-	-	-
test 3	10	1297	6.51	10	1	unknown	yes	yes	yes					100	
test 6		7807	6.28	57	1	unknown	yes	yes	yes				100		

Notes	
1	Due to differences of shear deformation in adhesive, the steel holders rotated
2	X 60* adhesive between steel holders, but this glue failed short after start of the test
3	Rubber bands failed to hold the steel parts parallel to each other
4	Timber failed due to tension perpendicular to the grain caused by the bending moment

* X 60 is a fast drying adhesive, used to attach the samples to the steel holders

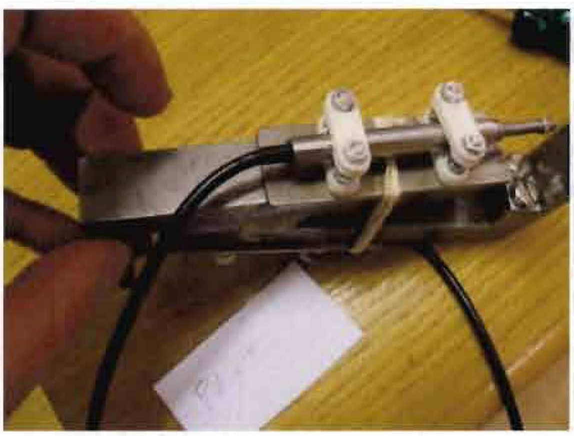

Figure 184: Rotated steel parts

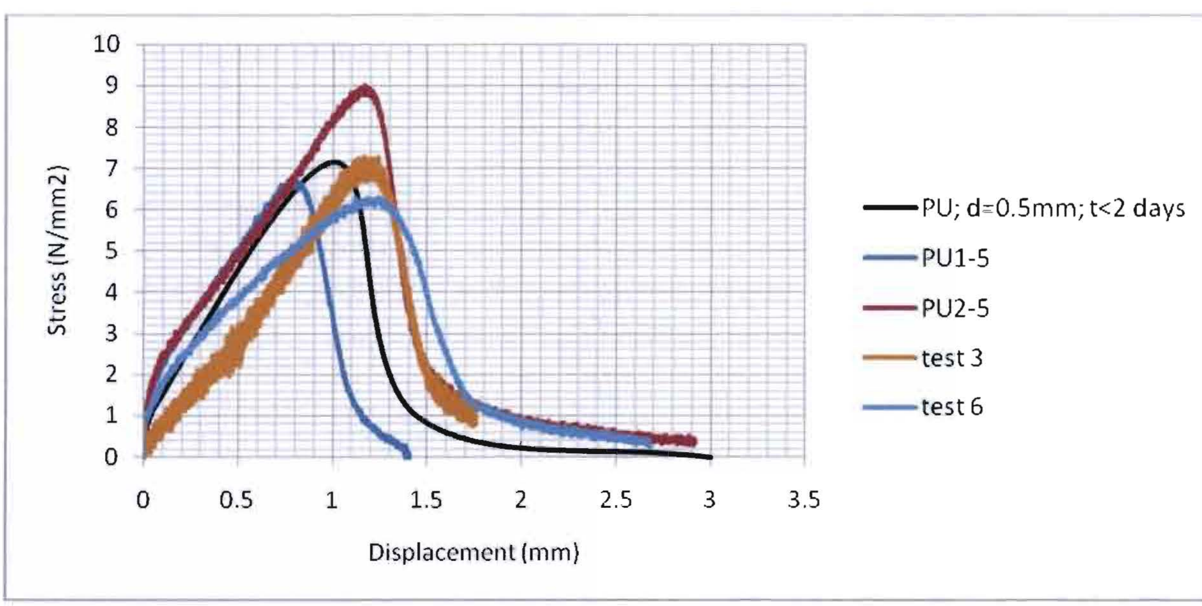

Figure 185: Results of shear tests with PU-based adhesive. d=0.5 mm; t<2 days

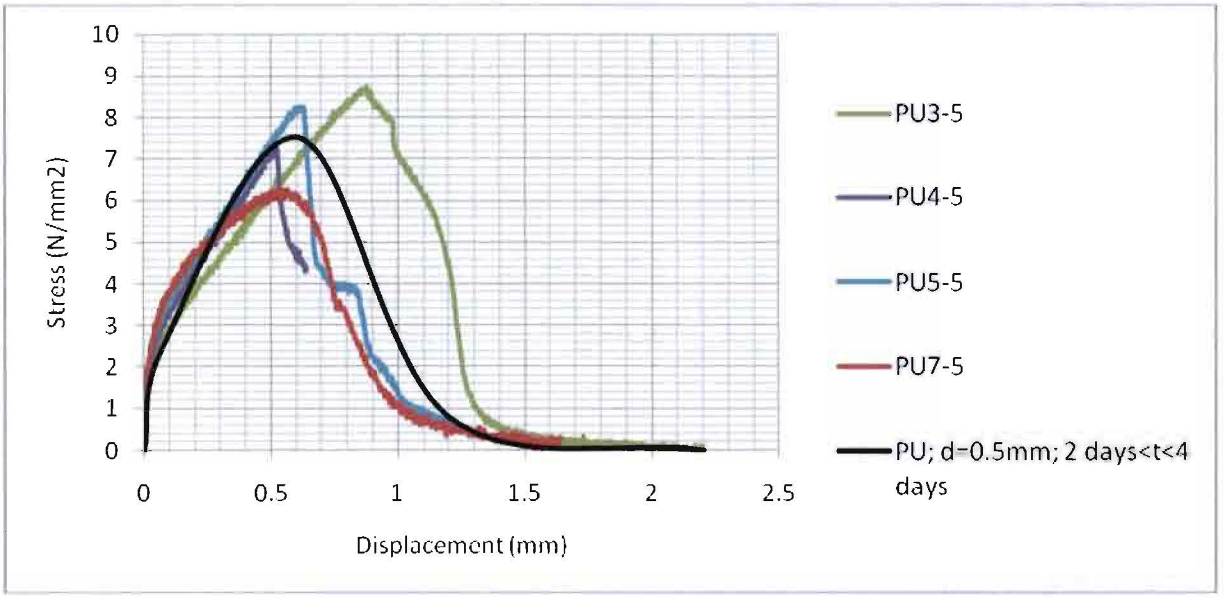

Figure 186: Results of shear tests with PU-based adhesive. d=0.5 mm; 2<t<4 days

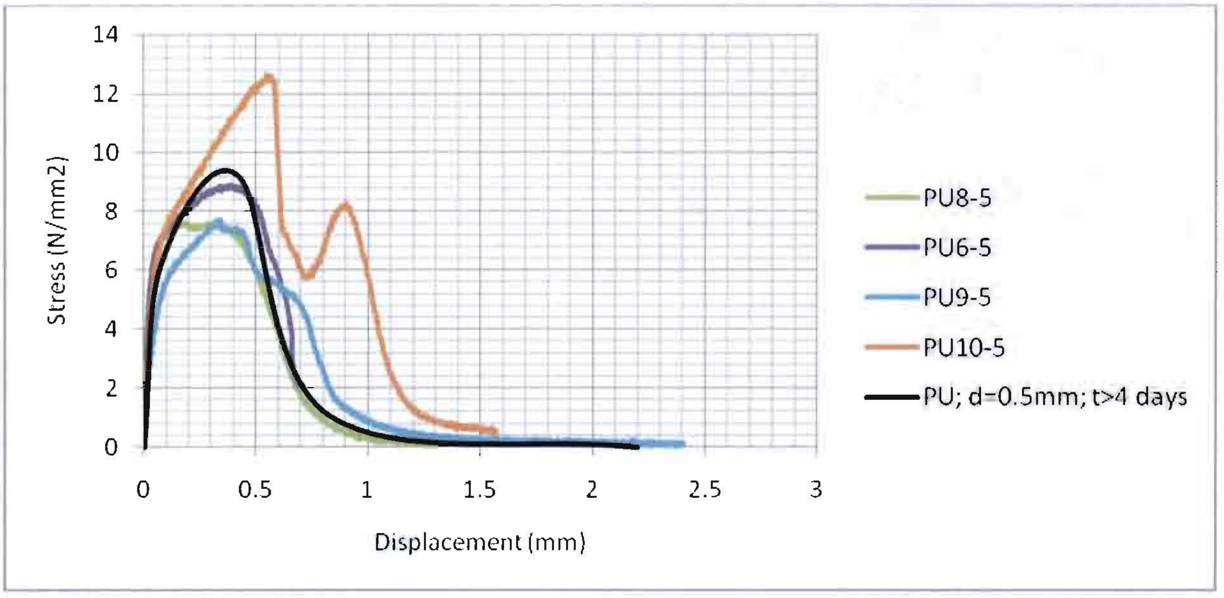

Figure 187: Results of shear tests with PU-based adhesive. d=0.5 mm; t>4 days


PU1-5
PU 2-5
PU 3-5
PU 4-5
Pulled apart after test
PU 5-5
PU 6-5
PU 7-5
PU 8-5

Apendices

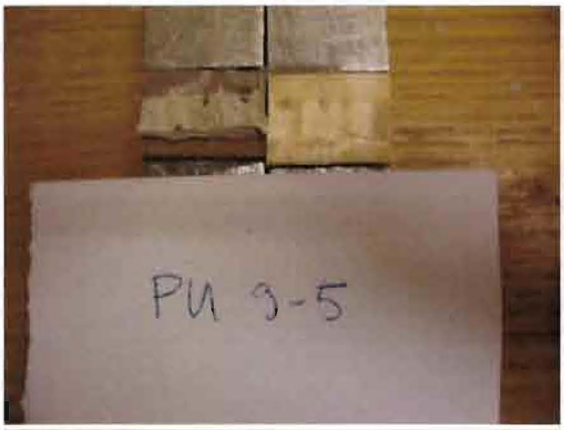

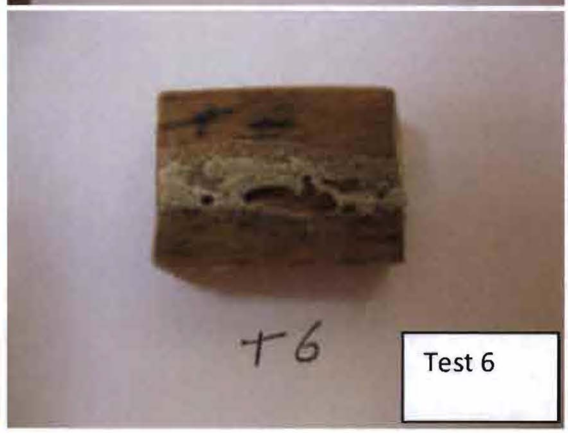

Epoxy; d=0,1 mm

							Used for the estimation of:				Percentage of bond surface failed:				
Sample	Angel of anual rings to loaded surface (°)	Fracture energy (J/m2)	Strength (N/mm2)	Initial stiffness (N/mm3)	days of drying	Glue thickness (mm)	Initial stiffness	Strength	Fracture energy	Notes	Timber	Interaction timber-adhesive	Adhesive	Interaction dvw-adhesive	Dvw
EPX1-1	15				3	0.12	no	no	no	1				100	
EPX2-1	unknown		9.37		3	0.13	no	no	no	1				100	
EPX3-1	30			1884234	2	unknown	yes	no	no	2	70			20	10
EPX4-1	30			5894	2	unknown	yes	no	no	2					100
EPX5-1	35		14.16	762	2	0.16	yes	yes	no	3			20	70	10
EPX6-1	45	3135	12.68	468	2	unknown	yes	yes	yes						100
EPX7-1	40				2	unknown	no	no	no	1	70			30	
EPX8-1	10		16.82		2	0.21	no	yes	no	4	80		15		5
EPX9-1	0				2	unknown	no	no	no	5					
EPX10-1	75	2175	15.43	4192	2	unknown	yes	yes	yes	6	50				50

Notes	
1	Much X 60* adhesive between steel holders
2	X 60* adhesive failed first
3	X 60* adhesive failed during the softening proces
4	X 60* adhesive between steel holders, but this glue failed short after start of the test
5	Timber failed due to tension perpendicular to the grain caused by the bending moment
6	Rubber bands failed to hold the steel parts parallel to each other at the end of the softening

* X 60 is a fast drying adhesive, used to attach the samples to the steel holders

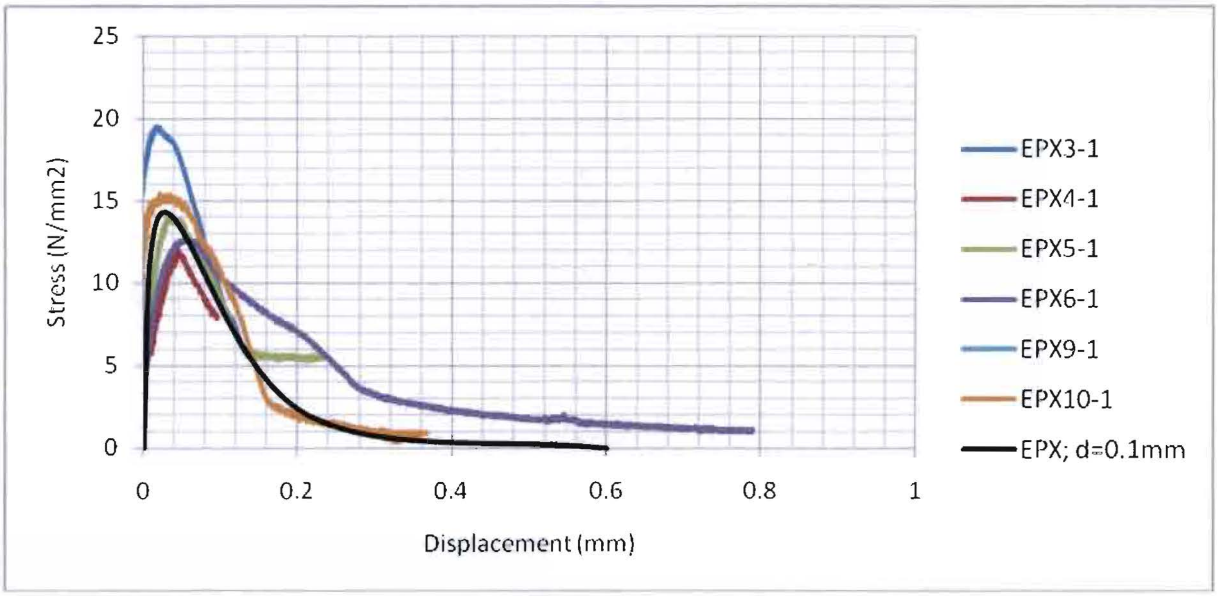

Figure 188: Results of shear tests with epoxy-based adhesive. d=0.1 mm

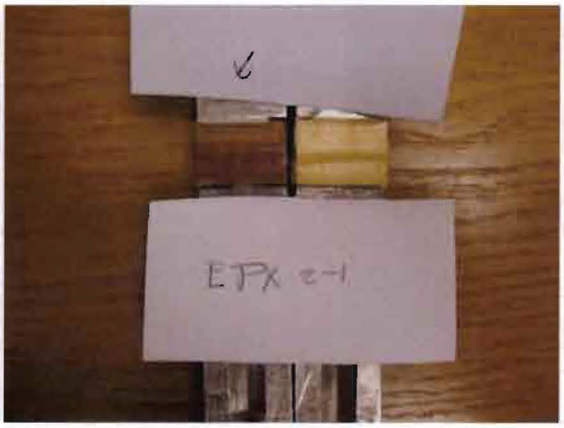

Apendices

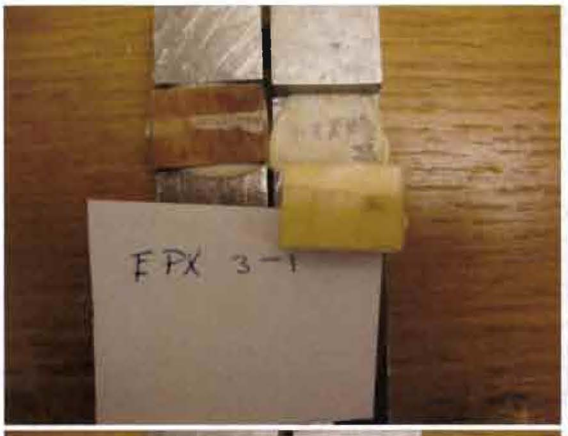

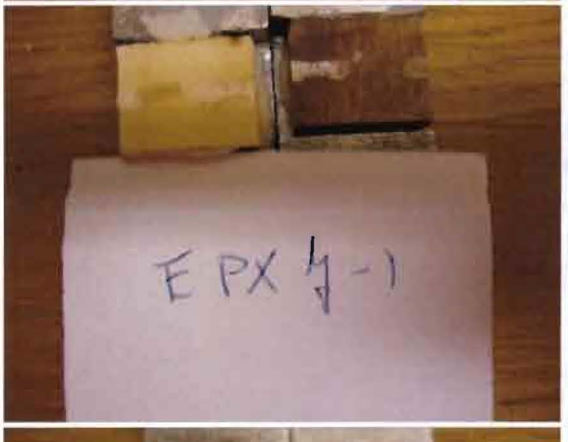

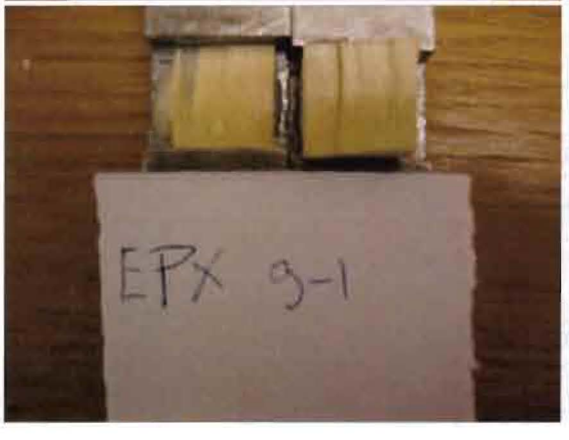

Epoxy; d=0,3 mm

							Used for the estimation of:				Percentage of bond surface failed:				
Sample	Angel of anual rings to loaded surface (°)	Fracture energy (J/m2)	Strength (N/mm2)	Initial stiffness (N/mm3)	days of drying	Glue thickness (mm)	Initial stiffness	Strength	Fracture energy	Notes	Timber	Interaction timber-adhesive	Adhesive	Interaction dvw-adhesive	Dvw
EPX1-3	0				3	0.34	no	no	no	1			100		
EPX2-3	close to center				3	0.38	no	no	no	1			100		
EPX3-3	80			218	2	0	yes	no	no	2					
EPX4-3	0				2	0.47	no	no	no	3	100				
EPX5-3	10	2756	16.16	512	3	0.47	yes	yes	yes		10			90	
EPX6-3	unknown	3503	19.88	138012	3	0	yes	yes	yes	4		50		50	
EPX7-3	90	4215	18.68	85421	3	0.4	yes	yes	yes		100				
EPX8-3	unknown		13.22	272	3	0.68	yes	yes	no	4	100				
EPX9-3	40	5467	17.89	2750	3	0	yes	yes	yes		100				
EPX10-3	0			511	2	0	yes	no	no	2	unknown	unknown	unknown	unknown	unknown

Notes	
1	Preparation failed
2	Timber failed due to tension perpendicular to the grain caused by the bending moment
3	Rubber bands failed to hold the steel parts parallel to each other
4	Test ended little bit early

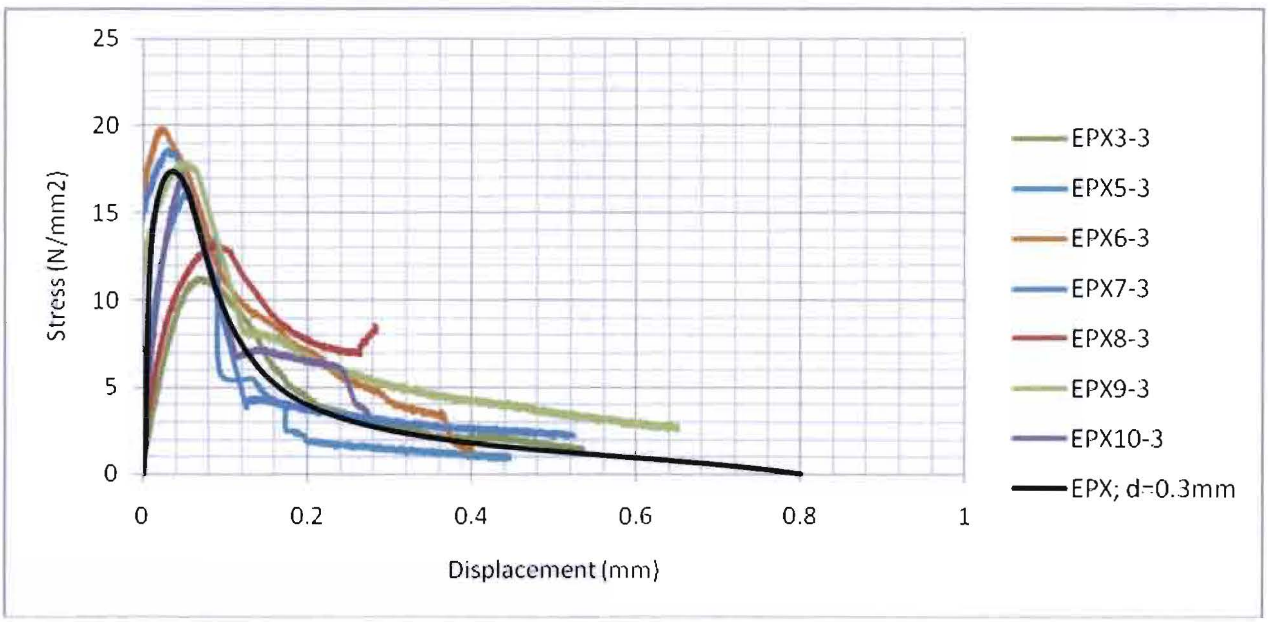

Figure 189: Results of shear tests with epoxy-based adhesive. d=0.3 mm


EPX 3-3


EPX 4-3


EPX 5-3

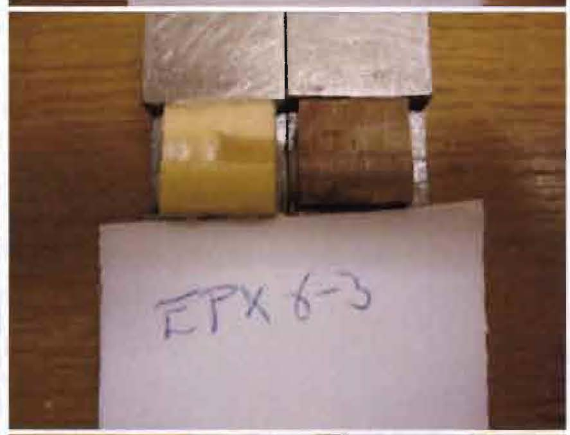
EPX 6-3

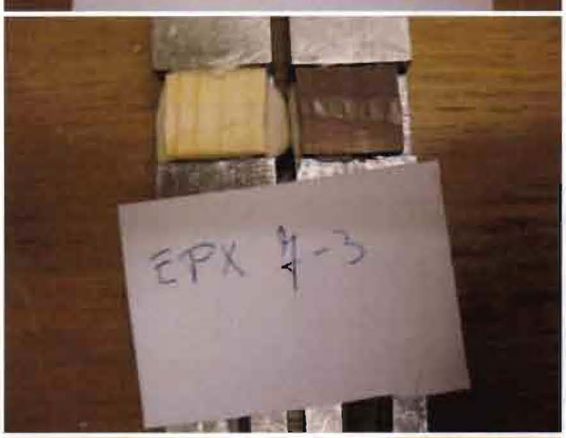
EPX 7-3


EPX 8-3


EPX 9-3

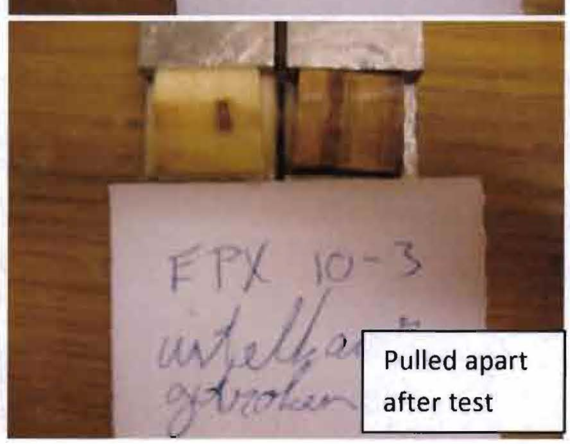
EPX 10-3
Pulled apart after test

Epoxy; d=0,5 mm

Sample	Angel of anual rings to loaded surface (°)	Fracture energy (J/m2)	Strength (N/mm2)	Initial stiffness (N/mm3)	days of drying	Glue thickness (mm)	Used for the estimation of: Initial stiffness	Strength	Fracture energy	Notes	Percentage of bond surface failed: Timber	Interaction timber-adhesive	Adhesive	Interaction dvw-adhesive	Dvw
EPX1-5	30				3	0.57	no	no	no	1					
EPX2-5	5				3	0.59	no	no	no	1					
EPX3-5	45		17.23	669	2	0.56	yes	yes	no	2	unknown	unknown	unknown	unknown	unknown
EPX4-5	30	3332	13.07	505	2	0.63	yes	yes	yes	3,5	100				
EPX5-5	0	2472	17.71	873	2	0.49	yes	yes	yes	5	100				
EPX6-5	unknown				2	0.68	no	no	no	1					
EPX7-5	45	2143	15.38	381	2	0.44	yes	yes	yes					50	50
EPX8-5	unknown			625	2	0.6	yes	no	no	1	100				
EPX9-5	25				2	0	no	no	no	4					
EPX10-5	unknown	3226	15.09	278	2	0	yes	yes	yes		100				

Notes	
1	Much X 60* adhesive between steel holders
2	X 60* adhesive between steel holders, but this glue failed short after start of the test
3	Much X 60* adhesive between steel holders, but it does not seem to effect the results.
4	Timber failed due to tension perpendicular to the grain caused by the bending moment
5	Brittle failure: softening part of curve is influenced by the elastic deformation of the set up

* X 60 is a fast drying adhesive, used to attach the samples to the steel holders

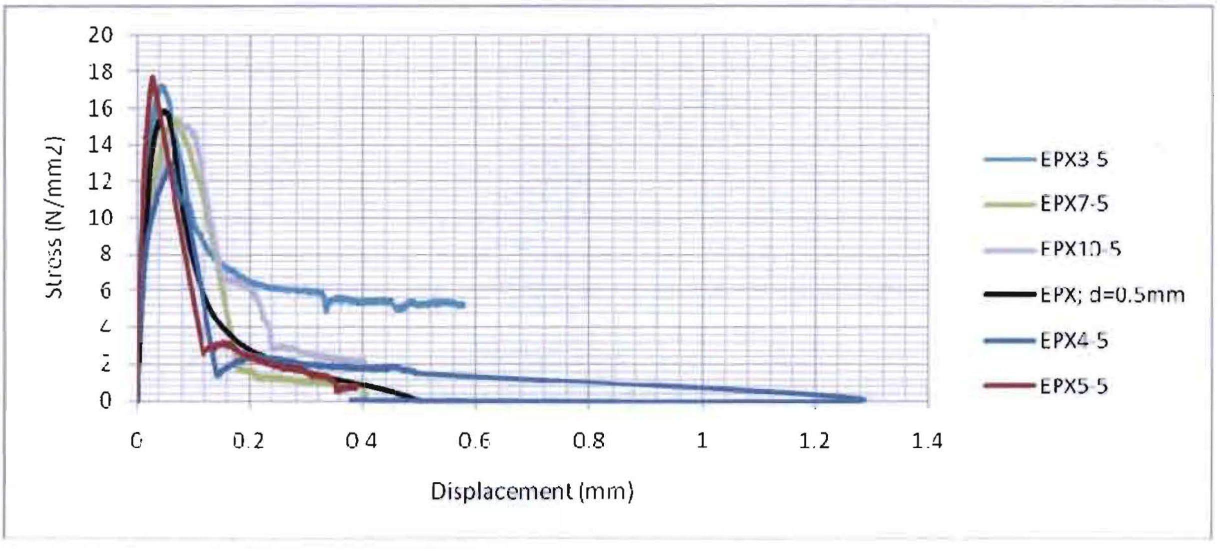

Figure 190: Results of shear tests with epoxy-based adhesive. d=0.5 mm

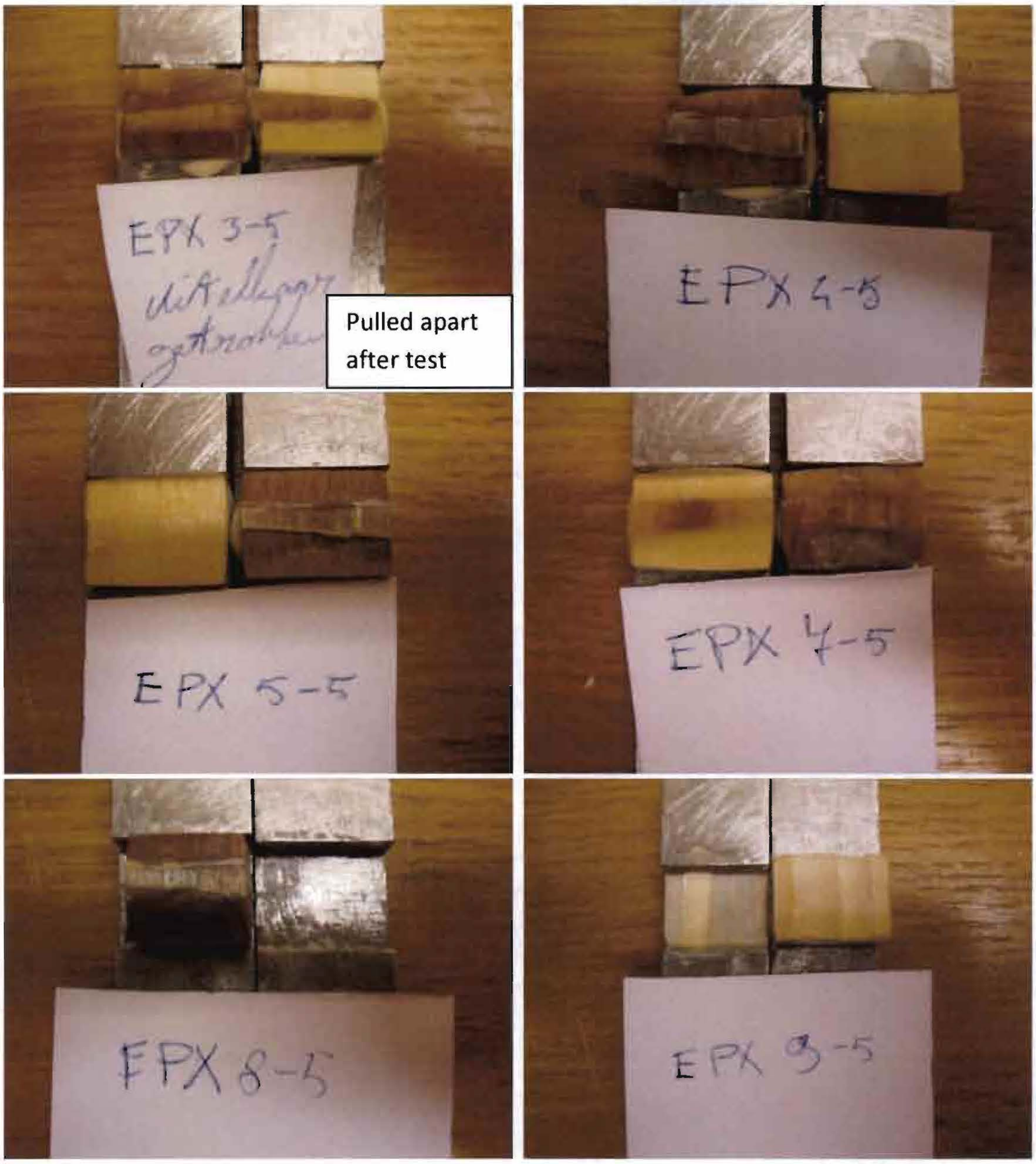
EPX 3-5
Pulled apart after test
EPX 4-5
EPX 5-5
EPX 7-5
EPX 8-5
EPX 9-5

Appendix 32: Detailed results of bond line tensile tests at Lund University

PU; d=0,1 mm

							Used for the estimation of:				Percentage of bond surface failed:				
Sample	Angel of anual rings to loaded surface (°)	Fracture energy (J/m2)	Strength (N/mm2)	Initial stiffness (N/mm3)	days of drying	Glue thickness (mm)	Initial stiffness	Strength	Fracture energy	Notes	Timber	Interaction timber-adhesive	Adhesive	Interaction dvw-adhesive	Dvw
PU1-1T	0				5	0.22	no	no	no	1	100				
PU2-1T	5	1327	4.72	72	5	0.26	yes	yes	yes		100				
PU3-1T	5	1447	4.23		5	0.26	no	yes	yes		100				
PU4-1T	unknown	2429	6.62	72	5	0.27	yes	yes	yes		90		10		
PU5-1T	5				5	0.31	no	no	no	2	70		10		20

Notes

1	Pressure of 9 kN on the specimen before starting the test
2	X 60* adhesive partly failed

* X 60 is a fast drying adhesive, used to attach the samples to the steel holders

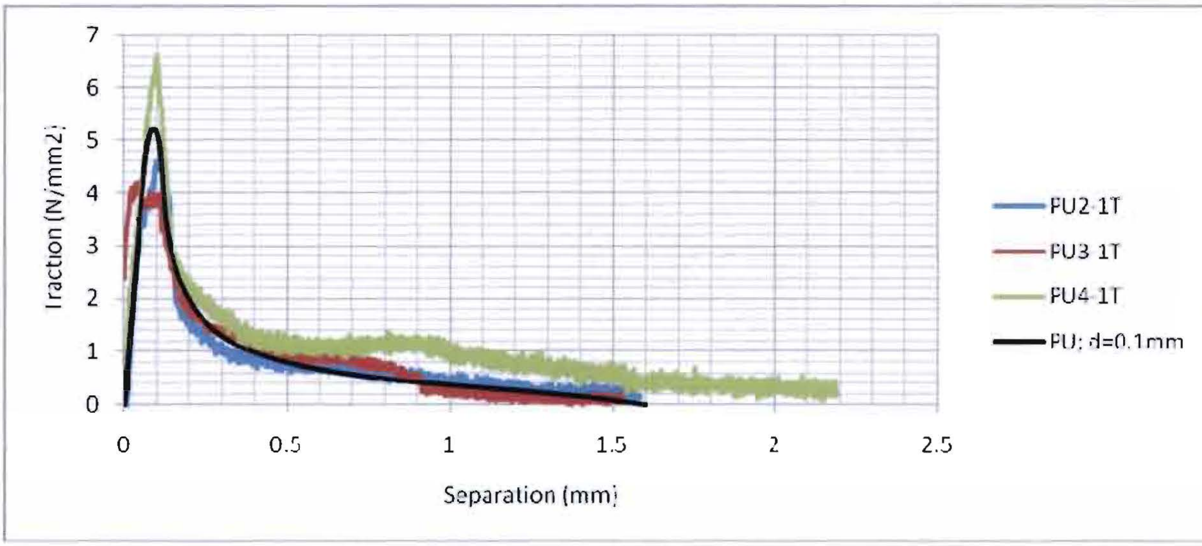

Figure 191: Results of tensile tests with poly-urethane based adhesive. d=0.1 mm

PU; d=0,3 mm

							Used for the estimation of:				Percentage of bond surface failed:				
Sample	Angel of anual rings to loaded surface (°)	Fracture energy (J/m2)	Strength (N/mm2)	Initial stiffness (N/mm3)	days of drying	Glue thickness (mm)	Initial stiffness	Strength	Fracture energy	Notes	Timber	Interaction timber-adhesive	Adhesive	Interaction dvw-adhesive	Dvw
PU1-3T	5	952	4.44	59	5	0.47	yes	yes	yes		90		10		
PU2-3T	0	1167	5.97	58	5	0.44	yes	yes	yes		100				
PU3-3T	5				5	0.54	no	no	no	1	80				20
PU4-3T	0				5	0.86	no	no	no	2					
PU5-3T	0				5	0.43	no	no	no	1	100				

Notes	
1	X 60* adhesive partly failed
2	Pressure of 6 kN on the specimen before starting the test

* X 60 is a fast drying adhesive, used to attach the samples to the steel holders

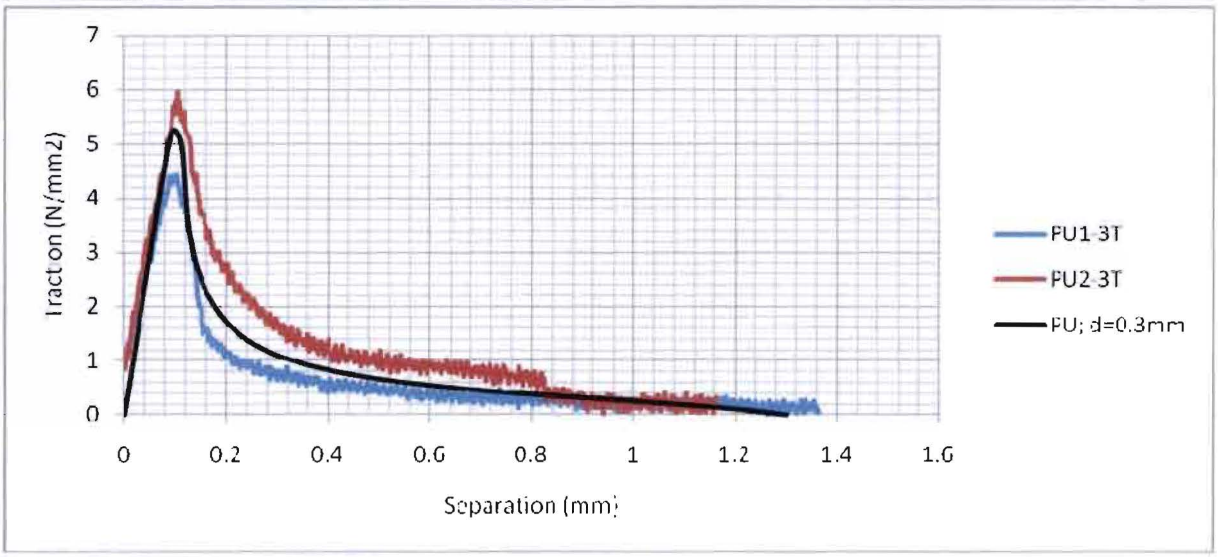

Figure 192: Results of tensile tests with poly-urethane based adhesive. d=0.3 mm

Apendices

PU; d=0,5 mm

Sample	Angel of anual rings to loaded surface (°)	Fracture energy (J/m2)	Strength (N/mm2)	Initial stiffness (N/mm3)	days of drying	Glue thickness (mm)	Used for the estimation of: Initial stiffness	Strength	Fracture energy	Notes	Percentage of bond surface failed: Timber	Interaction timber-adhesive	Adhesive	Interaction dvw-adhesive	Dvw
PU1-5T	25	1194	6.18	144	5	0.63	yes	yes	yes		100				
PU2-5T	5				5	0.66	no	no	no	1	100				
PU3-5T	0	1739	7.40	78	5	0.64	yes	yes	yes		90		10		
PU4-5T	0		5.00		5	0.63	no	yes	no	2	100				
PU5-5T	25				5	0.76	no	no	no	1	100				

Notes	
1	High Pressure on the specimen before starting the test
2	LVDT not properly installed. Only strength is measured

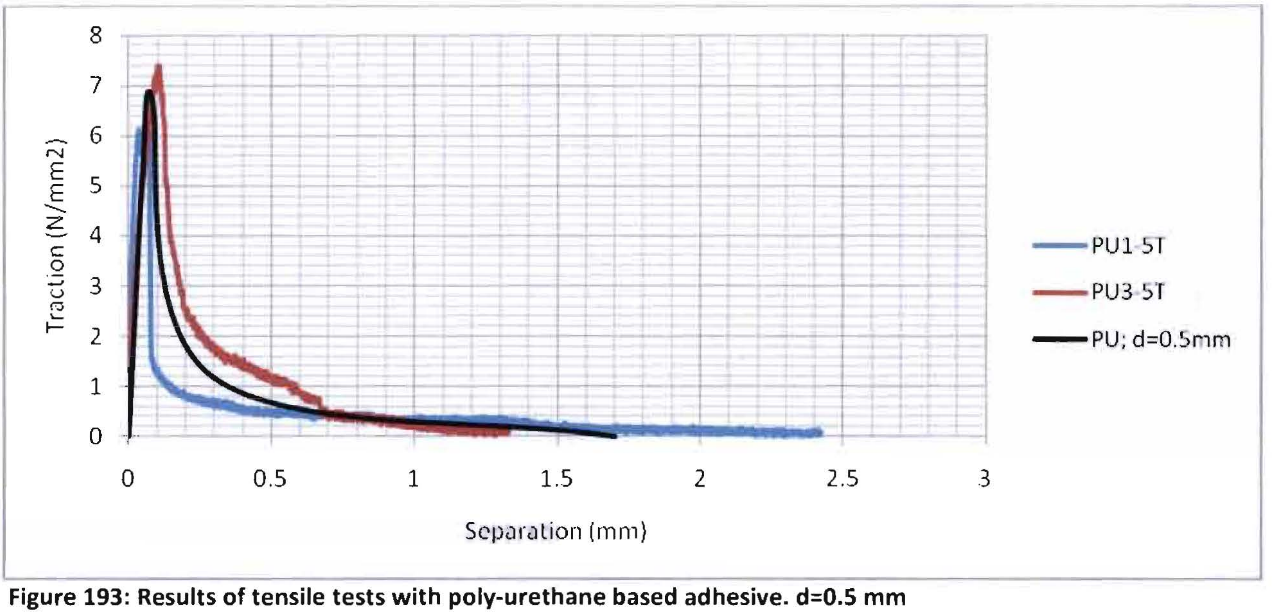

Figure 193: Results of tensile tests with poly-urethane based adhesive. d=0.5 mm

Epoxy; d=0,1 mm

							Used for the estimation of:				Percentage of bond surface failed:				
Sample	Angel of anual rings to loaded surface (°)	Fracture energy (J/m2)	Strength (N/mm2)	Initial stiffness (N/mm3)	days of drying	Glue thickness (mm)	Initial stiffness	Strength	Fracture energy	Notes	Timber	Interaction timber-adhesive	Adhesive	Interaction dvw-adhesive	Dvw
EPX1-1T	5	579	2.92	48	2	0.17	yes	yes	yes		100				
EPX2-1T	10	812	3.08	59	2	0.1	yes	yes	yes	1	80			20	
EPX3-1T	0	1240	8.02	142	2	0.18	yes	yes	yes		15			85	
EPX4-1T	0	937	6.58	86	2	0.37	yes	yes	yes		100				
EPX5-1T	5	1387	4.53	54	2	0.18	yes	yes	yes		50			50	

Notes	
1	X 60* partly failed

* X 60 is a fast drying adhesive, used to attach the samples to the steel holders

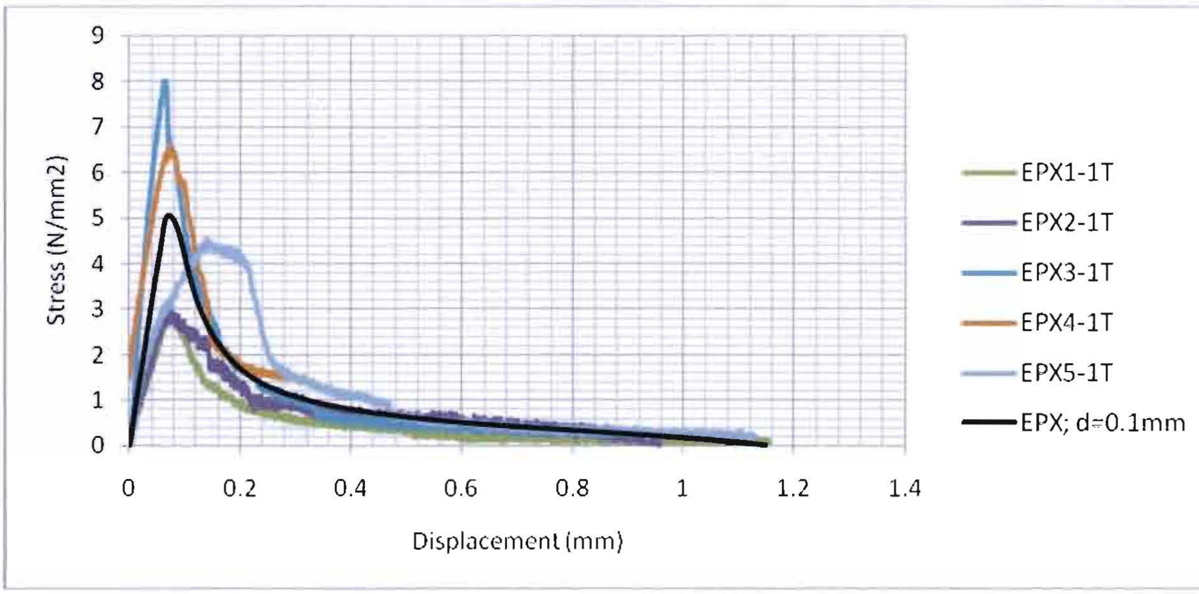

Figure 194: Results of tensile tests with epoxy-based adhesive. d=0.1 mm

Epoxy;   d=0,3 mm

							Used for the estimation of:				Percentage of bond surface failed:				
Sample	Angel of anual rings to loaded surface (°)	Fracture energy (J/m2)	Strength (N/mm2)	Initial stiffness (N/mm3)	days of drying	Glue thickness (mm)	Initial stiffness	Strength	Fracture energy	Notes	Timber	Interaction timber-adhesive	Adhesive	Interaction dvw-adhesive	Dvw
EPX1-3T	0	1681	6.43	82	2	0.35	yes	yes	yes		100				
EPX2-3T	0	727	4.83	57	2	0.34	yes	yes	yes		100				
EPX3-3T	10	1306	5.11	57	2	0.39	yes	yes	yes	1	70				30
EPX4-3T	0		3.97		2	0.4	no	yes	no	2	100				
EPX5-3T	5	482	6.42	179	2	0.44	yes	yes	yes		100				

Notes	
1	Pressure of 4 kN on the specimen before starting the test
2	LVDT's not installed correctly. Only the strength is measured

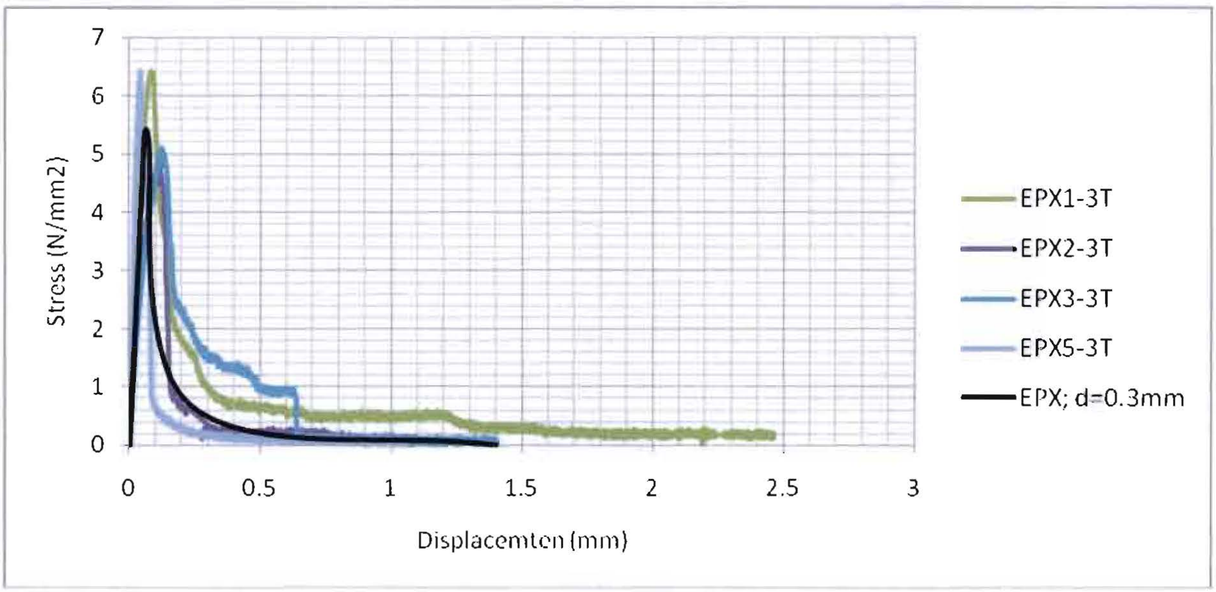

Figure 195: Results of tensile tests with epoxy-based adhesive. d=0.3 mm

Epoxy; d=0,5 mm

							Used for the estimation of:				Percentage of bond surface failed:				
Sample	Angel of anual rings to loaded surface (°)	Fracture energy (J/m2)	Strength (N/mm2)	Initial stiffness (N/mm3)	days of drying	Glue thickness (mm)	Initial stiffness	Strength	Fracture energy	Notes	Timber	Interaction timber-adhesive	Adhesive	Interaction dvw-adhesive	Dvw
EPX1-5T	5	867	4.55	59	2	0.53	yes	yes	yes		100				
EPX2-5T	0		5.51		2	0.81	no	yes	no	1	100				
EPX3-5T	0				2	0.92	no	no	no	2	100				
EPX4-5T	5		4.83		2	0.42	no	yes	no	1	100				

Notes

1	LVDT's not installed correctly. Only the strength is measured
2	X 60* adhesive failed at the start

* X 60 is a fast drying adhesive, used to attach the samples to the steel holders

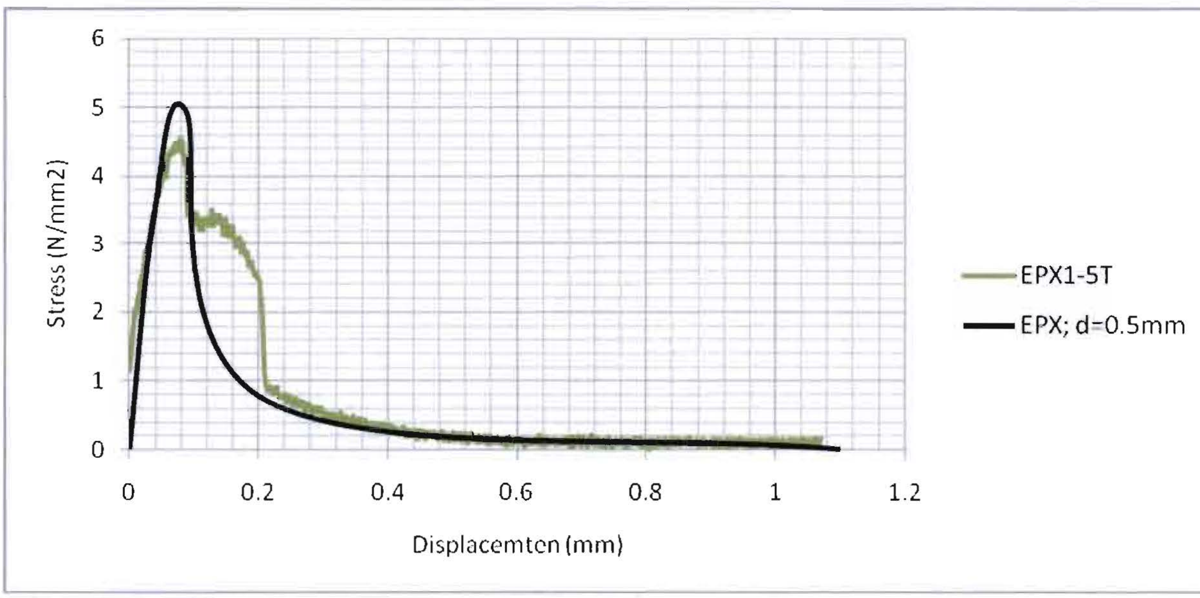

Figure 196: Results of tensile tests with epoxy-based adhesive. d=0.5 mm